GRABEN MECHANICS AT THE JUNCTION OF THE HARTFORD AND DEERFIELD BASINS OF THE CONNECTICUT VALLEY, MASSACHUSETTS

BY WILLIAM E. CHANDLER, JR.

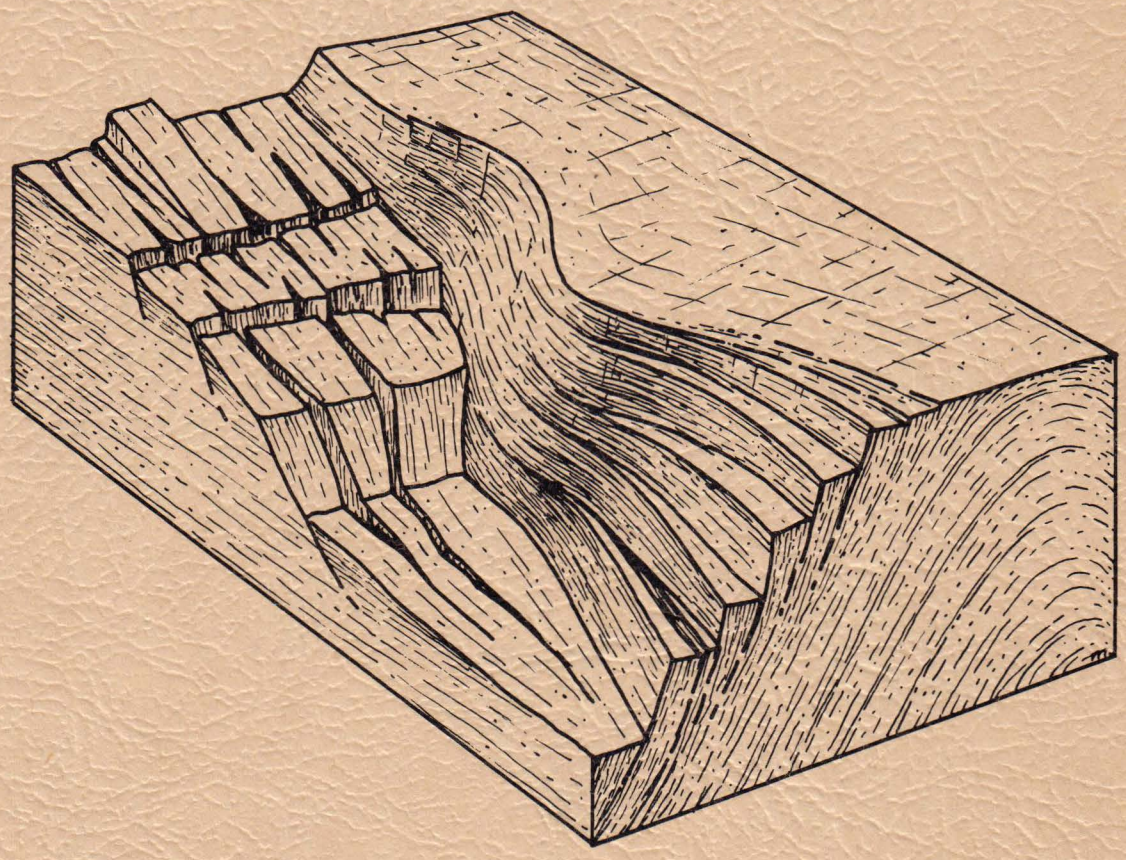

CONTRIBUTION NO. 33
DEPARTMENT OF GEOLOGY & GEOGRAPHY
UNIVERSITY OF MASSACHUSETTS
AMHERST, MASSACHUSETTS

GRABEN MECHANICS AT THE JUNCTION OF THE HARTFORD AND DEERFIELD BASINS OF THE CONNECTICUT VALLEY, MASSACHUSETTS

by

William E. Chandler, Jr.

Contribution No. 33

Department of Geology & Geography

University of Massachusetts

Amherst, Massachusetts

November, 1978

TABLE OF CONTENTS

TABLE OF CONTENTS
(Continued)

TABLE OF CONTENTS
(Continued)

ILLUSTRATIONS

ILLUSTRATIONS
(Continued)

DEDICATION

This thesis is dedicated to my family; my brother, Mark, and my mother and father, without whose encouragement, love, and support, the successful completion of this work could not have come about.

ABSTRACT

A structural high, here named the Amherst Block, separates the Mesozoic Deerfield and Hartford basins. The eastern border fault of these basins undergoes marked curvature in the same region, as does the strike of the basin fill. The graben mechanics of this area were examined in terms of gross geometry, bedrock anisoptropy, fault motions, fracture analysis, and sand model experiments.

The geometry of the basin fill was determined by regional isodip and generalized strike and dip maps compiled from published maps and from field work done in conjunction with this study. These were supplemented by water well data, gravity and magnetic data, and by one gravity traverse run for this study. The traverse showed a model solution with a 675m throw normal fault at the western edge of part of the Amherst Block. Significant elements of basement anisotropy are the west-dipping flanks of the Bronson Hill line of mantled gneiss domes, the Paleozoic Connecticut Valley-Gaspé synclinorium, the Devonian Belchertown and Hatfield plutons, and a possible connection between the plutons beneath the Amherst Block.

Fractures are dominated by N0E to N30E strikes. Of the 208 minor faults observed, 70% were dip-slip, 15% oblique-slip, and 15% strike-slip. Two major normal fault orientations predominate. A set of probable Mesozoic faults striking N30E are evident in rocks of Mesozoic

and pre-Mesozoic age and show slickensides plunging steeply west-southwest. A second set of probable pre-Mesozoic faults, evident only in rocks of pre-Mesozoic age, are oriented N55-70W with slickensides plunging steeply north-northeast and south-southwest. Model experiments were conducted to study fracture behavior in anisotropic sand masses with internal geometry analogous to the geometry of the dome flanks controlling faulting during the formation of the Connecticut Valley. Fracture behavior in the experiments showed curvature of the σ_3 and σ_2 stress trajectories in the vicinity of the anistropy and suggested that the eastern border fault may have started as a series of en echelon, splaying listric faults controlled by the geometry of the dome flank anisotropy. A tectonic model is proposed involving regional extension oriented N60W-S60E. The model makes use of these anisotropies to form the Amherst Block, with the Holyoke Range interpreted as a monoclinal flexure along the southern flank of the block, warped into its present orientation through differential subsidence of the Hartford Basin.

INTRODUCTION

The Problem

There is a growing interest today in planetary scale crustal extension and the associated mechanisms of graben formation (McGill, 1974; Koide, 1975; Stromquist, 1976). The relation of continental rifts to incipient ocean basins has also received much attention with investigations of the Rhine Graben (Illies et al., 1974), the East Africa Rift System (Willis, 1936; McConnell, 1972) and the Red Sea/ Afar Triangle region (Laughton, 1966; McKenzie et al., 1970; Coleman, 1974). In recent years, interest has grown to include lunar and martian graben systems as well as earth analogs for such systems. These studies are presently being conducted by the Planetary Geology Office of the National Aeronautics and Space Administration (N.A.S.A.).

One method of investigating the details of formation of these grabens is the examination of the effects of basement anisotropy on their geometry and the ways in which their deformational history produces internal structures in a basin fill. The Connecticut Valley, which in the context of plate tectonics might be looked on as an abortive attempt to open the Atlantic, provides an ideal setting for studying problems of this type.

Speculation about the interplay of Paleozoic geologic structure

and Mesozoic movement patterns in the Connecticut Valley have been numerous (Wheeler, 1937, 1939; Bain, 1941; Willard, 1951). The major Paleozoic geologic features bounding and underlying the valley are the Berkshire anticlinorium, the Connecticut Valley-Gaspé synclinorium with its "Vermont line" of gneiss domes, and the Bronson Hill anticlinorium with its gneiss domes. Within these terrains are rocks of metamorphic grades ranging from chlorite to sillimanite-orthoclase (Figure 1). Among the most complicated of the Connecticut Valley areas is the region in and around Amherst and Belchertown, Massachusetts. These involve range curvature, complex fault patterns, and basement anisotropy. The principal elements of this complex region are the border fault, its abrupt changes in strike, the Amherst Block, the bend in the Holyoke Range, the Pelham and Glastonbury domes, and the Belchertown Intrusive Complex (Figure 1, see also Figure 1a). It is these elements, with their genetic and geographic relationship to the eastern border fault, which complicate any interpretation of the Mesozoic structural history of the region.

The primary goal of this study is to answer a number of questions regarding the tectonic history of western Massachusetts and the more general mechanisms of graben formation and tilting. Some of the more important questions are:

1. What basement anisotropies are present?
2. What models can explain the effects of these basement anisotropies on the geometry of the basin as it formed?

3. What fracture patterns exist in the study area? From these, what limitations can be placed on the past stresses active over the region?
4. How do fractures derived from a single stress system behave as they propagate and encounter an anisotropy? How do their orientations change?
5. How might the eastern border fault have been initiated and evolved within the study area?
6. How and when did the apparent curvature of the Holyoke Range take place?
7. What is the nature of the Amherst Block and what is its relation to the Belchertown Intrusive Complex?
8. Was the Belchertown Intrusive Complex initially continuous across the area that is now the Connecticut Valley?
9. What limits can be proposed for the three-dimensional geometry of the basin in the Amherst-Belchertown region?

In an attempt to answer some of these questions, this thesis involves three basic types of study, each presented in a separate section: Local Border Fault and Basin Geometry, Brittle Petrofabrics, and Deformational Models.

Location and Topography

The study area (Figure 2) is located in west-central Massachusetts and includes major portions of the Mt. Toby, Mt. Holyoke, Springfield

Figure 1. Map showing general geologic setting of the Connecticut Valley with an outline of the study area.

LEGEND

A. Bronson Hill Anticlinorium (kyanite and sillimanite zones)

1. Pelham Dome
2. Belchertown Intrusive Complex
3. Glastonbury Dome

B. Connecticut Valley-Gaspé Synclinorium (kyanite-garnet and biotite-chlorite zones)

4. Hatfield Pluton
5. Vermont line of gneiss domes

C. Connecticut Valley

6. Border Fault
7. Holyoke Range
8. Amherst Block
9. Mt. Warner
10. Mt. Tom Range

D. Berkshire Anticlinorium (garnet-kyanite-sillimanite zones)

11. Pomperaug Outlier

Line of cross-section A-A′ (see Fig. 5)

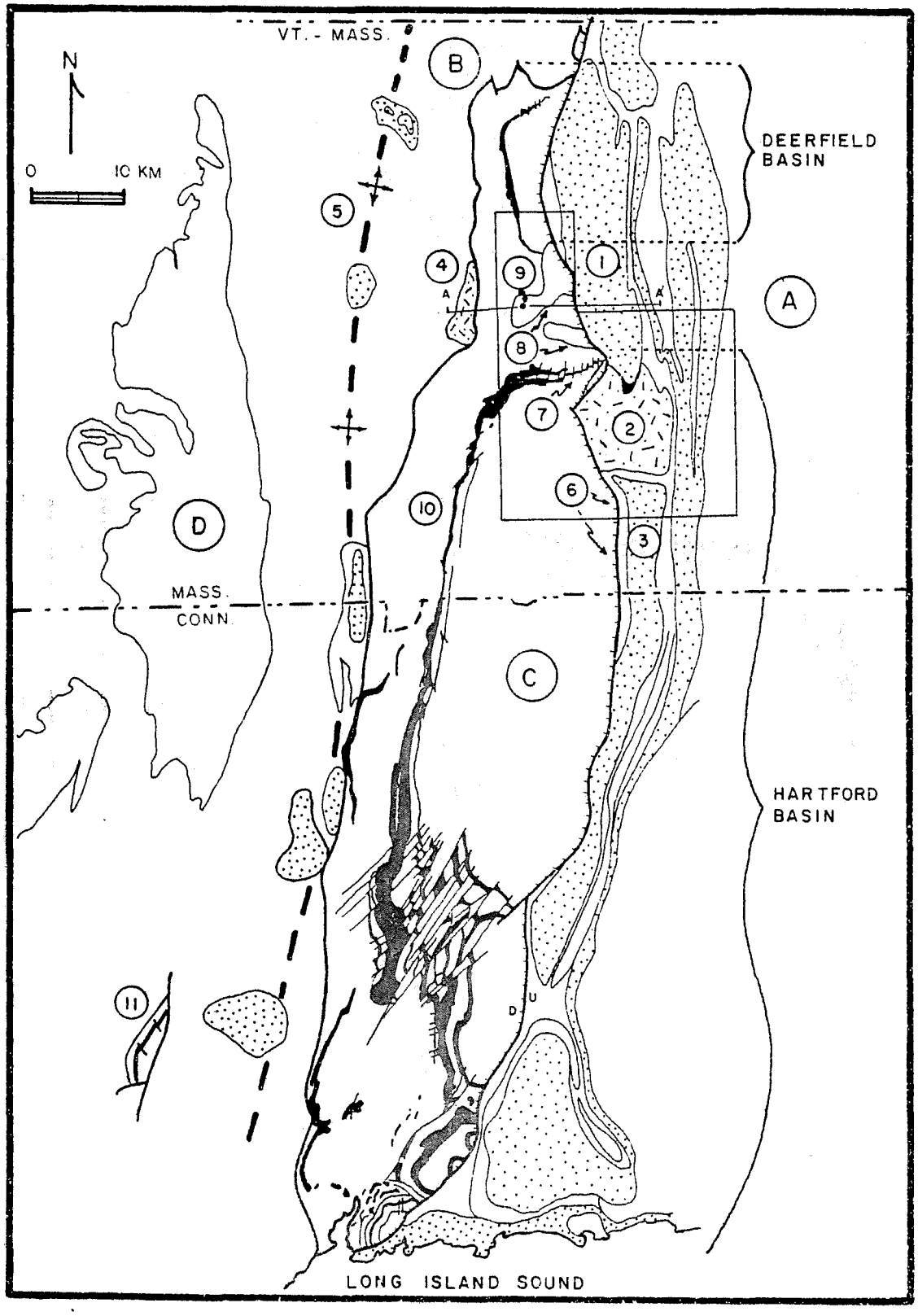
VT. - MASS.
N
0
10 KM
B
DEERFIELD
BASIN
A
5
4
9
1
8
7
2
6
3
10
D
MASS.
CONN.
C
HARTFORD
BASIN
11
U
D
LONG ISLAND SOUND

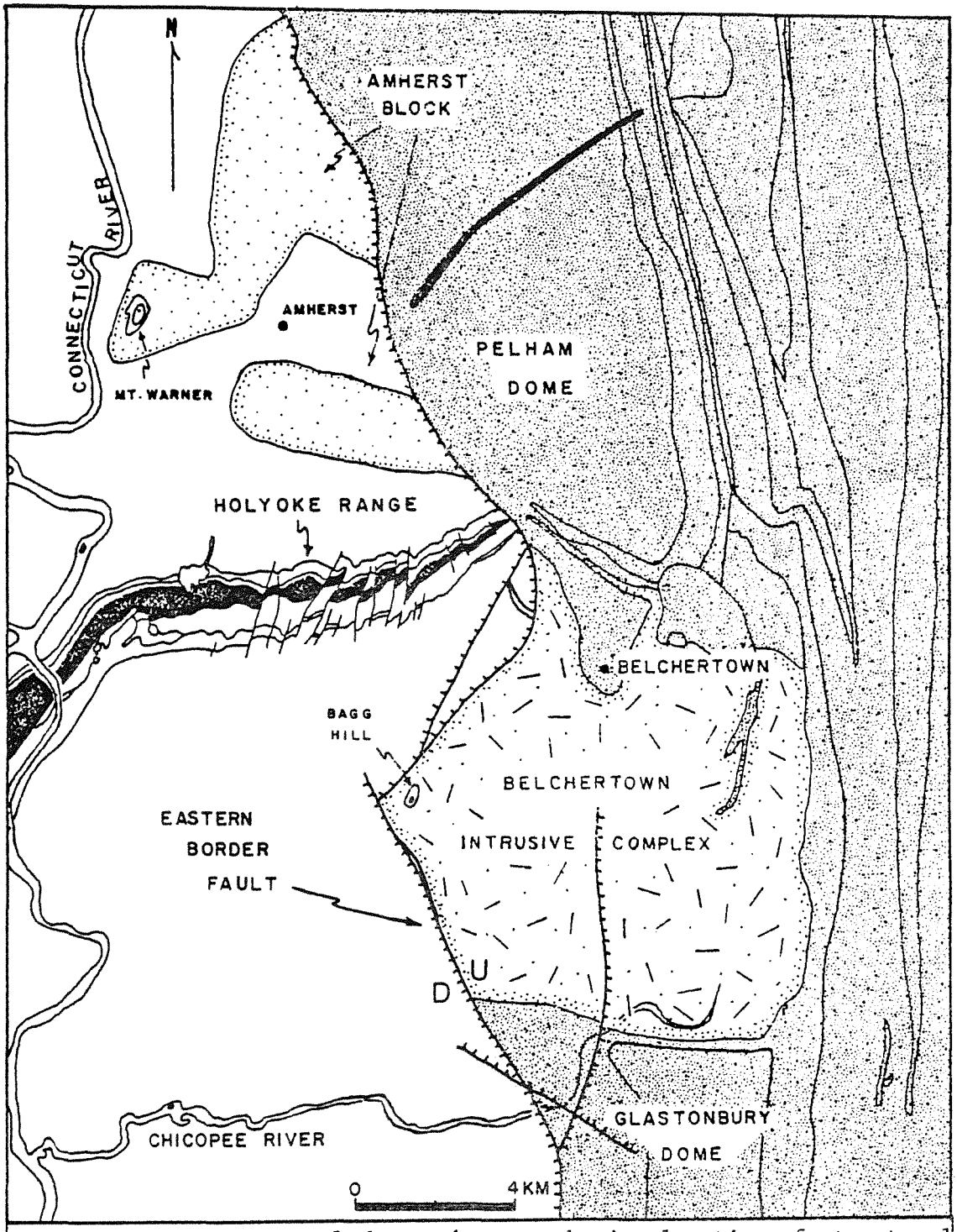

Figure 1a. Index map of the study area showing location of structural elements controlling the trend of the border fault. Mesozoic rocks are shown as black and un-patterned areas (Geology after Robinson, unpublished data, 1978).

North, Belchertown, Ludlow, Windsor Dam, and Palmer 7½-minute U.S.G.S. quadrangles. The area covers much of west-central Massachusetts, extending from the area in and around North Amherst, south to the Town of Granby, and from the Mt. Tom Range on the west to the Bronson Hill line of gneiss domes on the east. The prominent topographic features of the study area are Mt. Warner (156m), the Mt. Tom-Holyoke Range, and the Pelham Hills. These elements show clearly on the shaded raised-relief map of the region (Figure 3). The areas in the vicinity of the towns of Amherst and Belchertown appear as relative topographic lows. The Connecticut Valley as a whole also appears as a major topographic low and defines the approximate location of the eastern border fault by its boundary with the neighboring Paleozoic highlands.

Previous Work

A number of brittle fracture studies have been conducted in western Massachusetts and Connecticut by the University of Massachusetts fracture studies group. Piepul (1975) analyzed joint and fault patterns along the eastern border fault in southern Connecticut. Goldstein (1976) and Williams (1976) conducted similar studies for northern Massachusetts, in the Deerfield (Montague) Basin and the Pelham Dome, respectively. Recently, a substantial contribution was made to our present knowledge of the brittle fracture history of western Massachusetts by a number of workers under the direction of Professor Donald U. Wise through a research contract of the Nuclear

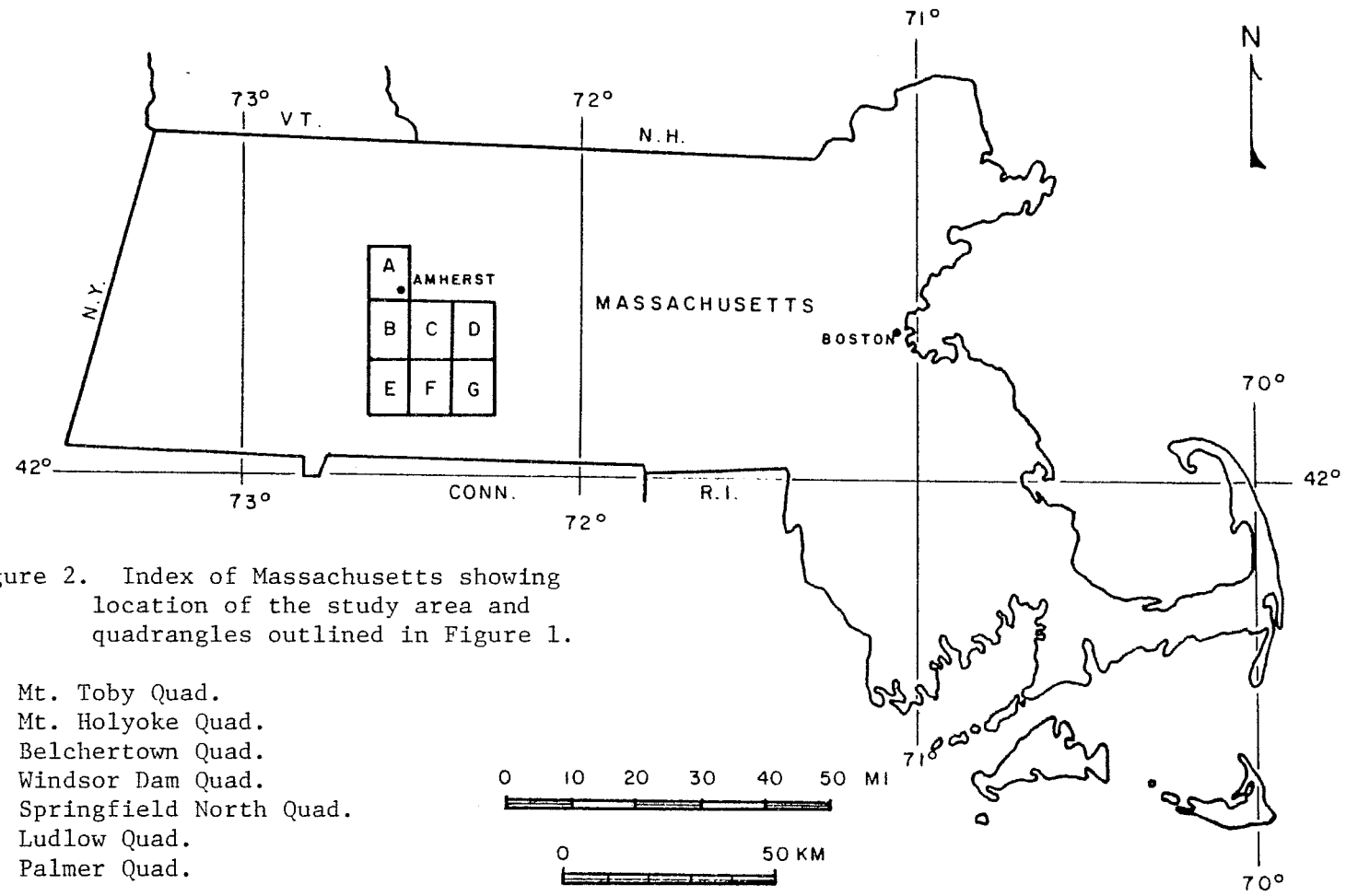

Figure 2. Index of Massachusetts showing location of the study area and quadrangles outlined in Figure 1.

A. Mt. Toby Quad.
B. Mt. Holyoke Quad.
C. Belchertown Quad.
D. Windsor Dam Quad.
E. Springfield North Quad.
F. Ludlow Quad.
G. Palmer Quad.

Regulatory Commission (1977-1978).

Data collection. Field methods and procedures used in this study in collecting fracture data have been evolved over the past few years by Professor Wise and his students and are described in detail by Pferd (1975), Piepul (1975), and Goldstein (1976). Computer-based data storage and retrieval systems for processing structural data were developed by Pferd (1975) and later modified by Piepul (1975) to accommodate a variety of fracture data.

Past geologic mapping and structural interpretations. The bedrock geology of the study area was established by Emerson (1898), Willard (1951), Balk (1957), Guthrie (1972), Hall (1973), Laird (1974), and Robinson (unpublished data, 1978). The structural complexity of the study area has resulted in a number of tectonic theories and interpretations of wide diversity. Speculations as to the nature and origin of Connecticut Valley structures were first summarized in detail by Emerson (1898). Some of the more recent "revolutionary" theories will be discussed here to establish a foundation and context for the models and theories to be proposed in this study.

Bain (1932, 1941, 1957) proposed a number of models for the origin and structure of the Connecticut Valley. His earliest work led him to suggest that the eastern border fault was a high-angle thrust fault with east to west displacement. In his two later papers, the idea of thrust faulting was abandoned. Instead, he suggested that the valley had undergone significant right-lateral strike-slip

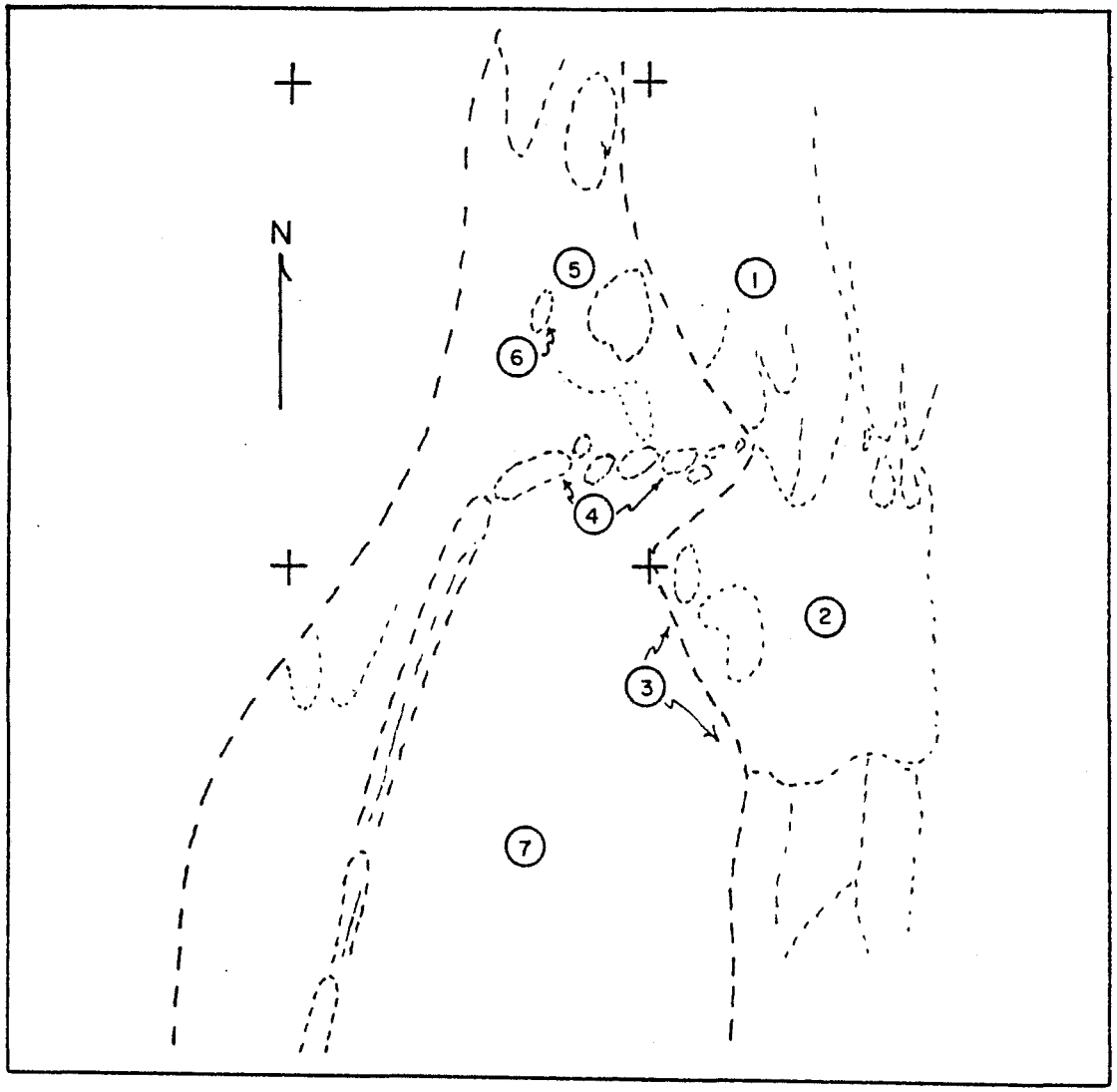

Figure 3. Shaded raised-relief map showing topographic expression of the principal geologic and structural elements in the study area (next page). Index sketch map shown above: 1) Pelham Dome, 2) Belchertown Intrusive Complex, 3) Border Fault, 4) Holyoke Range, 5) Amherst Block, 6) Mt. Warner, 7) Connecticut Valley.

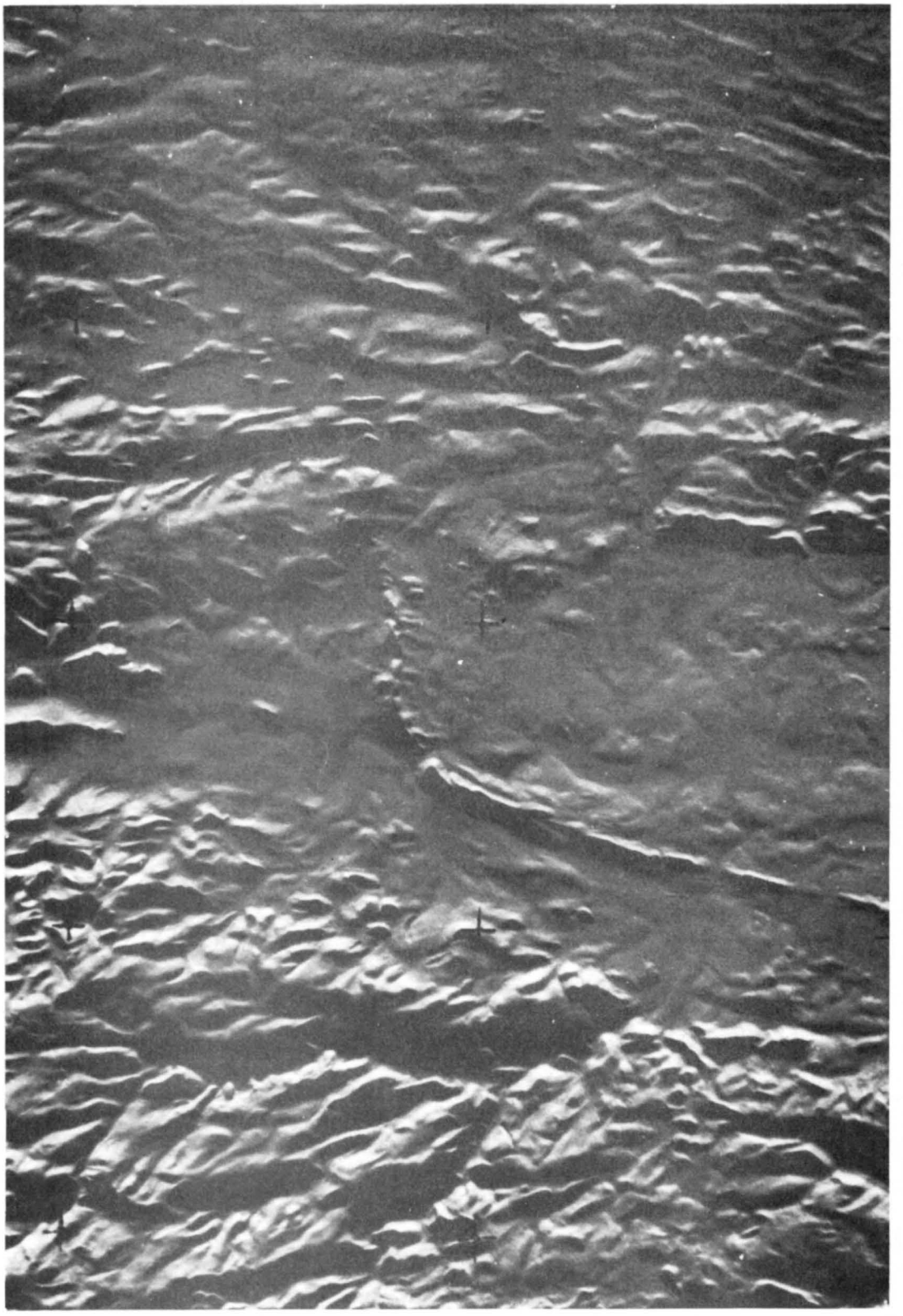

movement along its eastern "border" fault. Bain (1941) suggested that the sediments and volcanics being deposited in the basin were deformed by this southward movement of the eastern highlands, resulting in the bending of the Holyoke Range to its present orientation by faulting and flexuring. Bain's "evidence" for this is the generally vertical, north-south trending faults cutting the range with apparent strike-slip displacement. These faults may have originally been normal faults in the Holyoke Basalt with apparent erosional offset coupled with warping into their present orientation by the monoclinal flexuring of the Holyoke Range (see Section III).

Wheeler (1937) gave an excellent review of past models for Connecticut Valley formation. He concluded that the western boundary of the valley is locally an east-dipping normal fault, suggesting that at least parts of the valley represent a graben structure. In a later work, Wheeler (1939) proposed that irregularities in the eastern border fault resulted in differential movement of the basin fill along the fault plane to produce a warping of the fill. Salients in the fault plane defined areas where subsidence of the fill along the fault was minor, whereas subsidence was greatest in the re-entrants. This model has particular significance for the study area near the eastern end of the Holyoke Range and in the re-entrant created by the Amherst Block and the Belchertown Intrusive Complex.

Willard (1951) proposed a model for the formation of the northern portion of the Connecticut Valley based on observations made in the Mt. Toby and Greenfield quadrangles. He defined a sequence of four

events beginning with initiation of a "basin-forming" west-dipping normal fault, west of the present eastern boundary of the valley in the vicinity of the Connecticut River. Faulting was followed by erosion and sedimentation which eventually filled the basin, covering the fault. This was followed by a period of volcanic activity and further sedimentation. This period included a second episode of faulting. A second major normal fault occurred east of and parallel to the original fault, with movement occurring along both faults. The eastern extent of the basin was correspondingly increased with erosion continuing from the eastern highlands to fill the basin and cover the western fault. A final stage, according to Willard, involved consolidation of sediments, and tilting by later movements along the faults.

More recently, Sanders (1960, 1963) proposed the following structural history for the valley. A period of initial graben subsidence, sedimentation, and igneous activity was followed by longitudinal crustal arching in the graben with no associated faulting or igneous activity. A second period of graben subsidence occurred and was followed by a final late system of faulting, including both dip-slip and strike-slip faults, compressional folding, and igneous intrusion. Erosion is believed to have continued until Late Cretaceous time. Recently, Lindholm (1978) suggested that the Triassic-Jurassic border faults of all the basins in eastern North America were controlled by pre-existing planes of weakness (anisotropies) in the pre-Triassic rocks, dipping parallel to the foliation

in these rocks.

Research in areas geographically remote from the Connecticut Valley may offer some indication of the mechanisms involved during valley formation. Stewart (1971), on the basis of results of clay model studies, geophysical evidence, and field studies, suggested that Basin and Range graben structures are complex zones of listric (shallowing with depth) and antithetic (dipping in the opposite direction from the master fault) faulting over zones of deep-seated extension. These zones of extension are believed to be related to brittle crustal fracturing above a plastically extended substratum. Similarly, Profett (1977) explained the complex system of listric and antithetic faults in the Basin and Range as being due to deep-seated horizontal extension in the crust, analogous to a sea-floor spreading axis. A similar deep-seated extension system, active during continental break-up between Africa and North America, may have given rise to the crustal stresses active during the initiation of the Connecticut Valley.

Acknowledgments

I would like to express my appreciation to Dr. Donald U. Wise for his assistance in all aspects of this study. His enthusiasm and insight into the problem provided much of the motivation for this study and determined many of the directions the study would ultimately take. Many of the basic models presented are outgrowths of his ideas. Special thanks are due also to Dr. Peter Robinson, Dr. Laurie Brown,

and Dr. John Hubert, who provided many helpful suggestions and critically reviewed the thesis. Dr. George McGill assisted in the model studies undertaken and in related photography. Dr. Alan Niedoroda assisted in computer programming. Field assistance was provided by James Beard and Gerald Williams. Financial support for this project came from grants from the National Aeronautics and Space Administration and the Nuclear Regulatory Commission. To each of these institutions and to the persons above, the author expresses his thanks.

REGIONAL GEOLOGIC SETTING

Geologic Timing Relationships for the Connecticut Valley Region

The timing of the formation of Connecticut Valley structures relative to basin sedimentation and volcanic activity can be determined in a number of ways. Radiometric age dating techniques can be used to date fault movements, periods of igneous activity, and metamorphism (Table 1). The location and identification of fossils in sedimentary rocks above and below major basalt units places some restrictions on ages of depositional events and facilitates stratigraphic correlation (Figure 4). Stratigraphic displacements of Mesozoic and Paleozoic rocks, and displacements of metamorphic isograds in the vicinity of the Amherst Block (Figure 5), provide information as to the age and extent of faulting and the stress field active at the time. Depths of erosion provide another useful tool for correlating the timing of basin stratigraphic units (sedimentation) with levels of erosion of the Paleozoic crystalline rocks to the east (Table 1).

General Setting

The study area is centered on the boundary between the Connecticut Valley synclinorium and the Bronson Hill anticlinorium (Figure 1). Bedrock geology of the Connecticut Valley region includes rocks from essentially three periods of geologic time; Precambrian, Early to

Table 1. Geologic Timing

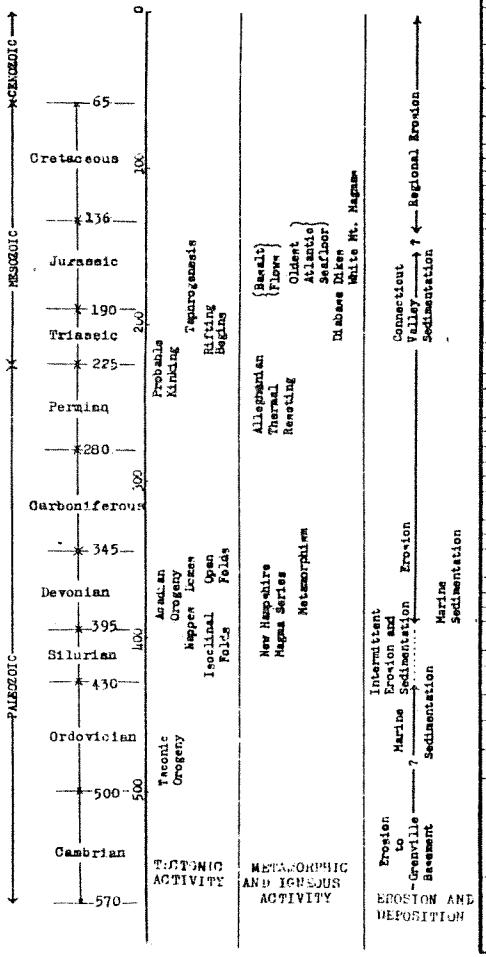

Table 1. Geologic Timing

Method	Age in M.Y.	Geologic, Structural Events and/or Lithologic Units	Reference
K-Ar	115 ± 15	Lamprophyre dikes, younger White Mt. Magma Series, New England	McHone (in press)
	Jurassic (unknown)	Differential subsidence and tilting of basin and gradual warping of Holyoke Range to present configuration	Chandler (1978)
K-Ar	140 - 180	Major age grouping from gouge and mylonite in normal faults	N.E. Utilities (1975)
Stratigraphy Petrology	Lower Jurassic	First erosional unroofing of Belchertown Intrusive Complex	Hall (1973)
K-Ar	143 - 182	Mylonite, gouge at fault contact Erving and Upper Gile Mt. Fm. (Mt. Toby site)	N.E. Utilities (1975)
K-Ar	154 ± 6	Fault in Standing Pond Volcanics (Gill site)	N.E. Utilities (1975)
K-Ar	177 - 180	Sericitized feldspar in Gile Mt. Fm. (Mineral Hill site)	N.E. Utilities (1975)
K-Ar	189 ± 9	Deerfield Basalt (Poet's Seat site)	N.E. Utilities (1975)
K-Ar	171 - 196	All Connecticut Valley Basalts (Holyoke, Talcott, Hampden, Deerfield)	Baeseman et al. (1973)
K-Ar	180 ± 20	Diabase dikes, New England, older White Mt. Magma Series	McHone (in press) 1978
K-Ar	180 - 190	Major age grouping Deerfield Basalt, sericitized feldspar	N.E. Utilities (1975)
	Lower Jurassic	Initial formation of Amherst Block (isolation of Hartford and Deerfield Basins)	Chandler (1978)
		Spores, pollen, and fishes in Portland and Shuttle Meadow Fms. of Hartford Basin	Cornet et al. (1973)
Stratigraphy Petrology	Upper Triassic	Erosion to level of nappes and high grade metamorphics of Bronson Hill	Krynine (1950)
	~210	Beginning of Connecticut Valley Sedimentation	
K-Ar	211 ± 8	Ultramylonite at contact Erving - Lower Gile Mt. Fm. (Mt. Toby site)	N.E. Utilities (1975)
K-Ar	206 - 233	Mylonite in Gile Mt.Fm. (Mineral Hill site)	N.E. Utilities (1975)
K-Ar	200 - 235	Major age grouping of mylonites, breccias, and cataclasized gneisses in Gile Mt. Fm.	N.E. Utilities (1975)
K-Ar	230 ± 15	Oldest White Mt. Plutonic activity	McHone (in press) 1978
K-Ar	227 - 242	Slickensides in Gile Mt. Fm. (Mineral Hill site)	N.E. Utilities (1975)
K-Ar	259	Pseudotachylite in Hampo zone, New York	Ratcliffe (1977)
K-Ar	284 ± 10	Shear zone in Standing Pond Volcanics (Gill site)	N.E. Utilities (1975)
Rb-Sr	140 - 311	Barre Pluton, Vermont	Naylor (1971)
Rb-Sr whole rock	349 ± 13	Standing Pond Volcanics (metamorphic date ?) (Gill site)	N.E. Utilities (1975)
K-Ar	349	Adamant Granite, Vermont	Fmal (1963)
Rb-Sr	354 - 357	Echo Pond Pluton, Vermont	Naylor (1971)
Rb-Sr whole rock	359 ± 11	Concord Granite, last of New Hampshire Magma Series	Lyons et al. (1977)
Rb-Sr	363 - 380	Derby Pluton, Vermont	Naylor (1971)
Rb-Sr	380 ± 3	Barre type plutons (above)	Naylor (1971)
U-Pb	382 ± 5	Belchertown Intrusive Complex	Ashual et al. (in press) 1979
Rb-Sr whole rock	380	Gile Mt. Fm. (metamorphic date ?)	N.E. Utilities (1975)
Rb-Sr	385 ± 20	Prescott Intrusive Complex (post-nappe formation, pre-doming)	Naylor (1971)
	Lower Devonian	Cardigan Pluton and Hardwick Granite (folded with nappes)	Robinson (1967)
Rb-Sr whole rock	402 ± 5	Blackwater Pluton of Spalding Quartz Diorite	Lyons et al. (1977)
Rb-Sr whole rock	405 ± 76	Bethlehem Gneiss	Lyons et al. (1977)
Rb-Sr whole rock	411 ± 19	Cardigan Pluton of Kinsman Quartz Monzonite	Lyons et al. (1977)
Stratigraphy	Lower Devonian	Waite River Fm.	
		Standing Pond Volcanics - Putney Volcanics	
		Gile Mt. Fm.	
		Littleton Fm.	Boucot & Arndt (1960)
Fossils	Silurian	Fitch Fm.	Boucot (1961)
		Clough Fm. (brachiopods and corals)	Boucot (1961)
Stratigraphy	Ordovician	Partridge Fm.	Robinson (1967)
		Ammonoosuc Volcanics	
		Paleozoic Gneiss	Naylor (1967)
	O2	Monson Gneiss - Fourmile Gneiss	Robinson (1967)
		Poplar Mt. - Dry Hill Gneiss	Naylor et al. (1973)

Middle Paleozoic, and Mesozoic; specifically the Triassic and Jurassic (Robinson, 1967; Hubert et al., 1978).

The Mesozoic fill of the Connecticut Valley extends from Long Island Sound to the Massachusetts-Vermont border. It can be separated into two basins characterized by sequences of generally east or southeast dipping sedimentary rocks of Triassic-Jurassic age and Early Jurassic extrusive igneous rocks of basaltic composition (Figure 4). The larger of the two basins, the Hartford Basin (Figure 1), is Late Triassic to Early Jurassic in age (Table 1) based on spores and pollen dated from lacustrine mudstones (Cornet, 1975). The basin is approximately 32 km wide and 140 km long. It is generally regarded as an isolated (Klein, 1969) half-graben, bounded on the east by a west-dipping normal fault (Barrell, 1915; Wheeler, 1939; Hall, 1973). The exact nature of the western boundary of this basin is still subject to dispute, but most speculation has involved variations from an east-dipping normal fault to a simple unconformity. The development of these ideas was discussed in detail by Wheeler (1937). The sedimentary sequence of the Hartford Basin (Figure 4) is believed to have been derived from the erosion of Paleozoic igneous and metamorphic rocks forming the fault scarp highlands to the east (Stevens, 1977). There have also been proposals that some of the basin sediments were derived from a western source-land (Russell, 1878, 1880; Longwell, 1922; Sanders, 1960, 1963; Klein, 1969). The precise nature of the sedimentary and extrusive igneous basin fill has been studied in detail by Krynine (1950) and others.

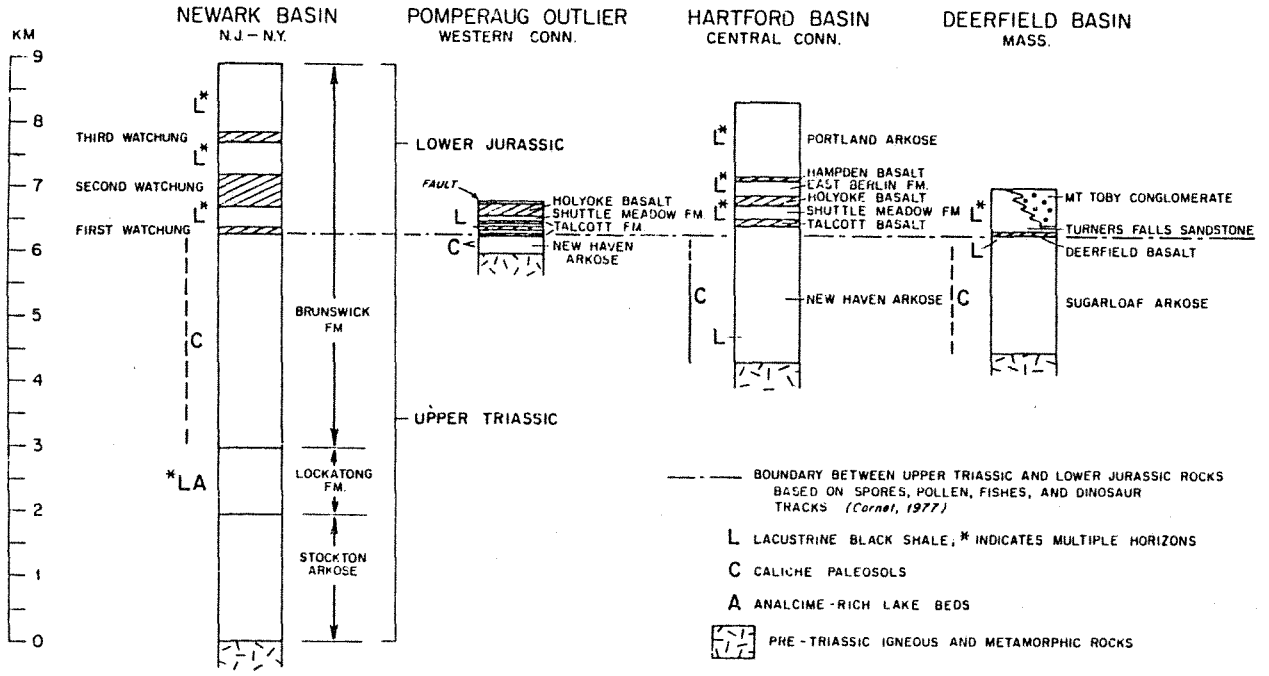

Figure 4. Stratigraphy of Upper Triassic and Lower Jurassic rocks in the Newark, Hartford, and Deerfield basins and in the Pomperaug outlier from Hubert et al., 1978).

Figure 5. East-west cross-section through Amherst as proposed by Robinson (manuscript data, 1978). See Figure 1 for line of section A-A´.

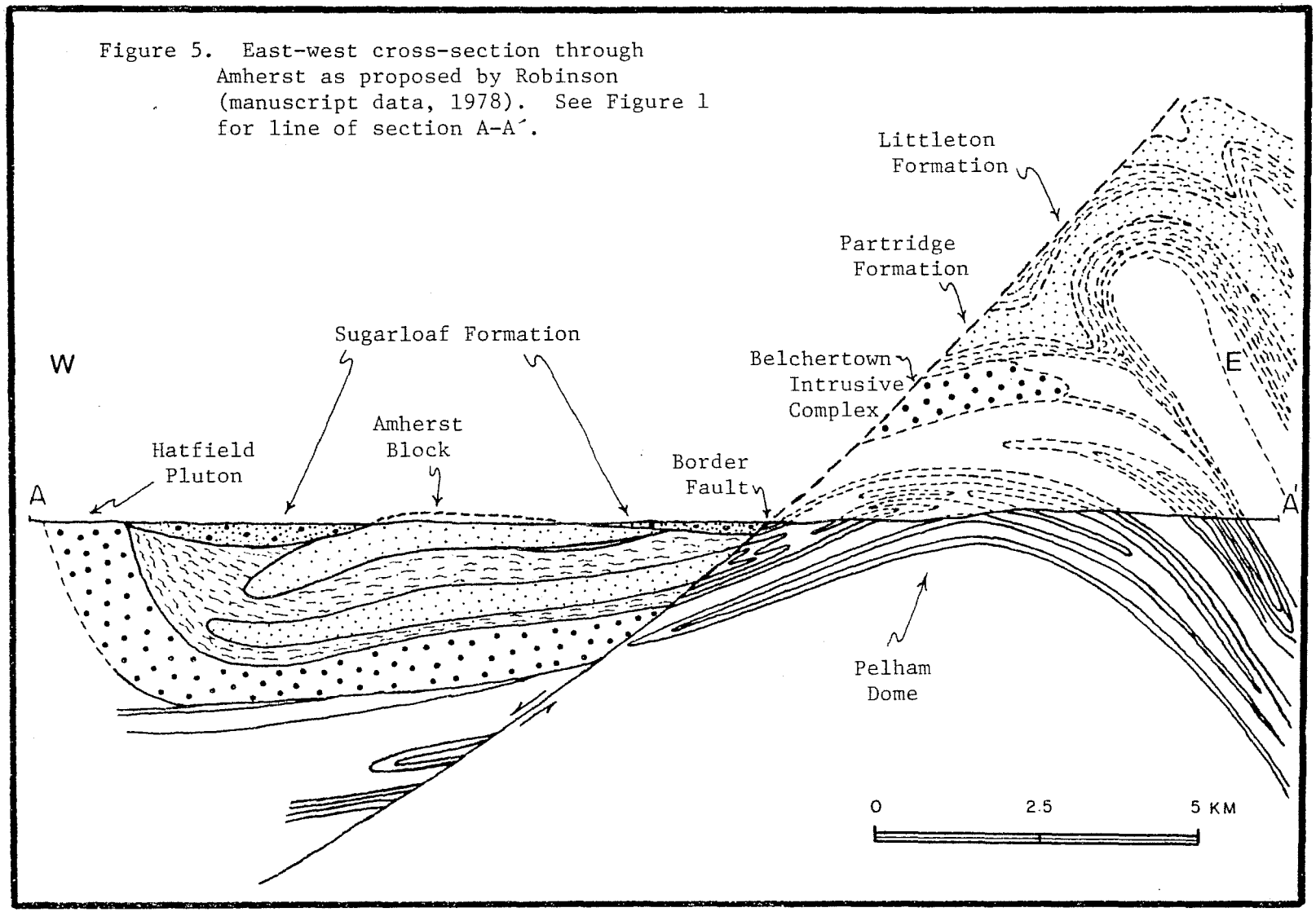

The paleogeography and environments of deposition for much of the Connecticut Valley have been summarized recently by Hubert et al. (1978).

The more northerly basin is commonly referred to as the Deerfield (Bain, 1957; Hubert et al., 1978) or the Montague Basin (Emerson, 1898; Goldstein, 1976). It is separated from the Hartford Basin by a transverse block, possibly a horst, cutting diagonally across the head of the Hartford Basin in the vicinity of Amherst, Massachusetts. The evidence for and the geometry of such a structure will be developed in later sections. The Deerfield Basin is bounded on the east by a northern continuation of the eastern border fault. It is approximately 14 km wide, 24 km long, and is also of Late Triassic to Middle Jurassic age (Hubert et al., 1978). This basin differs in a stratigraphic sense from the Hartford Basin (Figure 4) in that it contains only one volcanic unit, the Deerfield Basalt, in contrast to the three distinct volcanic units of the Hartford Basin; the Talcott, Holyoke, and Hampden basalts. Stratigraphic correlation between the two basins is now on fairly firm ground as a result of recent studies of spores, pollen, and fossil fishes (Table 1, Cornet et al., 1973, 1975).

The crystalline rocks underlying the basin fill are part of the Paleozoic Connecticut Valley Gaspé synclinorium and Bronson Hill anticlinorium. The synclinorium includes metamorphosed Upper Precambrian to Lower Devonian sedimentary, volcanic, and plutonic rocks. Infolded zones of biotite and chlorite schists (Figure 1) locally define a central

low grade metamorphic core of the synclinorium (Robinson, 1967). A zone of en echelon domes cored by gneiss of uncertain age and overlain by metamorphosed Middle Ordovician, Silurian, and Lower Devonian sedimentary and volcanic rocks characterizes the Bronson Hill anticlinorium (Figure 1). The development of nappes with east to west overfolding preceded the formation of these domes (Table 1; Robinson, 1967).

To summarize briefly, the following sequence of geologic events characterizes the tectonic history of western Massachusetts and provides the context for understanding the structural complexities of the study area (see Table 1 for details):

1. A period of intense deformation and metamorphism during Grenville time, of the Precambrian rocks now exposed in the core of the Berkshire anticlinorium, with subsequent erosion.
2. Deposition of miogeosynclinal and eugeosynclinal sedimentary and volcanic rocks of Eocambrian to Lower Devonian age followed by Acadian metamorphism (Ordovician Taconic Orogeny involved deformation and some metamorphism as an intervening episode).
3. Formation of recumbent folds (nappes) with general east to west overfolding after the close of Lower Devonian sedimentation.

4. A Middle to Upper Devonian period of gneiss dome formation and intense isoclinal folding about north-south axes, with Middle Devonian intrusion and folding of the Belchertown Intrusive Complex into the synclinal region between the Pelham and Glastonbury domes.
5. Initial faulting in the Connecticut Valley region probably during Early Triassic time. Major normal faulting forming the eastern boundary of the valley is controlled by the geometry of the basement rocks creating a strength and/or structural anisotropy in the crust.
6. Continuation of valley subsidence with periods of faulting. Late Triassic sediments were derived from highlands to the east. Extrusion(s) of Early Jurassic age basaltic lavas from fissures in the basin floor separated sedimentary strata throughout most of the Connecticut Valley. Partial separation of the Hartford and Deerfield basins occurred as a transverse crystalline ridge formed in the vicinity of Amherst.
8. Late stage faulting, tilting, and differential subsidence within the basin gave rise to major isolation of the Hartford and Deerfield basins by the Amherst Block. General warping (formation of the Holyoke Range) and

internal deformation of the basin fill continued due primarily to the irregularities in the basin floor (Amherst Block), irregularities in the plane of the eastern border fault (salient of the Belchertown Intrusive Complex), and differential rates of subsidence.

Principal Geologic and Structural Elements

It is important to examine in some detail, the nature of the principal geologic structures within the study area so that some knowledge of the existing basement structural and strength anisotropies is available for reference. Special attention will be paid to the basement geologic structures within the study area, bordering the valley to the east, and those geologic features within and bordering the basin which appear structurally and/or genetically related to it.

Some of the more significant anisotropies controlling structural behavior are the following:

1. The west-dipping flanks of the north-south trending Pelham and Glastonbury domes provide a 30-40^{o} west-dipping anisotropy associated with internal stratigraphy and foliation.
2. The Belchertown Intrusive Complex is a major disruption in the dome pattern where it warps dome stratigraphy and foliation. At a minimum, the complex reorients the

stratigraphic and foliation planes of the domes. In addition, the complex has its own foliation orientation which varies throughout the intrusion (Guthrie, 1972; Hall, 1973; Ashwal et al., 1979) and may contribute to a strength anisotropy between the complex and domes. The postulated continuation of a sill-like projection of the complex across the valley to the Hatfield Pluton (Robinson, personal communication, 1978) creates another anisotropy which may have influenced the formation of the Amherst Block.

3. The crustal rocks of the Connecticut Valley synclinorium including a low grade biotite-chlorite zone of mechanically weaker rocks create further discontinuities both at shallow depths and possibly in the deep structure of the continental crust itself.
4. The silicification of the eastern border zone may be Late Paleozoic in age and may have had a controlling effect on later faulting along the dome flanks.
5. A questionable fracture anisotropy oriented N55-70W is found only in Paleozoic rocks. It is unclear whether these fractures were associated with a Paleozoic stress system or were Mesozoic in age and developed only in the Paleozoic rocks because of mechanical differences between

crystalline rocks and the basin fill.

The border fault. The eastern border fault of the Connecticut Valley appears on geologic maps (Robinson, unpublished data, 1978) as a continuous fault which extends from Long Island Sound into western New Hampshire, following the approximate boundary between the Bronson Hill anticlinorium and the Connecticut Valley synclinorium (Figure 1). This boundary is shown clearly by the topography (Figure 3), but actual surface exposures of the fault are rare and its position is commonly inferred. Many abrupt changes in the strike of the border fault are evident from its surface trace (Figure 1). In Massachusetts, the most notable irregularities in strike occur within the study area. The controlling effects of Paleozoic basement anisotropy on the trend of the fault are reflected by the salient created by the fault-bounded corner of the Belchertown Intrusive Complex; by the re-entrant between the complex, the Pelham Dome, and the southern flank of the Amherst Block; and by the more gentle irregularities along the entire extent of the border fault (Wheeler, 1939) (Figures 1 and 1a).

The actual nature of the border fault has been the subject of considerable speculation. The eastern border fault has been considered a simple unconformity (Northeast Utilities, 1974) and a west-dipping thrust fault of Paleozoic age (Northeast Utilities, 1975). These arguments, while intriguing, have little evidence to support them and considerable evidence against them. The major problem with

regarding the border fault as an unconformity is that the rock units within the basin appear truncated (Figure 6) along the eastern boundary of the Connecticut Valley basin, a feature that is difficult to explain without the presence of some type of major faulting. It is conceivable that the border fault could involve some Paleozoic thrusting, but the predominance of Mesozoic age dip-slip normal faulting in many outcrops along the eastern half of the Connecticut Valley (Figure 10) strongly suggests that the present border fault primarily represents an extensional environment. Evidence for major normal faulting has come from the offset of crystalline rocks in the Keene-Brattleboro area as shown by Moore (1949) and reconstructed by Ahmad (1975).

At present, the border fault is regarded by most as a west-dipping normal fault, with suggested dips ranging from 30^{o} to nearly vertical in places (Emerson, 1898; Wheeler, 1937, 1939; Willard, 1951; Sanders, 1963; Robinson, 1967). These dips may depend in large part on the orientation and geometry of the basement anisotropy determining the character of the fault plane at depth. Exposures near French King Bridge have yielded a variety of fault surfaces that, taken together, suggest the main border fault has a dip of approximately 40^{o} (Ashenden, 1973). Drill hole data east of Mt. Toby have yielded an estimated dip in the vicinity of 35^{o} (Northeast Utilities, 1975; Robinson, personal communication, 1978).

Vertical displacements of from 5 to 8.5 km have been suggested for the border fault based on the thickness of stratigraphic sequences in the basin, apparent stratigraphic and isograd displacements, and displacement along some of the plutons in New Hampshire (Emerson, 1898; Robinson, 1966, 1967; Hall, 1973). Further evidence for the existence of the border fault includes the presence of localized zones of mineralization and silicification that are believed to be genetically associated with the initiation of the border fault in Early Triassic time (Table 1). An extensive copper-bearing silicified zone (Chandler, personal observation, 1978) on the Hampshire-Hampden County line just south of Bagg Hill (Appendix I, map N) is located directly along the border fault. Localized occurrences of apparent Mesozoic age quartz-barite-sulfide mineralization are also associated with the eastern border fault in the area southeast of Mt. Toby and at the Leverett Lead Mine (Wheeler, 1937).

The term "Triassic border fault" was often used in reference to the age of the fault (Emerson, 1898; Wheeler, 1939; Robinson, 1967). Ages based on radiometric dates (Table 1) from mylonites, brecciated schists, cataclased gneisses, and fault gauge show three relevant age groupings: one between 235 and 200 m.y.b.p., a second grouping 190 to 180 m.y.b.p., and a third between 180 and 140 m.y.b.p. (Northeast Utilities, 1975). These data suggest that the Connecticut Valley formed over a considerable span of geologic time, but that initial

faulting began in the lowermost Triassic, approximately 225 m.y.b.p., and that the first sediments of the basin were preserved in Upper Triassic time. The volcanism and much of the displacement were Jurassic. Thus, the term "Mesozoic border fault" seems more appropriate.

The Pelham Dome. The Pelham Dome is located directly east of the Deerfield Basin on the west flank of the Bronson Hill anticlinorium, where its western limb is truncated by the Mesozoic border fault (Figure 1). Situated in a staurolite-kyanite zone of regional metamorphism, the dome is cored by three major gneiss units; the Dry Hill Gneiss and the Poplar Mountain Gneiss of probable Late Precambrian age, and the younger Fourmile Gneiss (Table 1; Laird, 1974). These gneisses (ρ=2.67 g/cc) are mantled by Middle Ordovician rocks of the Partridge Formation (ρ=2.82 g/cc) (Hall, 1973). The rocks of the dome have been intruded by Devonian age pegmatite dikes and sills and Early Jurassic diabase dikes and sills. The regional stratigraphic relationship of the Pelham Dome to other principal elements is shown in Figure 5.

The dome forms a relative topographic high with a strong correlation between lithology and topography (Figure 3). The highest hills are the manifestation of the granitic gneisses, with the valleys underlain by quartzite and biotite gneisses (Laird, 1974). A complex sequence of deformative episodes led to the present structure of the Pelham Dome (Robinson, 1967; Laird, 1974). A period of doming

followed early recumbent folding, with northwest to southeast overfolding, during the Devonian Acadian Orogeny (Table 1). This doming of existing metamorphic rocks resulted in a broad arch of originally gently dipping foliation that presently trends generally north-south and is superimposed on the axial plane foliation of the early recumbent folds (Laird, 1974). The author proposes that the orientation and angle of dip of the border fault in the vicinity of the Pelham Dome may have been controlled by the orientation and degree of doming and the trend and dip of the resulting foliation.

The Belchertown Intrusive Complex. A pronounced topographic low marks the location of the Belchertown Intrusive Complex along the axis of the Bronson Hill anticlinorium (Figure 3). The complex was intruded into the synclinal region between the Pelham and Glastonbury domes (Figure 1) where it crops out over approximately 64 square miles (Guthrie, 1972). The westernmost boundary of the complex was created by the border fault which is believed to dip approximately 40^{o} to the west in this area. The southwest contact of the complex may not have lain far beyond the present location of the border fault (Hall, 1973). The complex is composed of three main rock types: (1) a hypersthene-augite-quartz monzodiorite (inner zone), (2) a hornblende-biotite-quartz monzodiorite gneiss near the outer margins and in localized shear zones, and (3) an augite-quartz monzodiorite in a gradational region between the inner and outer zones. Minor

inclusions of hornblendite and pyroxenite are present along with late stage pegmatite and aplite dikes (Hall, 1973). Aplite and pegmatite dikes in the complex trend predominantly N10E, N30E, and N60E, and dip northwest. These attitudes appear related to location within the complex. Dikes in the northeast portion trend northeast and dip west, whereas those in the northwest portion of the complex strike northwest (N60W) and dip southwest. These dikes are most abundant near the margins of the complex, becoming less abundant with no preferred orientation toward the center (Guthrie, 1972).

The age of the complex is generally believed to be Devonian (Table 1), with intrusion taking place during the late stages of regional matamorphism (Guthrie, 1972, Ashwal et al., 1979). Foliation within the complex is weakly to strongly developed except in the massive unaltered core (Hall, 1973; Ashwal et al., 1979). The strongest foliation exists in the outer zone of the complex, in the vicinity of Bagg Hill (Hall, 1973, Figure 11; stations 19 and 20). Here the foliation shows a dominant N55-70W trend. The exposed contacts of the complex appear concordant, but map relationships suggest that the northern contact is regionally discordant with the structure of the surrounding metamorphic rocks.

During Triassic-Jurassic time, the complex was faulted, intruded by diabase dikes, in the vicinity of the border fault; hydrothermally altered and silicified, and unroofed and eroded (Table 1; Hall, 1973).

The Longmeadow Sandstone lies in fault contact along the western edge of the complex and contains cobbles of rocks from the complex. The absence of these cobbles further north in deeper horizons suggests that the complex was first unroofed during Longmeadow time (Hall, 1973), but was apparently not unroofed near the Amherst Block (Figure 5).

Density measurements show that the complex and related metamorphic rocks have a higher average density (2.82 g/cc) than the adjacent Mesozoic sedimentary rocks and dome gneisses (2.67 g/cc , dome mantling rocks 2.82 g/cc). The simple-bouguer gravity anomaly map and models examined by Hall (1973) suggest that the complex is nearly disc-shaped, with a diameter greater than six times its thickness (approximately 12.9 km wide and 2.1 km thick). Hall (1973) also suggests a minimum vertical extent for the complex of between 1.4 and 1.65 km, i.e., a large sill.

The mechanism of emplacement for the Belchertown Intrusive Complex as proposed by Guthrie (1972) involved forceful intrusion and stopping, evidence for which lies in the intrusive breccias and contact relationships with surrounding metamorphic rocks (see also Ashwal et al., 1979).

The Hatfield Pluton (Figure 1) may or may not be related to the Belchertown Complex at depth (Figure 5). Separated from the complex by the Connecticut Valley lowlands, the Hatfield Pluton is

unconformably overlain by the Triassic Sugarloaf Arkose (Willard, 1956; Stevens, 1977). The composition of the Hatfield Pluton is essentially the same as the complex (Stoeck, 1971) and may be a continuation of it underlying the basin sediments of the Connecticut Valley (Robinson, personal communication, 1978).

The Amherst Block. The Amherst "Block" was first mapped by Emerson (1898) and later Willard (1951). It is now interpreted as an inlier of Paleozoic basement down-dropped along the border fault and consisting of rocks of sillimanite grade Ordovician Partridge schist, Silurian Clough conglomerate, and Devonian Littleton schist (Figure 5; Table 1). Displacements in metamorphic grade and structure, evident from the contact between rocks of the Amherst Block and the Pelham Dome, have served to locate the border fault more precisely in the vicinity of Amherst. Comparatively little else is known about the Amherst Block. Its three-dimensional geometry remains the subject of considerable speculation.

The Amherst Block appears as a topographic low with the exception of Mt. Warner and a series of hills near Leverett, Massachusetts which represent the highest surface exposures of rocks of the Partridge and Littleton formations within the block (Figure 3). The block separates the Hartford and Deerfield basins and is believed by the author to represent the surface exposure of upwarped and faulted basin floor. In effect, the block represents a lag point during the subsidence of the pre-Triassic basement. Through faulting,

it stands as a transverse "horst" (fault-bounded block, possibly triangular in nature) trending diagonally N55-70W across the head of the Hartford Basin. Evidence for the geometry of the Amherst Block will be examined in later sections.

The Mt. Tom-Holyoke Range. The Mt. Tom Range trends along the generalized strike of the Connecticut Valley and becomes the Holyoke Range through its abrupt curvature to a more east-west transverse trend (Figure 1). The Mt. Tom-Holyoke Range is held up by the Holyoke Basalt, a massive basalt of variable texture which consists of a number of thick flows totalling as much as 300m and extruded from fissures into large lava lakes (Sanders, 1963; Hubert et al., 1978). Within the basin, the Mt. Tom-Holyoke Range stands as the prominant topographic high (Figure 3).

The strike of the basalt changes abruptly from generally north-south to east-west as reflected by the adjacent basin sedimentary rocks (Figure 6). The dip of the basalt clearly steepens along the length of the Holyoke Range (Bain, 1941) from 15^{o} on the western part to 80^{o} on the east end (Figure 7), where it appears truncated by the border fault. The Holyoke Basalt is also cut by numerous, generally north-south trending faults showing significant apparent horizontal displacements (Bain, 1941).

Recent evidence (Figure 4) suggests that the Holyoke Basalt is Early Jurassic in age. Previous radiometric age dates (Table 1) gave a range of ages for the Talcott, Deerfield, Holyoke, and Hampden basalts that support this finding.

LOCAL BORDER FAULT AND BASIN GEOMETRY

Introduction

It is the purpose of this section to examine carefully the geometry of the basin within study area and present some evidence on this subject based on newly compiled geologic maps, available water well data, and geophysical data.

Strike and Dip of Mesozoic Bedding

A series of maps describing the basin fill and the geology surrounding the Connecticut Valley have been compiled recently by Wise, Chandler, and Golombek (unpublished data, 1977) at the University of Massachusetts. Two of these maps are of special interest here: a generalized strike and dip map and an isodip map, parts of which are reproduced in Figures 6 and 7, respectively. The lines comprising the map in Figure 6 are formlines showing the changing strike of the basin rocks and their average dip along strike. The formlines reflect the curvature of the Holyoke Range and suggest that the Amherst Block has had a warping effect on the basin fill related to the curvature of the range. Thus, the Holyoke Range may represent the outcrop of an east-west striking monoclinal flexure on the south flank of the Amherst Block.

The isodip map (Figure 7) defines areas where the sedimentary rocks have a common range of dips. It shows a sharp steepening

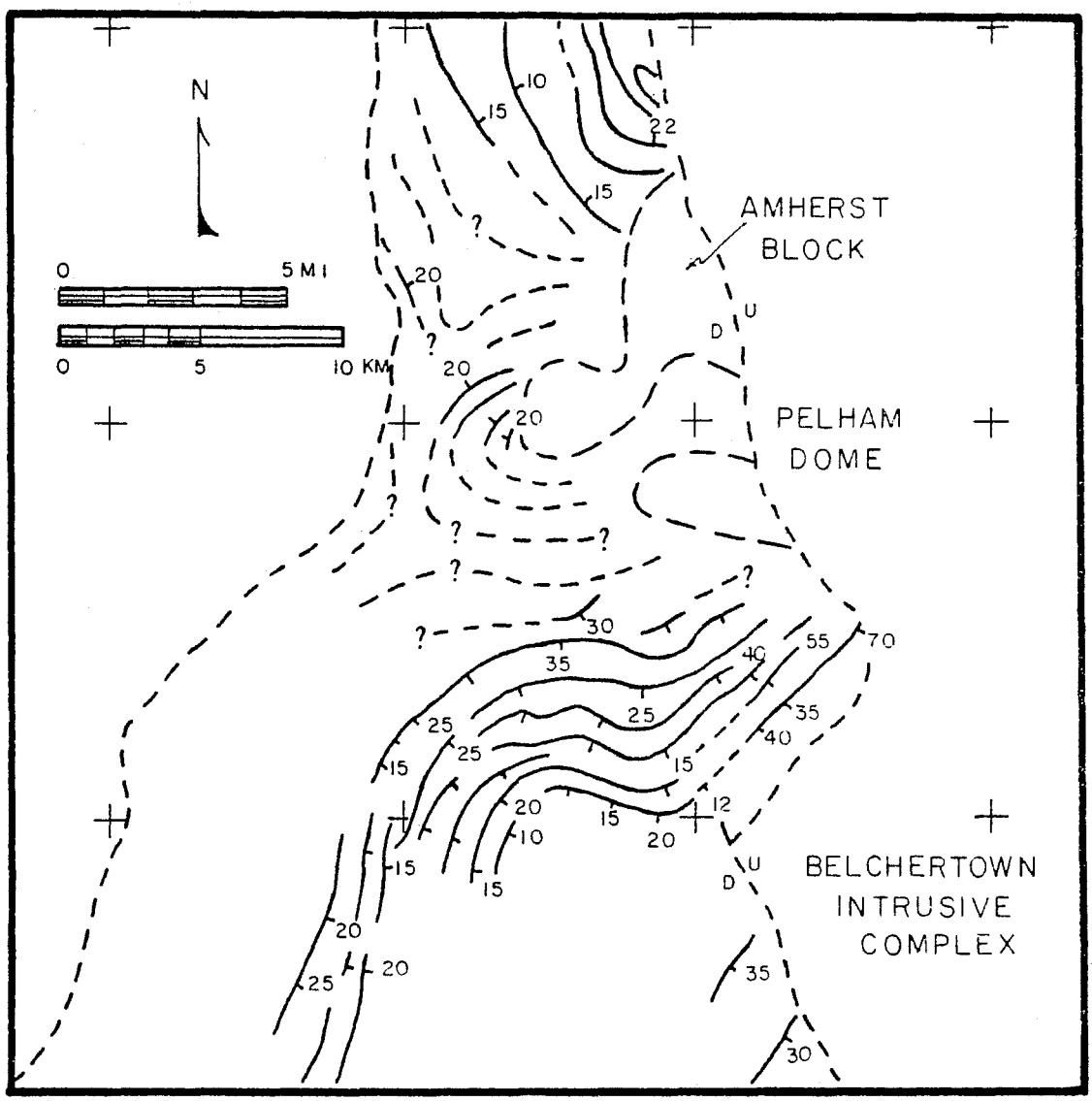

Figure 6. Generalized strike and dip map of the study area.

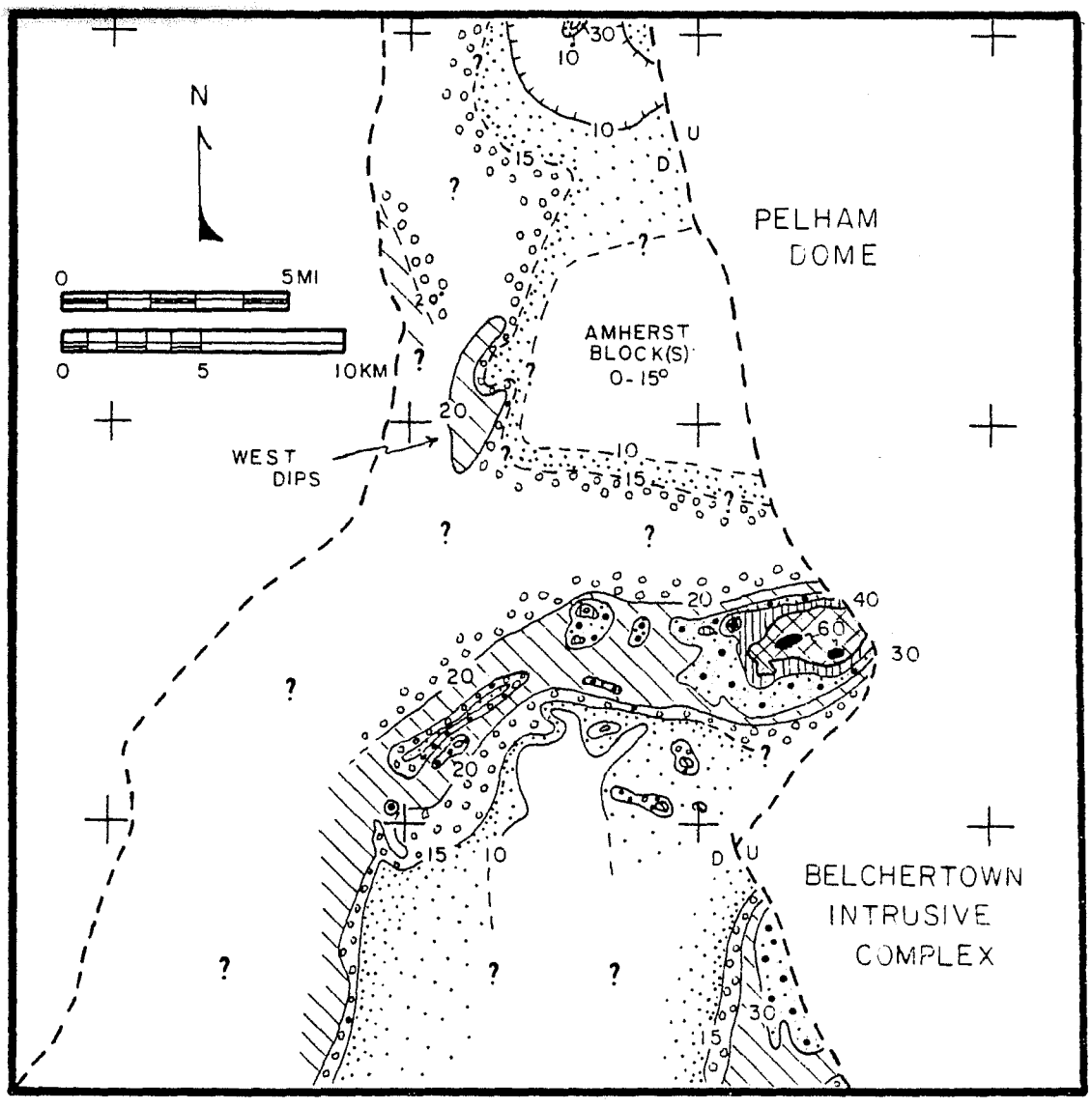

Figure 7. Isodip map of the study area.

of the basin sedimentary rocks toward the east end of the Holyoke Range suggesting that the basin floor suddenly becomes deeper within the re-entrant created by the northern portion of the Belchertown Intrusive Complex and the southern flank of the Amherst Block. The map also shows a general flattening (and probable thinning) of the basin fill over the central area of the Amherst Block, and a corresponding steepening along the southern and western edges of the block. This again suggests a genetic relationship between the Amherst Block and the warping of the basin fill to produce the apparent curvature in the range.

Water Well Data

The usefulness of water well data was limited to some extent by the degree of cooperation of local drillers, the ambiguity of the information contained in the well logs, and the difficulties encountered in trying to locate the wells precisely. Approximately 240 wells were located; 60 of the more significant wells are located on the maps in Appendix I. Wells located on maps H and O are of special interest as they cross the border fault and generally support the mapped fault location (Robinson, unpublished data, 1978).

Although ambiguities do exist, as can be seen in Appendix I, the potential of these wells is obvious. With more wells, properly located, a precise location of the contact between Paleozoic crystalline and basin sedimentary rocks could be determined in the study area, where outcrop is scarce. Perhaps of greater importance

is the possibility of mapping the topography of the basin fill beneath the glacial cover. From the data contained in the logs, structure contour maps could be constructed which, with sufficient coverage, might on a broad scale, provide some indication of the topography of the basin floor. Data similar to these contained in the logs for zone 1, zone 2, and zone 3 in Appendix I would be ideal for such a task.

One other piece of well log data should be pointed out. Well #92 (map M), located on Taylor Street in Granby, along with well #88 (map G) suggest the possible existence of an anomalous basalt "flow" or intrusion in the vicinity of Granby, Massachusetts. The log for this well is as follows: "total depth, 97'; ledge at 25' ('redrock'); at 60' encountered 'traprock' to 75'; 'puddin rock' at 75'." The certainty of the existence or extent of the basalt "flow" is fair at best, but the possibility of a 15' thick flow or sill located just south of the Holyoke Range is interesting nonetheless in terms of its surprisingly shallow depth and possible relation to the range.

Magnetics

A potentially useful tool in placing restrictions on the surface and subsurface geometry of the Connecticut Valley region is aeromagnetic maps. On a broad scale, magnetics (Gilbert et al., 1968, 1969) define the outline of the basin and correlate reasonably well with bedrock mapping. The Belchertown Intrusive Complex appears as

a broad, somewhat circular magnetic low (2800 to 3200 gammas) with a relative high (3300 gammas) corresponding to the inner zone of hypersthene granodiorite (Hall, 1973; Ashwal and Hargraves, 1977). There is essentially no sharp magnetic contrast between the complex and the basin fill directly to the west. The Amherst Block is virtually indistinguishable in the magnetics from the surrounding basin fill. Relative magnetic highs also correlate with portions of the Pelham Dome and Triassic-Jurassic basaltic dikes in the area. A linear series of closely spaced, generally east-west trending magnetic highs define the Holyoke Range. A recent ground magnetic study of the east end of the Holyoke Range suggests that the Holyoke Basalt is not in fault contact with Paleozoic crystalline rocks, but rather pinches out against a west-dipping alluvial fan near the eastern edge of the basin floor (Harris, 1974).

Gravity

Due to a lack of density contrast, available gravity maps (Ellen, 1964; Bromery, 1967; Hall, 1973; Kick, 1975) do not define precisely the outline of the basin and the surrounding geology. The Pelham and Glastonbury domes correlate with distinct gravity lows. A moderate-amplitude gravity low correlates with the basin to the west of the border fault. The Belchertown Intrusive Complex correlates with a broad, low-amplitude gravity high (+4 mgals), with a relatively gentle gradient that steepens sharply in the vicinity of the fault contact between the complex and the sedimentary basin to the

west (Hall, 1973; Kick, 1975). On the residual gravity map of Hall (1973), the complex correlates with a roughly circular gravity high (+9 mgals) whereas the Pelham and Glastonbury domes correlate with distinct lows relative to the complex. Within the basin, portions of the Amherst Block appear as gravity highs (0 to -1 mgal) relative to the surrounding Mesozoic basin fill (-9 to -12 mgals). Ellen (1964) notes a linear trend in relative gravity highs in the vicinity of the Belchertown Intrusive Complex, Mt. Warner, and the Hatfield Pluton. It is interesting to note that a line can be drawn through these three highs which trends N45-55W, suggesting some relation to the proposed trend of the Amherst Block at depth across the valley. Gravity map contours (Kick, 1975) behave much the same as the lines on the strike and dip map (Figure 6) and the isodip map (Figure 7) in grossly defining the outline of portions of the Amherst Block, particularly in the area between the Holyoke Range and Mt. Warner. Here, the contours grade from a low of -9 milligals in a broad trough correlating with the Holyoke Range, to a relative high of 0.0 to -1.0 milligals in the vicinity of Mt. Warner. This is shown clearly on the simple-bouguer gravity maps for the Mt. Toby, Mt. Holyoke, and Belchertown quadrangles compiled by Kick (1975), and may reflect the existence of a continuation of the more dense rocks of the Amherst Block at depth, dipping gently southward beneath the Holyoke Range.

The study area is characterized by small gravity contrasts between rock types and a total anomaly with respect to surrounding areas ranging from +4 to -12 milligals. Anomalies of not more than several milligals occur near the lithologic contacts. To study such areas further, it seemed appropriate to look for a method of accentuating the gravity signature with the hope of defining contacts and/or faults not clearly defined by the gravity contours. The method chosen was developed by Stanley (1977) and is described briefly in Appendix IIID. A gravity traverse was conducted in the Mt. Toby quadrangle along Comins Road, from the benchmark in North Amherst, west to Route 47. The locations of the traverse and the gravity stations are shown in Appendix IIIA. This particular line of traverse was chosen to test the method because it crossed a contact, the exact location and nature of which is uncertain. The objective was to determine geometric and density parameters which could be used to establish reasonable starting points for initial Talwani (1959) two-dimensional block models for the geometry of the rocks causing the observed gravity anomaly. The method proved to be surprisingly useful in this respect as shown by the similarity between calculated and final model values for d, the angle of dip of the contact, and t, the depth to the shoulder of the contact (Appendix IIIK).

The results of the traverse are shown in Appendix III along with the methods used to interpret the results. In summary, the

contact previously located by Willard (1951) can be relocated (Appendix IIIA) and modeled as a west-dipping (77^{o}W) fault contact with approximately 675 meters of throw between basin sediments (ρ=2.67g/cc) and Paleozoic crystalline rocks of the Amherst Block (ρ= 2.74g/cc to 2.82g/cc), mantled by 100 to 120 meters of glacial debris (ρ= 2.4g/cc) (Appendix IIIK). There is excellent agreement between the observed Bouguer anomaly and the calculated Bouguer anomaly curve for the best fit Talwani two-dimensional block model (Appendix IIIC). The depth to bedrock (t) in the block model and the calculated value of t also agree well with depth to bedrock data from wells in the area (Appendix I, A and B).

Map Changes

The water wells and limited geophysical data support the approximate location of the border fault as shown by Robinson (unpublished data, 1978). A geophysical traverse in the Mt. Toby quadrangle has resulted in the relocation of the western contact between the crystalline rocks of the Amherst Block and the basin sedimentary rocks as mapped by Willard (1951). The exact trend of the new fault contact will remain uncertain until further gravity and/or seismic work is done. Finally, a previously unknown basalt "flow" may exist in the vicinity of the Town of Granby, Massachusetts, but its actual location and extent remain uncertain.

BRITTLE PETROFABRICS

General Statement

Tectonic forces undoubtedly play a role in upward and lateral propagation of basement fractures into overlying meta-sediments and basin fill. With erosional unloading, the compressional stresses in the rock masses may undergo a gradual release and reorientation. This can give rise to fractures which propagate upward and laterally to encounter anisotropies in the surface rocks. The resulting fracture patterns are functions of the topography, level of erosion, orientation of stresses, and the geometry of the anisotropy at that level. These concepts are applied to the study area in this and in the final section on deformational models.

Results of Previous Brittle Fracture Studies in Western Massachusetts

A summary of some of the fracture data from recent studies conducted in and around the Connecticut Valley is shown in Figure 8, with the location of these studies shown in Figure 9. Goldstein (1976) postulates a complex brittle fracture history for the Deerfield (Montague) Basin. He notes a greater complexity of jointing in crystalline rocks than in basin sedimentary rocks and the predominance of strike-slip faulting in the basin showing a conjugate relationship suggesting north-south compression. Piepul (1975) concludes from analysis of jointing and faulting in the vicinity of the southern end

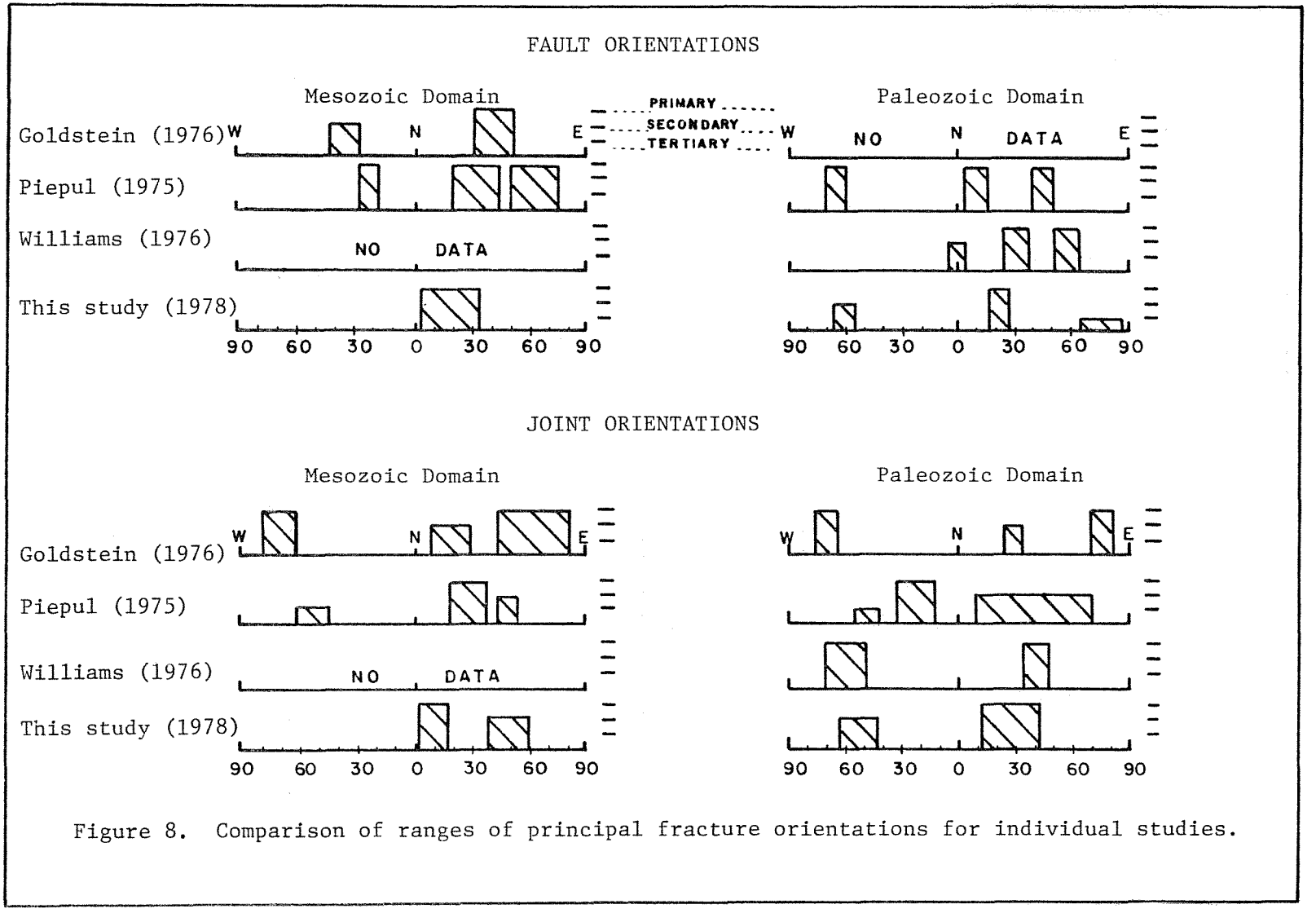

Figure 8. Comparison of ranges of principal fracture orientations for individual studies.

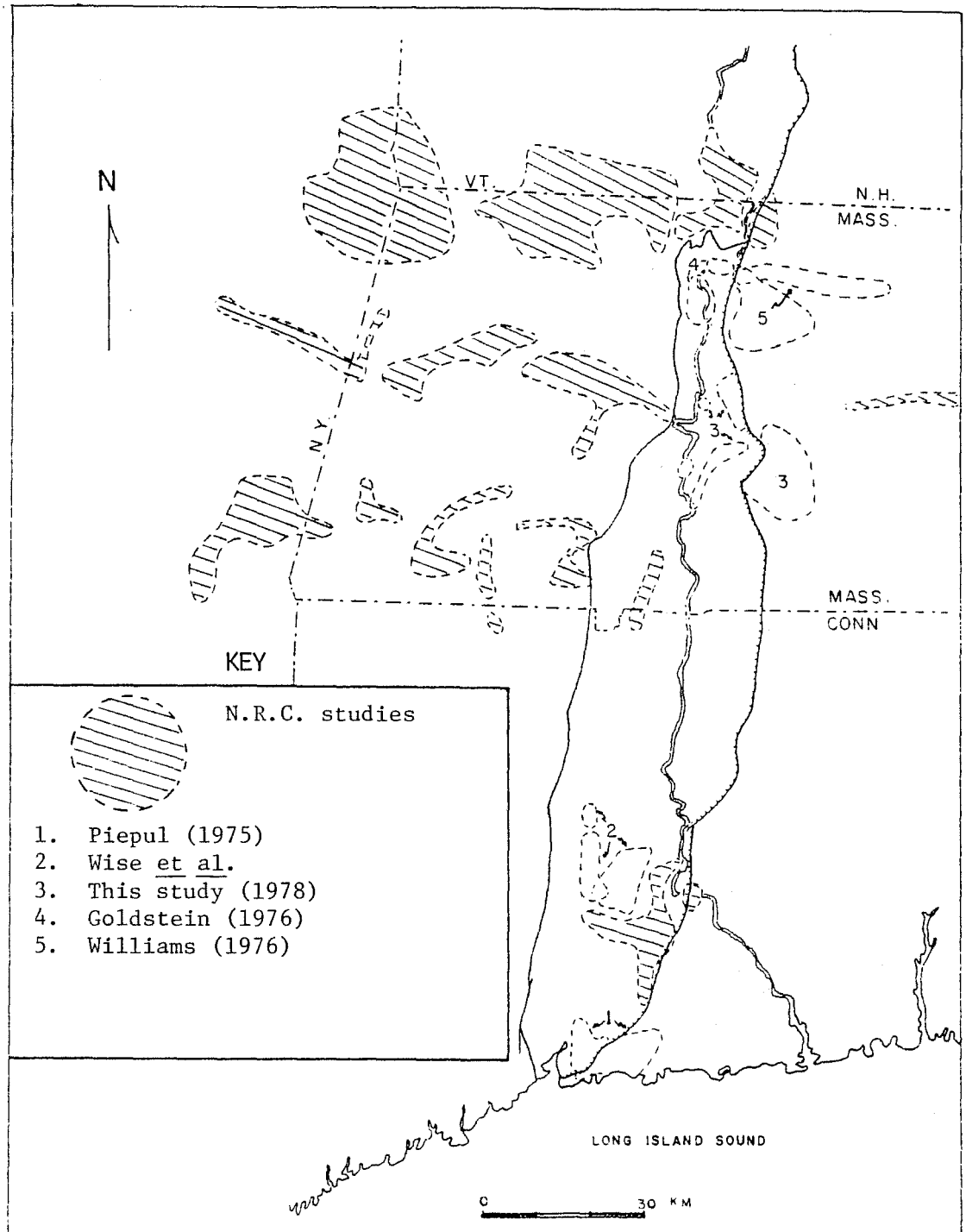

Figure 9. Location of fracture studies in western Massachusetts (from preliminary report to N.R.C., 1978).

of the border fault, that a pre-Mesozoic structural grain existed in the crystalline rocks and may have been related to the Paleozoic deformational history. Piepul's area shows predominantly dip-slip faulting in contrast to the western portion of the valley (Figure 10, from preliminary report to N.R.C., 1978). Piepul notes a pervasive N30E strike of almost all Mesozoic extensile features. He believes a northeast trending structural weakness of probable Paleozoic origin controlled the pattern of much of the faulting observed in the Mesozoic rocks. This faulting shows evidence of both northeast and northwest extension. Williams (1976), working in the west-central region of the Pelham Dome (Figure 9) found predominantly dip-slip faulting striking N30E over the area. His joints were relatively unsystematic in orientation. The nature of faulting observed in the studies above, this study, and those conducted by groups supported by the Nuclear Regulatory Commission can be summarized by the fault domain map in Figure 10.

Introduction to This Fracture Study

The principal stations from which most of the fracture data were collected are located in Figure 11 and described in Appendix IID. The study area as a whole is relatively devoid of outcrop which would be considered of adequate size for fracture stations (Goldstein, 1976). The ratio of joints to faults at most stations is also unusually low. Fracture data are analysed here by domain so that

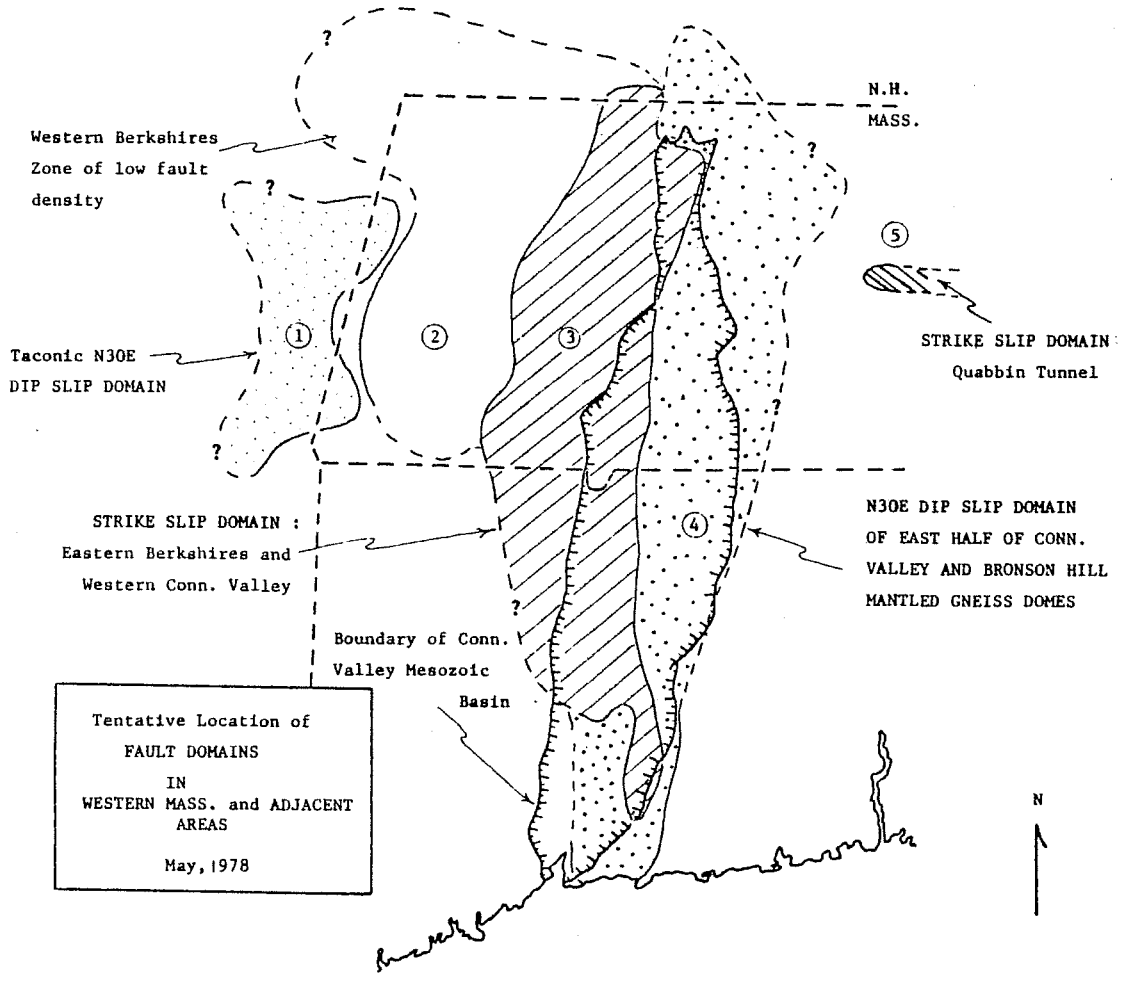

Figure 10. Fault domain map of western Massachusetts (from preliminary report to N.R.C., 1978).

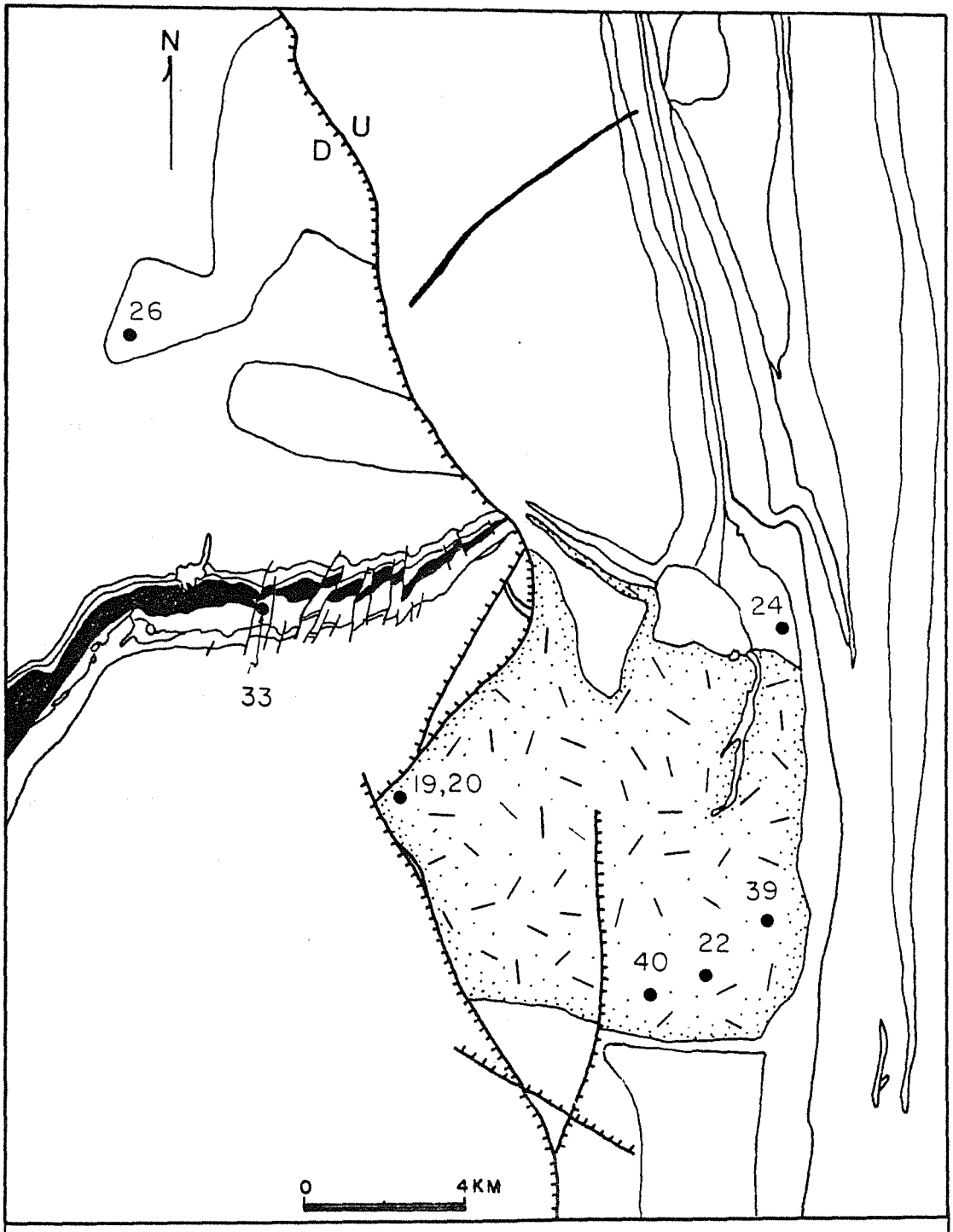

Figure 11. Generalized geologic map of the study area showing principal fracture station locations (Geology after Robinson, unpublished data, 1978).

patterns which exist can be isolated and interpreted in the context of their relative age and structural setting in the study area.

Cumulative fracture data. The study area lies in a domain of predominant dip-slip faulting characterizing the eastern margin of the Connecticut Valley (Figure 10). Cumulative fracture data for the entire study area are plotted on annotated equal-area nets in Figure 11a. and summarized here. All planar fracture data (dikes, veins, joints, and faults) for the area show a principal fracture maximum oriented N28E, 60°-80°NW with two minor sets, one oriented essentially north-south, 80°-90°W and another at N52W, 75°SW. Faults for the area show a dominant set oriented N24E, 55°-60°NW with minor fault sets oriented N3W, 80°-90°W; N15W, 35°W; N58W, 80°SW; and N65E, 65°NW. Rotation axes (σ_2) for these faults are essentially horizontal and trend primarily between N7E and N36E with a secondary set oriented around N45W, 25°SE. Slickensides show dip-slip motion in a predominantly S80W direction. Some minor maxima plunging to the north-northeast are due almost entirely to the station at Bagg Hill (Figure 11, stations 19 and 20) to be discussed later. Of the 208 faults observed, 70% were dip-slip whereas oblique-slip and strike-slip motions were each shown by only 15% of the faults.

All dikes and veins in the study area are essentially vertical and are oriented predominantly from N0E to N14E with the possibility that these constitute two separate maxima. The dikes and veins are quartzo-feldspathic in composition and are located almost entirely

within pre-Mesozoic rocks (Figure 12). Joints in the area show a principal maximum at N30E, 80°NW and two minor sets at N14E, 65°NW and N52W, 80SW. These joint sets correlate to some extent with raised-relief map and Landsat lineament maxima for the region (Wise and Goldstein, unpublished data, 1978).

Paleozoic and Mesozoic domains. These domains represent separation of data by stations located either in Paleozoic or Mesozoic age rocks (Figure 12). All planar fracture data for the Mesozoic domain (MD hereafter) are oriented between NOE, 85°W and N30E, 70°NW with the dominant set at N12E, 70°W. The Paleozoic domain (PD hereafter) in contrast shows a dominant fracture set oriented N30E, 60-85°NW and a minor set at N54W, 70SW. Faults in the MD are oriented predominantly between maxima at N3E, 80°W and N34E, 65°NW whereas in the PD, three distinct fault maxima are present oriented N24E, 55-80°NW; N56W, 70°SW; and N64E, 65°NW. Slickensides for faults in the MD showed predominantly dip-slip motion to the northwest whereas in the PD, motion is to the west-southwest, with minor motion to the northeast (due to Bagg Hill). Rotation axes (σ_2) for MD faults are predominantly horizontal and trend between N4E and N36E. In the PD, the rotation axes plunge 10-20°, with dominant trends at N86W, N16E, and N55W. Joints in the MD are slightly more randomly oriented than in the PD due largely to stations in well jointed basalt. Maxima are oriented N10E, 70°W; N39E, 70°NW; and N62E, 45°SE whereas joints in the PD are oriented predominantly N28E, 80°NW and N52W, 80°SW. Orientations of dikes and veins from

Figure 11a. Cumulative fracture data for the entire study area.

Annotation:

A. Data from "pre-Mesozoic" system.
B. Data from "pre-Mesoizoic" system.
C. Data from Mesozoic system.

Contouring varies as indicated.

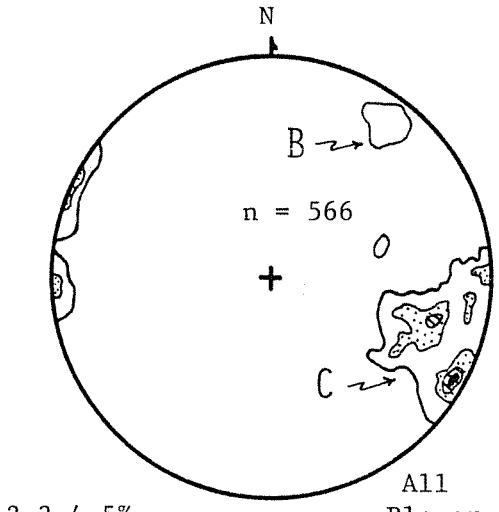

2,3,4,5%

All Planar Data

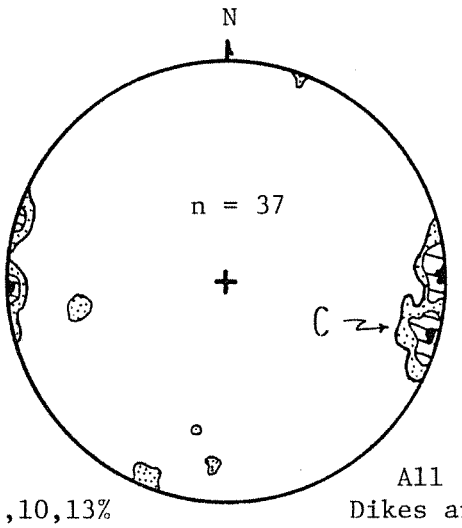

5,10,13%

All Dikes and Veins

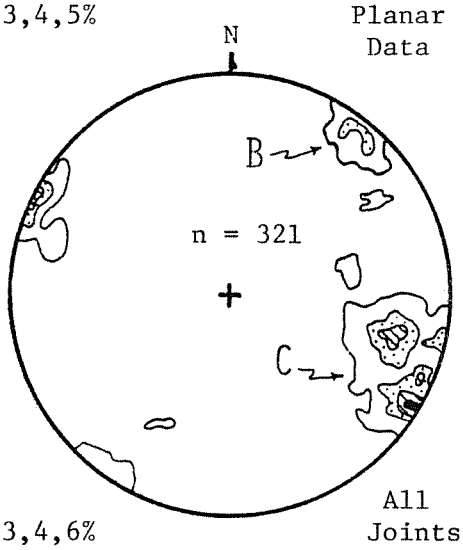

2,3,4,6%

All Joints

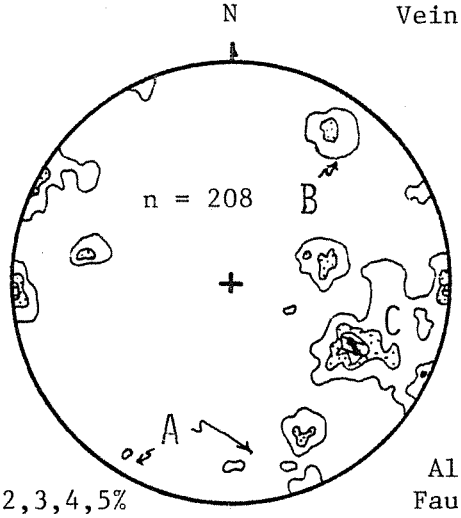

2,3,4,5%

All Faults

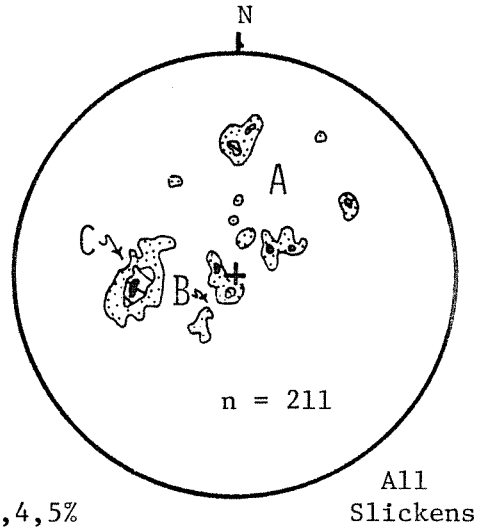

3,4,5%

All Slickensides

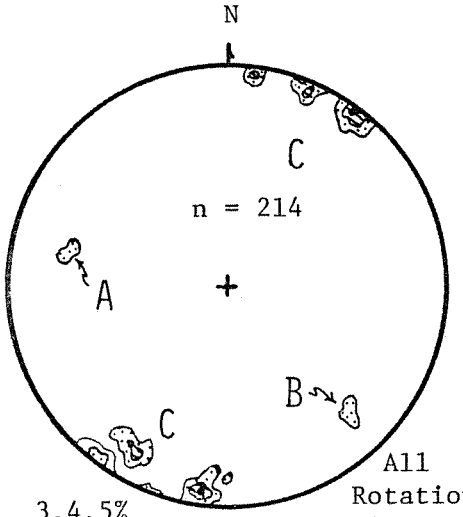

3,4,5%

All Rotation Axes

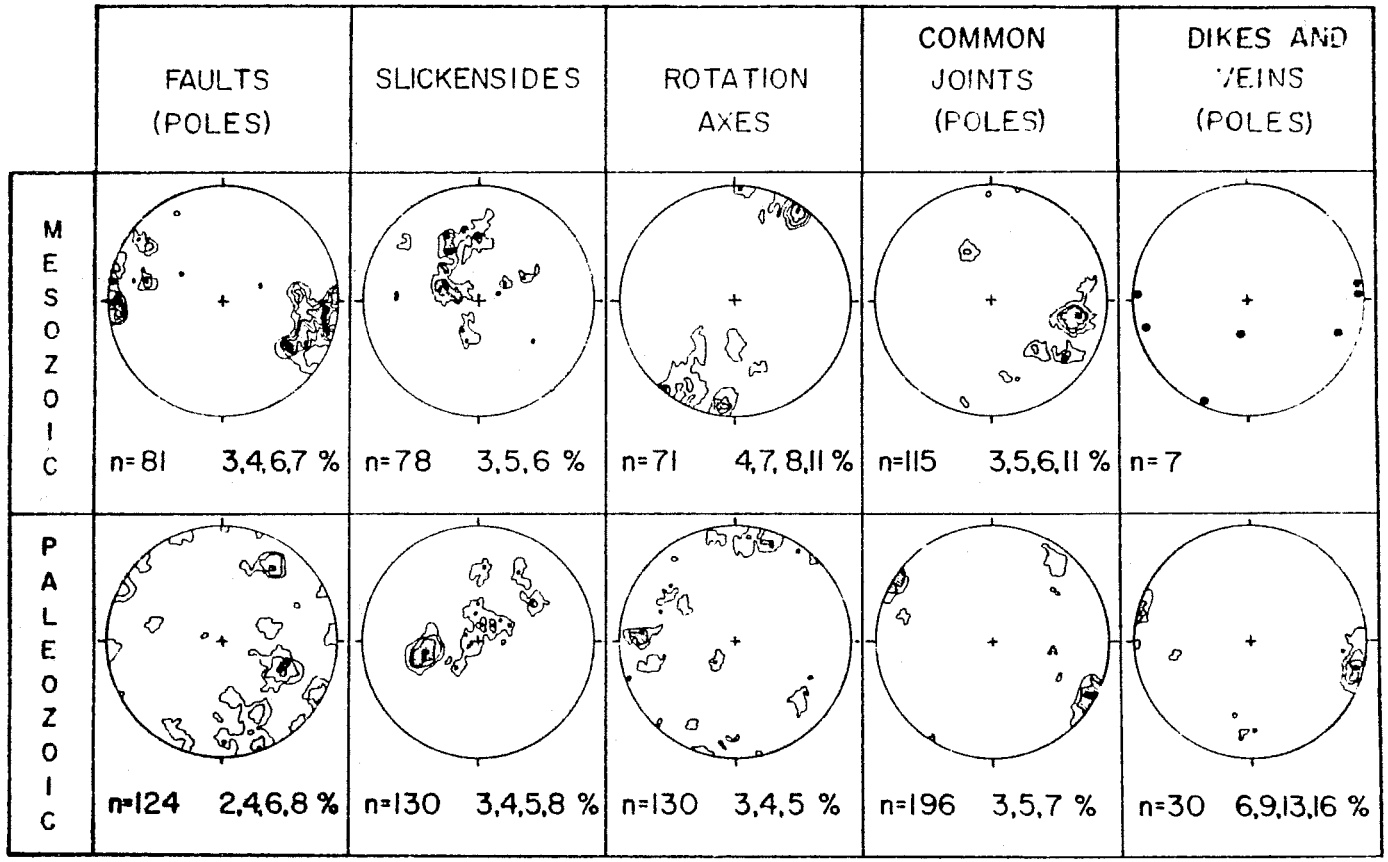

Figure 12. Separation, by lithologic age, of the cumulative fracture data for the Amherst-Belchertown region.

both domains are very similar, being nearly vertical and oriented between NOE and N14E.

Belchertown Intrusive Complex domain (BCD). Cumulative planar data from stations within the Belchertown Intrusive Complex (Appendix IIA) show essentially the same orientations as all planar data for the Paleozoic domain. Faults in the BCD show three dominant orientations at N28E, 55-80°NW; N57W, 70°SW and NE; and N66E, 65-80NW. Slickensides again show dip-slip motion to the west-southwest and to the northeast (Bagg Hill). Rotation axes (σ_2) are randomly oriented, but maxima do occur trending N84W, 15°W; N12E, horizontal; S76W, 20°W; and S48E, 20°SE.

Joints in the BCD show a well developed maximum oriented N28E, 80-90°NW with a number of poorly developed sets around N50W, 80°SW and 60NE. Dikes and veins measured were oriented N14E, vertical. It should be noted that joints in the Hatfield Pluton show two dominant sets, one oriented N50W and another at N60E (Stoeck, 1971).

Amherst Block domain. Cumulative fracture data for stations located in the Amherst Block are shown in Appendix IIB. Exposures of the block providing abundant fracture data are absent so that fracture orientations are not well represented on the nets.

Joints in the Amherst Block domain (ABD) show two dominant orientations at N45E, 80-90°NW and N53W, 80-90°SW. Faults have a wide range of orientations, but a dominant set oriented N32E, 45°NW is evident. Faults in the vicinity of Mt. Warner are oriented be-

tween NOW and N50W, 45-70°SW. Slickensides for the ABD show dominant dip-slip motion to the west-southwest, but also significant motion to the south and the southeast. The more south-southwest plunging set of slickensides correspond to the faults in the vicinity of Mt. Warner (station 26). Rotation axes (σ_2) show a dominant horizontal N30E trend as well as minor N4W and N45W trends again corresponding to the Mt. Warner faults.

Regional Stresses: Mechanisms, Timing, and Orientations

Mechanics. With some knowledge of the regional fracture patterns, it is possible to define further the orientation and timing of the stresses active over the study area. In order to interpret the stress field(s) which gave rise to the observed fracture patterns, it should be realized that: (1) in the upper level of the earth's crust, one principal stress must be normal to the surface, and (2) for homogeneous isotropic rocks, the intermediate principal stress (σ_2) will lie in the plane of a fault (Anderson, 1951). When rocks already cut by fractures are subjected to new stresses, new fractures will develop only where the stresses are oriented at highly oblique angles to the pre-existing fractures. For small angles, movement would be expected along the original fracture planes (Donath, 1962). The formation of initial fractures results in a complex alteration of the existing stress system as well as creating a new set of anisotropies. This in conjunction with pre-existing anisotropies makes accurate interpretation of the stress history of the study area

difficult and speculative.

Timing and orientations. Mesozoic age basaltic dikes in New England trend approximately N30E suggesting a regional σ_3 orientation around N60W during part of Mesozoic time (May, 1971; McHone, 1978, in press). Sanders (1963) notes two periods of igneous activity separated by a period of deformation in Early Mesozoic time, but there is still some uncertainty as to whether the basaltic dikes were emplaced during the Late Triassic-Early Jurassic period of valley formation or during a separate period of slightly earlier or later structural and igneous activity.

Examination of the annotated nets in Figure 10a. and comparison with nets from individual domains suggest that at least two distinct stress systems have been active over the region since Paleozoic time. A system of faults restricted to the pre-Mesozoic rocks and probably of pre-Late Triassic age had an intermediate principal stress (σ_2) orientation between N55W, 10-20^{o}SE and N86W, 10-20^{o}W with an average around N70W (Figure 11). The minimum principal stress, σ_3, for this system was oriented between N4E and N35E with an average around N20E, horizontal. The maximum principal stress, σ_1, would have been nearly vertical.

A system of probable Mesozoic age fractures is present over the entire study area in rocks of all ages. Dikes and veins recorded in the area are composed almost entirely of quartz and feldspar. Similarity in their composition and orientation within Paleozoic rocks and the existence of extensive silicified zones along the border fault, suggest

that the dikes and veins were injected during a latest Paleozoic or Early Mesozoic period of tectogenesis. Thus, they should be related to the stress field active at that time. The existence of quartz veins in rocks of Mesozoic age is evidence of later Mesozoic periods of injection. The orientations of the older dikes and veins between NOE and N14E suggest a N90W to N76W, horizontal orientation for σ_3 during this period. This orientation contrasts a N60W regional σ_3 orientation suggested by May (1971) on the basis of basaltic dikes. The difference may be due to the fact that the quartzo-feldspathic dikes and veins represent an older (latest Paleozoic to earliest Mesozoic) stress system whereas the basaltic dikes probably reflect a younger Mesozoic stress system. The gross radial pattern of the dikes around an early Atlantic, the basis for May's (1971) stress system, may suggest a σ_2 orientation around N30E. It could also represent the orientation of σ_1, depending on the broad scale mechanism involved in pre-Atlantic continental breakup and dike formation.

The orientation of the Mesozoic intermediate principal stress, σ_2, within the study area (from rotation axes of measured faults) falls between N4E and N36E with an average around N20E, horizontal. The range of measured orientations for σ_2 is interpreted as the result of rotation of the apparent stress trajectories by basement anisotropies. Consequently, the maximum principal stress, σ_1, would be essentially vertical. A large basaltic dike located near the southern end of the Pelham Dome (Figure 1a.) is oriented around N55E

(σ_2, and σ_3, N35W) suggesting that the eastern border zone and the neighboring basement anisotropies have had a decided effect in re-orienting principal stress trajectories.

This stress system was evidently in operation, at least in residual form, throughout most of the formation of the Mesozoic Connecticut Valley; propagation of the basement fractures upward into the late sedimentary rocks of the basin is evident. Reorientation of stresses and resulting fractures by existing anisotropies in the vicinity of the border fault and by the anisotropies present in the crystalline and sedimentary rocks, probably gave rise to the range of fracture orientations seen and the lack of distinct fracture maxima. However, the paucity of outcrops makes the testing of this hypothesis impractical.

To summarize, the study area is characterized by predominant dip-slip faulting (Figures 10 and 12a.). Considerable curvature of the σ_3 and σ_2 principal stress trajectories for both the Mesozoic and proposed pre-Mesozoic stress systems has taken place within the study area. For the probable pre-Mesozoic system, σ_2 was oriented around N70W, 10-20^{o}W and σ_3 around N20E, horizontal. The Mesozoic system shows an approximate 90^{o} rotation of the σ_2 and σ_3 stress trajectories. Rotation axes defining σ_2 are oriented around N20E, horizontal. Dike and fault orientations defining σ_3 are more variable but suggest an orientation between N90W and N60W, horizontal.

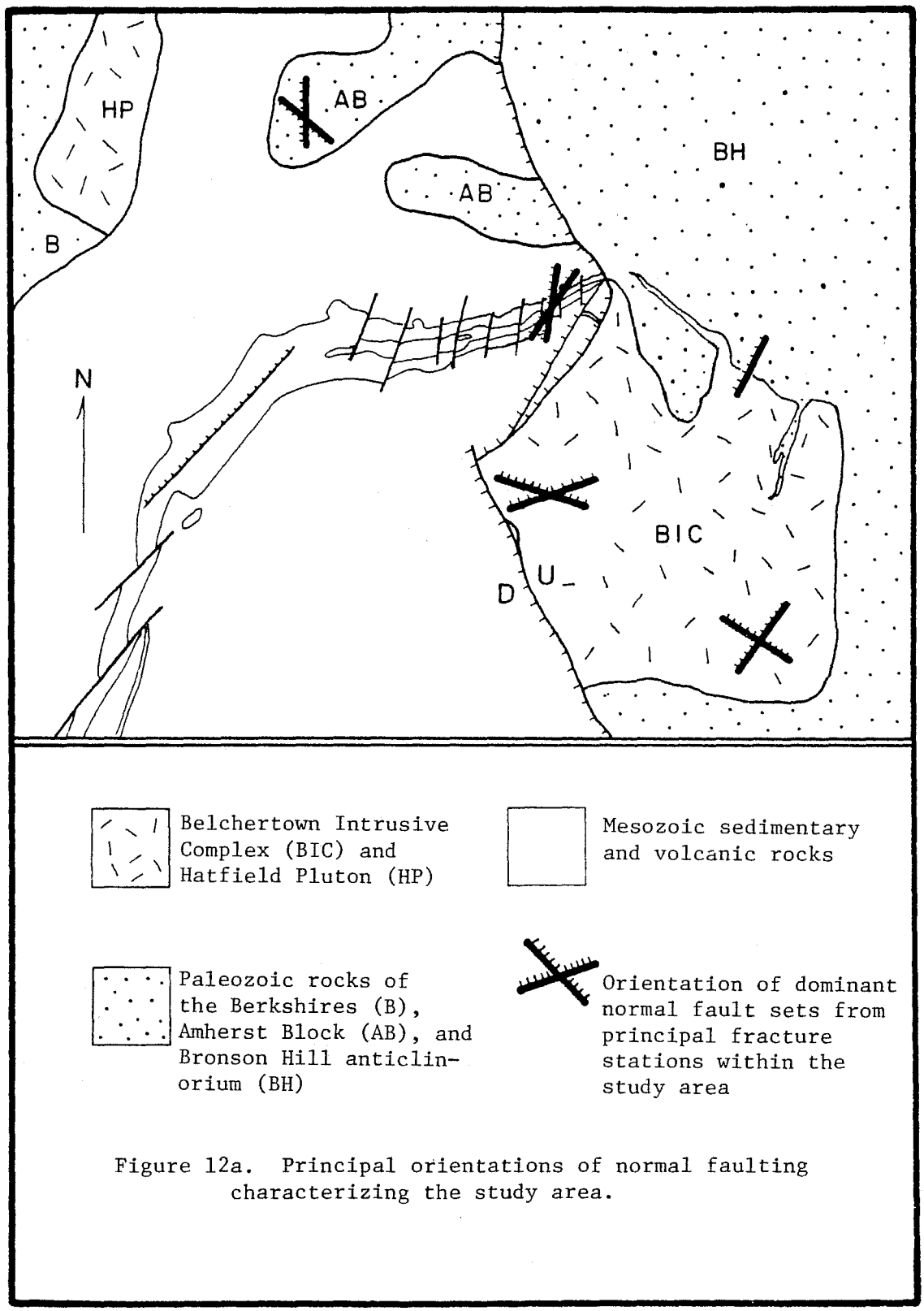

Figure 12a. Principal orientations of normal faulting characterizing the study area.

DEFORMATIONAL MODELS

Introduction

Having summarized some of the past deformational models and established the boundary conditions in previous sections, this section seeks to examine some possible new deformational models. Some of the basic facts to be incorporated into the models being considered are: the crustal extension environment, the predominance of dip-slip faults, their orientations, the warping effects of the Amherst Block on the basin fill, and the resulting dip patterns. Another factor to be considered is the possible development of the border fault as a series of splaying faults along the deeper boundaries of the domes and the Belchertown Intrusive Complex.

General Statement on Experimental Models

Most geologic processes are complex and extensive in terms of the time and space over which they operate. It is this factor that makes them difficult or impossible to observe. In an effort to understand these processes, geologists commonly have utilized operational scale models. The value of scale models is perhaps best characterized by Beloussov (1961):

> "Observation of scale models used to simulate tectonic processes helps sharpen the geologist's perception of real geologic structures and to check some of the deductions that result from observations made in the field . . . experimental tectonics has thus come to serve as an important supplement to classical geologic method. In many cases it

> can explain aspects of tectonic processes that are unaccessible to these methods, and it can open the geologist's eyes to important details in these processes that he might otherwise overlook."

The problems which inevitably arise in constructing a true scale model involve the conditions of similarity between model and prototype (Hubbert, 1937; Gzovsky, 1959). In determining the properties of the model materials and surrounding conditions necessary to construct and operate the model, all known properties of the prototype must be considered. The nature and deformational behavior of the rocks as well as time factors and the duration of tectonic stresses are just a few of the properties that must be considered in order to assure a valid scale model (Currie, 1966).

It is precisely this requirement that makes application of true scale modeling to the Connecticut Valley impractical if not impossible. The wide range of rock types, multiple periods of deformation, and complex stress systems that have been active over western Massachusetts would be difficult to reconstruct with conventional model materials under any laboratory conditions. Rather, a series of simple sand models have been used as geometric demonstrations of possible fracture systems resulting from proposed stress and anisotropy orientations. The limited extent of scaling done for these models is discussed in the next section.

Sand Model Experiments

Purpose. A series of sand model experiments were run to provide some understanding of the processes by which fracture patterns may

have developed during initial valley formation and the behavior of these fractures as they encountered an anisotropy. The value of these experiments does not lie in the possibility of duplicating known fracture patterns, but in the experience gained in detecting relationships between cause and effect in fracture behavior near an anisoptropy.

Materials and equipment. The usefulness of granular materials, e.g., sands and clays, in constructing models displaying fracture development has been well established (Bain, 1954; Cloos, 1955; Currie, 1966; Nettleton et al., 1947; Oertel, 1965; Sanford, 1959). Materials used in this study were powdered limestone and sand passed through a #18 (1mm) sieve. The models were constructed on the extension table described in Figure 13. This table was designed and constructed by a fellow student, Bert Stromquist, and modified slightly by the author for the purpose of this study.

Experiments and results. Time sequential photographic results of some of the more significant sand model experiments are shown here. A schematic representation of the internal composition and geometry for the model accompanies each sequence of photographs, along with reasons for specific starting geometries, extension directions, and a brief discussion of the significance of the results.

Model 8, shown in the following sequence of photographs, is perhaps the most significant. The source and direction of extension, and the starting geometry are shown in Figure 14. The model was constructed in a wooden frame from damp (5cc water/500cc dry sand)

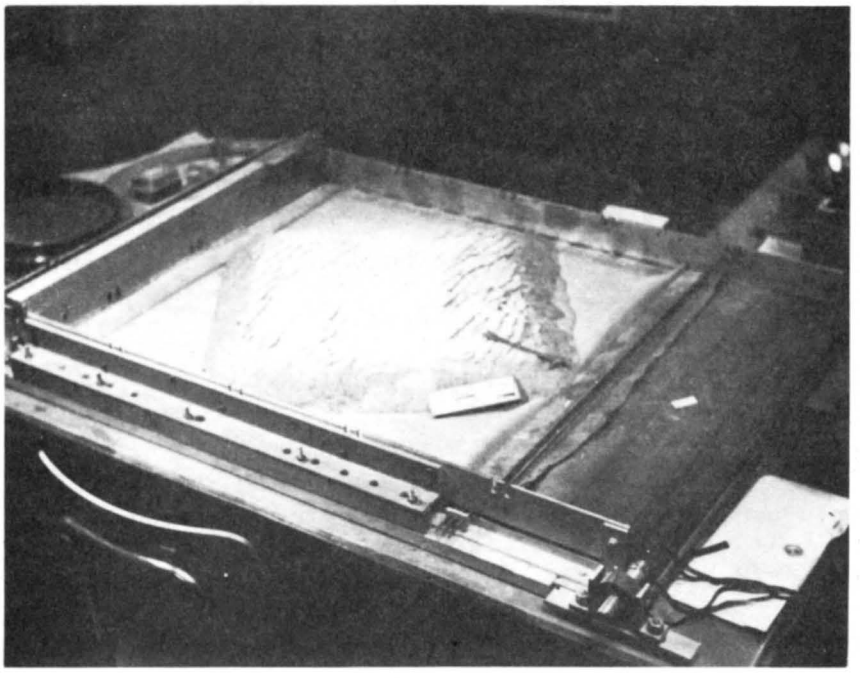

Figure 13. Extension Table Set-up: Sand models were constructed on a rubber sheet which could be stretched by means of a geared motor. The rubber was solidly fixed at one end and attached to a canvas sheet at the other. The canvas was slowly rolled onto a metal rod turned by the geared motor. The sides of the rubber sheet were restrained by attached metal runners which limited compression in the direction perpendicular to the direction of extension.

and dry sand, and dusted with powdered limestone to accentuate fracture development. The dry-damp sand boundary created a strength anisoptropy in the model, the geometry of which, at depth, was meant to be roughly analogous to the boundary between the medium to high grade metamorphic zone of gneiss domes (orientation of dome limbs and foliation = damp sand). Dry sand represented the low grade biotite-chlorite zone underlying the region in which the Connecticut Valley would eventually form.

Although not a true scale model, some attention was paid to scale factors. If 30 km is chosen for the present width of the Connecticut Valley and a depth of 15 km corresponds to the deep crustal boundary marking flattening of listric faults at the transition from brittle to ductile deformation, then the ratio between the two dimensions is 2 to 1. Therefore, in model 8, for a sand pile height of 4 cm above the rubber sheet (analog: deep crustal boundary), a zone 8 cm wide corresponds to the width of the region in which the valley would initiate.

The model was oriented on the extension table so that the relationship between source of extension and dip direction of listric faulting would agree with the findings of Cloos (1955). In short, Cloos noted that in clay model experiments, listric faults would form dipping toward the source of extension.

The sequential results of sand model experiment #8 are shown in Figures 14a, b, c, d, e, and f. A N60W extension direction (σ_3) gives rise to faulting oriented N30E. The most significant result is the

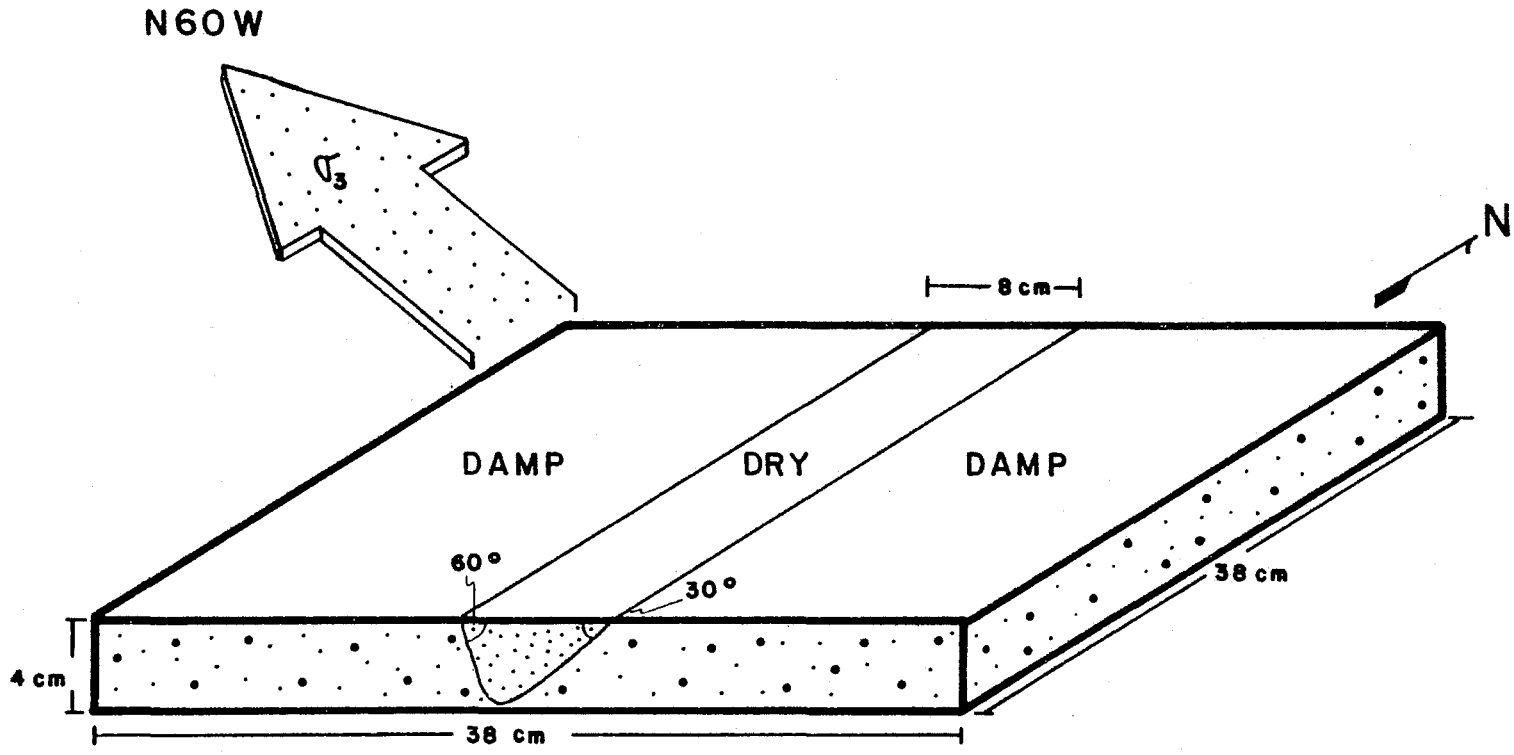

Figure 14. Schematic diagram of the starting geometry for model 8.

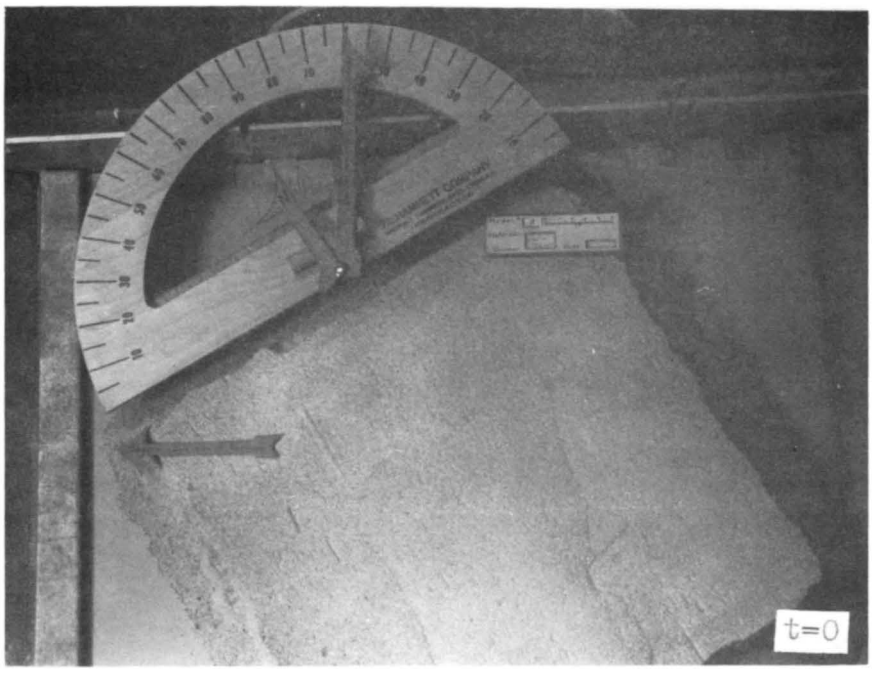

Figure 14a. Initial set-up for model 8.

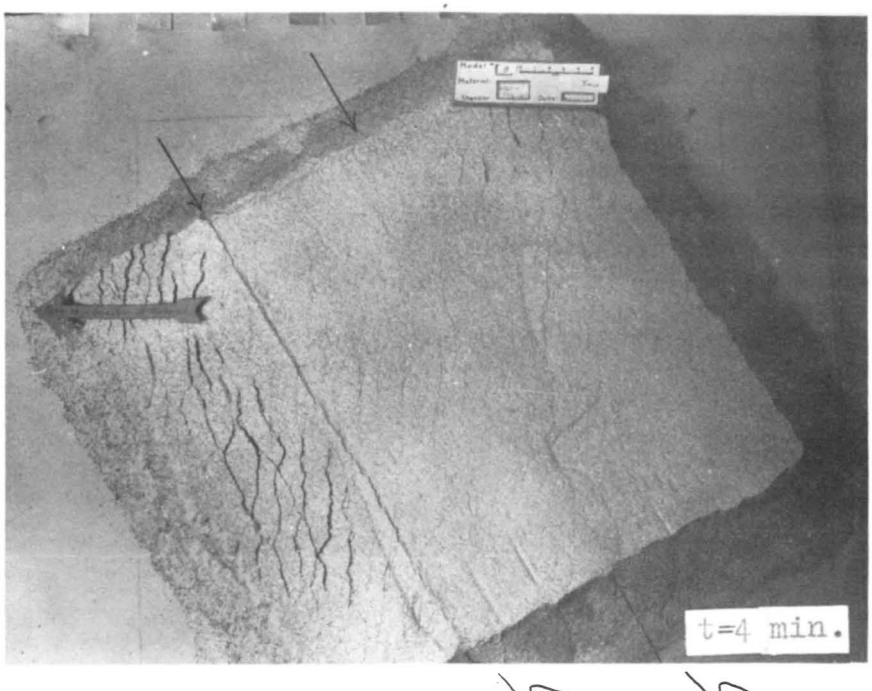

Figure 14b. Rubber sheet extended 6% (assumes linear rate of extension).

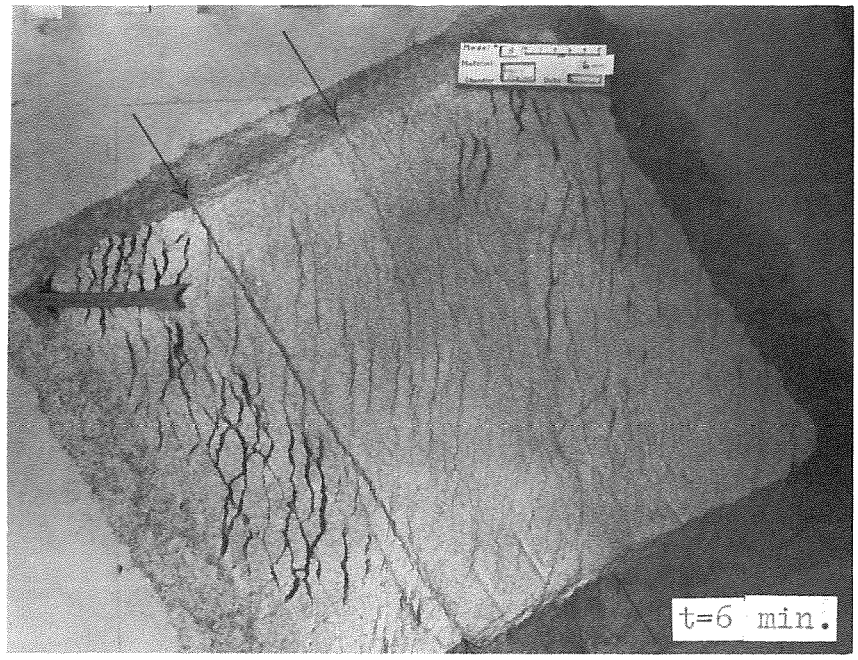

Figure 14c. Rubber sheet extended 9%.

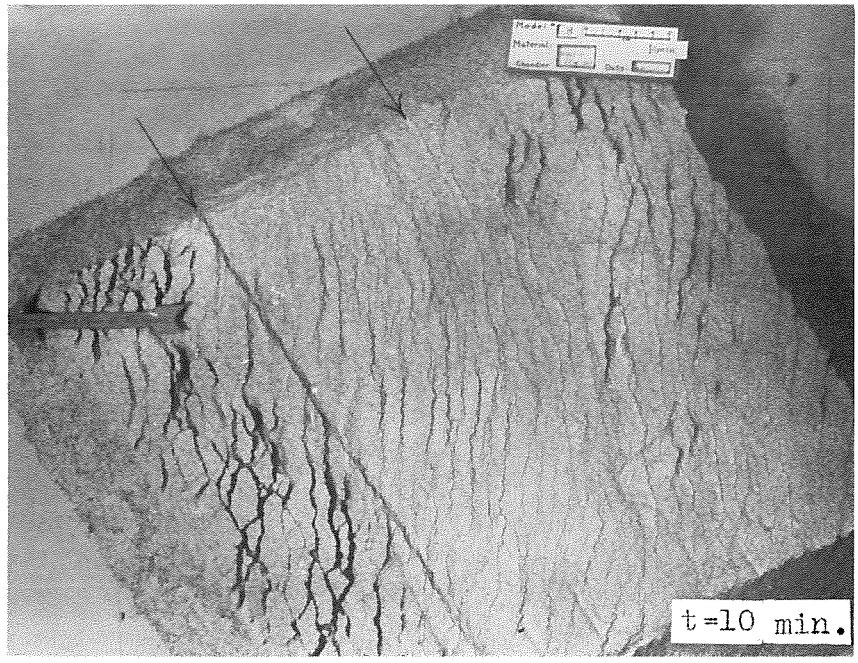

Figure 14d. Rubber sheet extended 15%.

Final stages of deformation.

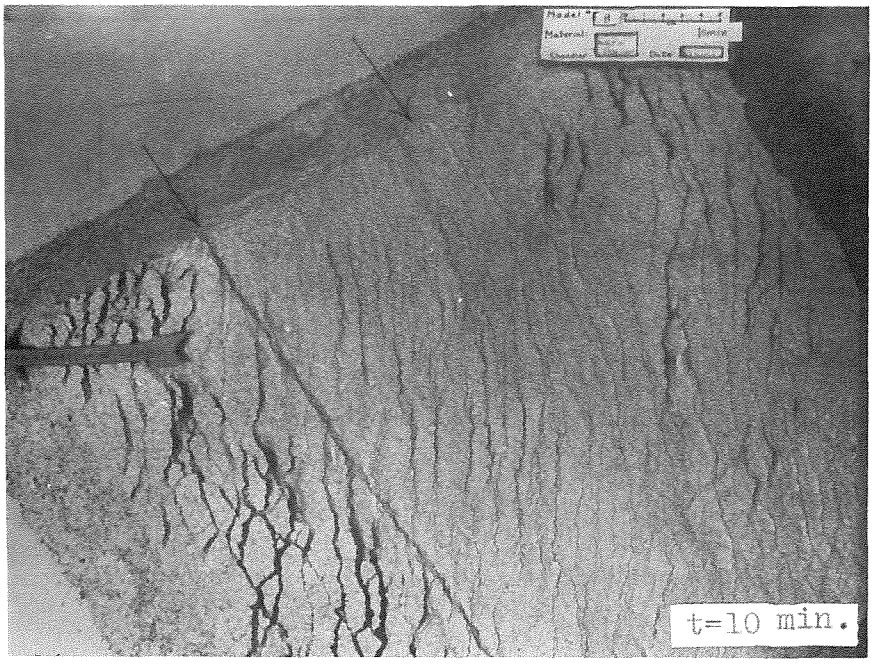

Figure 14e. Final deformation of model 8, 15% extension.

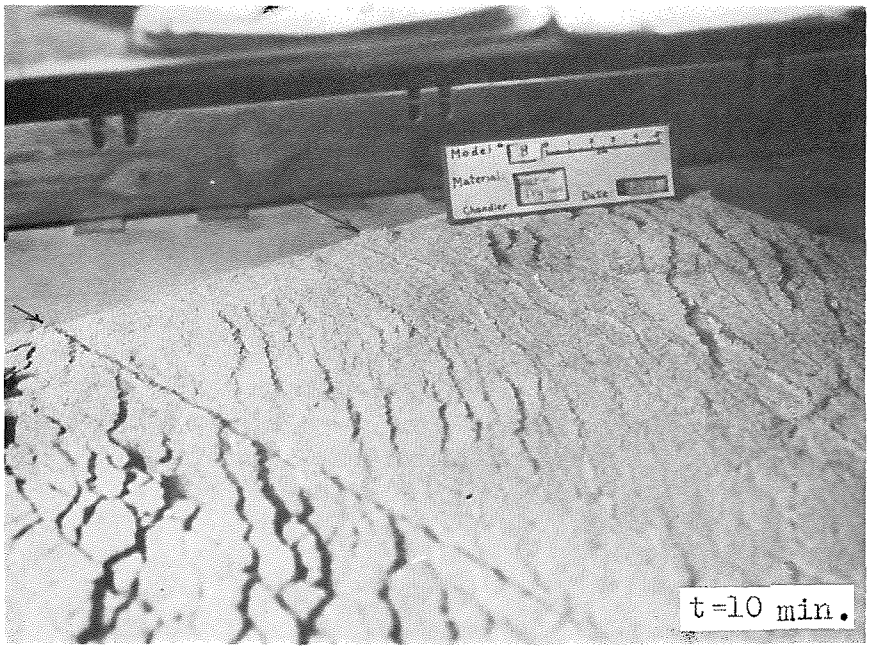

Figure 14f. Oblique view of the results of model 8 showing en echelon nature of faulting along eastern 30° dry-damp sand boundary. Rubber sheet extended 15%.

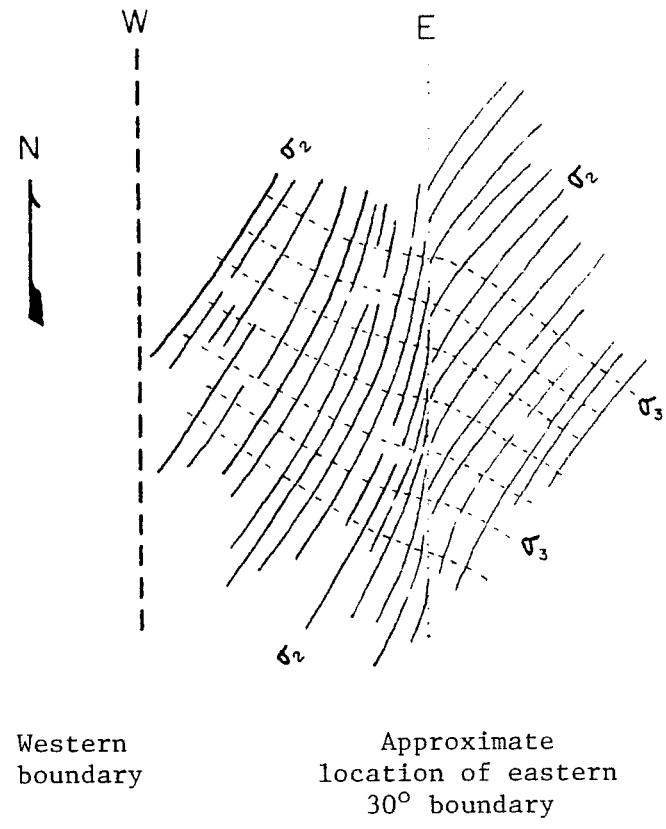

Figure 14g. Sketch showing curvature of σ_3 and σ_2 stress trajectories in model 8.

behavior of these fractures as they encounter the 30° dipping dry-damp sand boundary. There is a decided curvature of the fractures and of the corresponding stress trajectories, σ_3 and σ_2 (Figure 14g), near the surface trace of the 30° dipping boundary. The curvature of these fractures from a N30E trend to a more en echelon north-south trend in the vicinity of the wet-dry boundary, strongly suggests that the eastern border fault may have initiated, not as a continuous fault, but as a series of en echelon listric faults dipping toward the source of extension, stepping up the anisotropy created by the domes and complex, and controlled by their surface and subsurface geometry.

The range of Mesozoic fractures and apparent stress orientations seen in the study area may have originated from just the type of fracture behavior seen in model 8. The gradual curvature of fractures as they encounter the anisotropic boundary could account for the lack of distinct fracture orientation maxima evident in Figure 11a. It should be noted that the major displacement which occurred along the western 60° boundary in model 8 differs from the prototype in that the present western boundary of the valley was a zone of local steepening and minor faulting of the unconformity (Wheeler, 1937; Hubert et al., 1978).

Model 5

This model was one of the initial experiments run to test the effects of various wetnesses on material strength and the effects of

the orientation of the anisotropy to the direction of extension (Figure 15). Here, "wet" sand consists of 25cc of water/500cc of dry sand, and "damp" sand consists of 15cc water/500cc sand. The geometry of model 5 differs from that of model 8 only in the degree of wetness used and in the dimensions of the dry sand region shown in the accompanying drawing (Figure 15). By orienting the model so that extension would occur S60E, the processes of development of N30E fractures could be observed.

Results and conclusions. The results of model experiment #5 are shown in sequential order in the accompanying photographs (Figures 15a, b) for time t = 0,2,5 and 10 minutes (extension: 0,3,7.5, and 15%) proceeding from left to right. Note first how faults and graben turn from N30E to north-south and then back to N30E once they have propagated some distance along the anisotropy. The fracture behavior here is similar to that observed in model 8. The development of an extensive system of grabens in the dry sand is most likely due to the effect of opening up cracks in the stronger underlying wet sand.

One final type of fracture behavior can be pointed out here. The 60^{o} dipping boundary forms a distinct discontinuity sufficient to cause faults entering the boundary from outside the dry sand zone to turn toward it rather than turning parallel to it as seen along the 30^{o} dipping boundary.

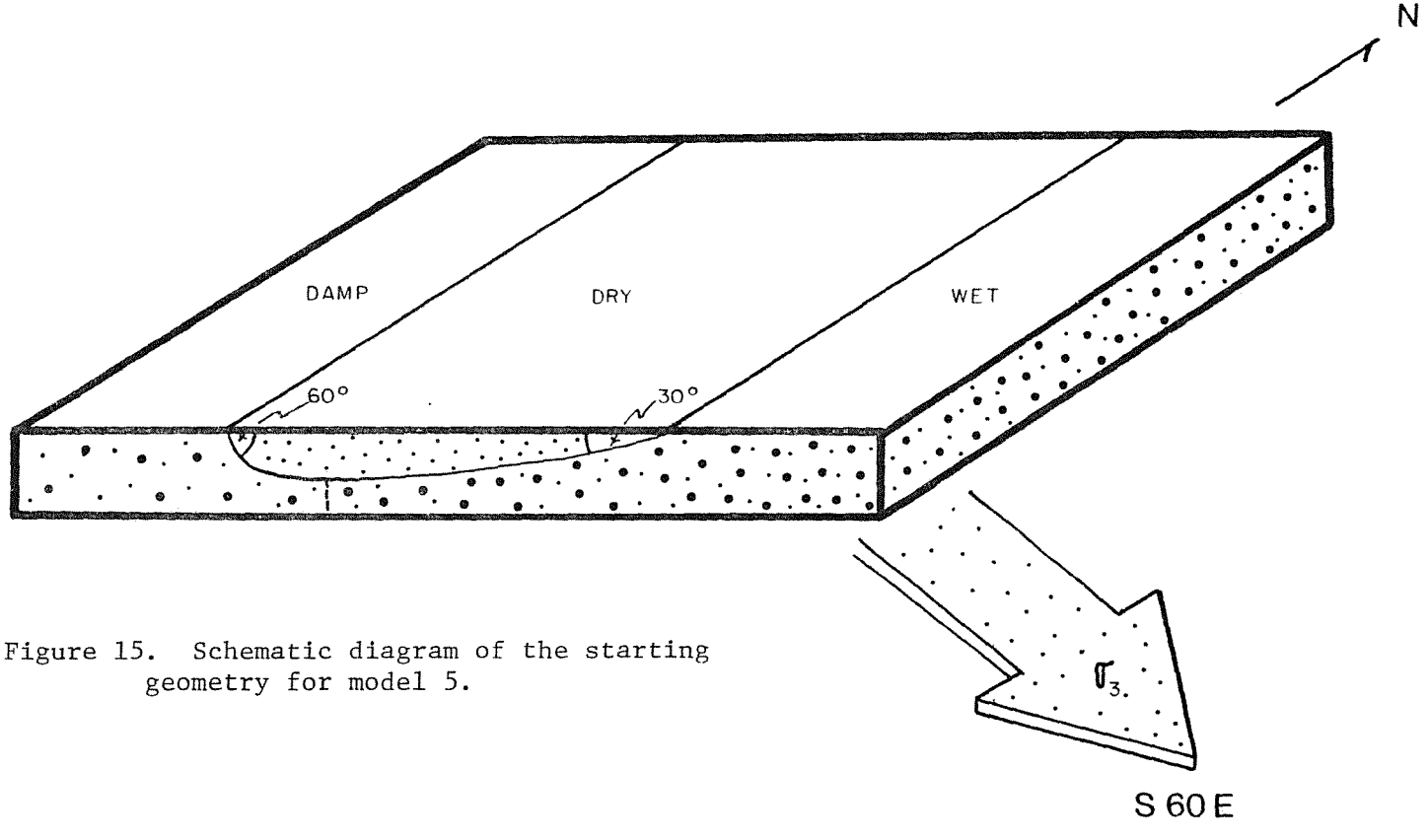

Figure 15. Schematic diagram of the starting geometry for model 5.

Figure 15a. Model 5

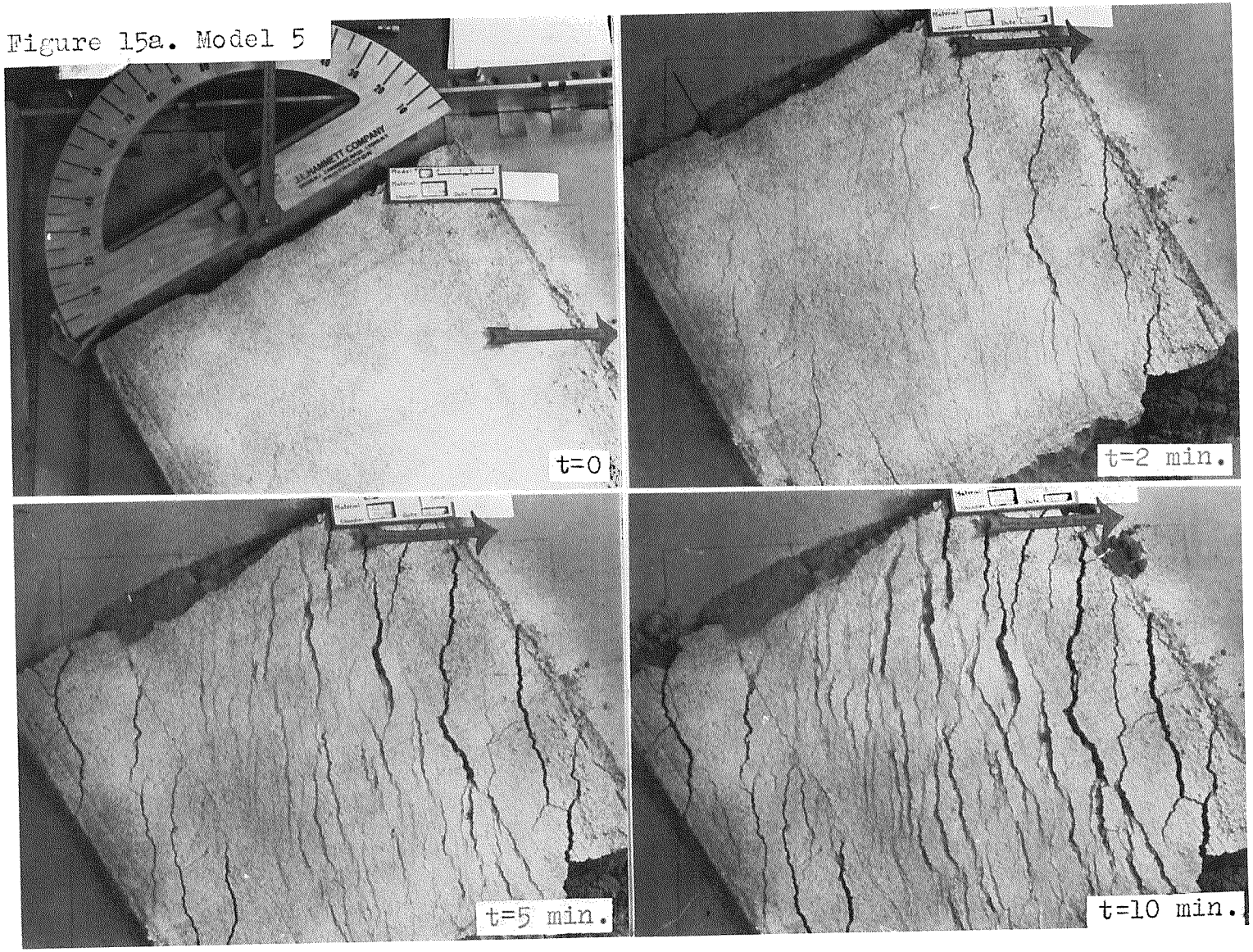

Figure 15b.

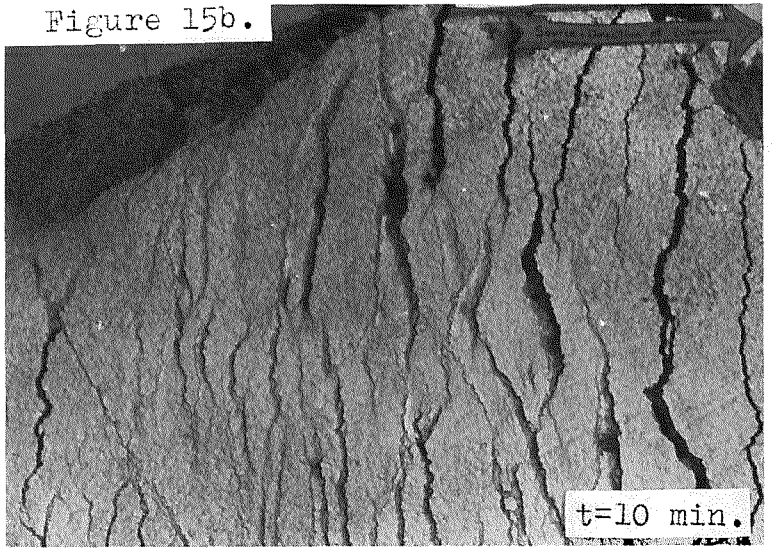

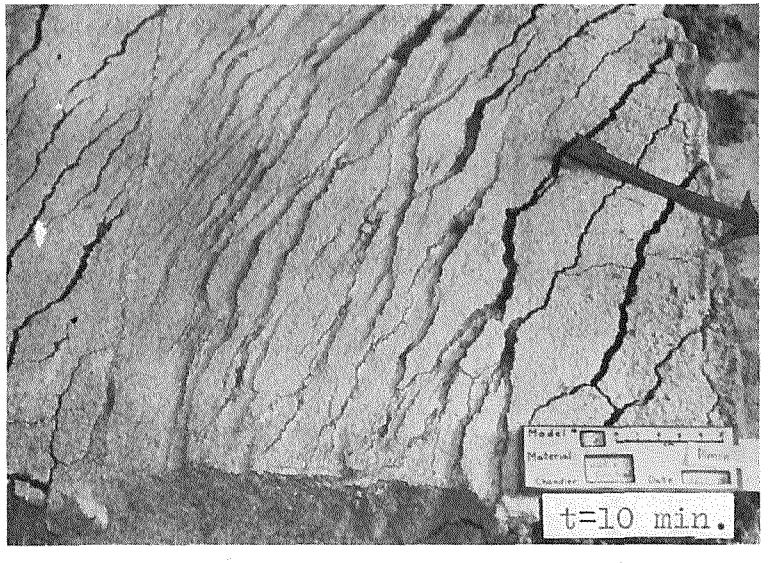

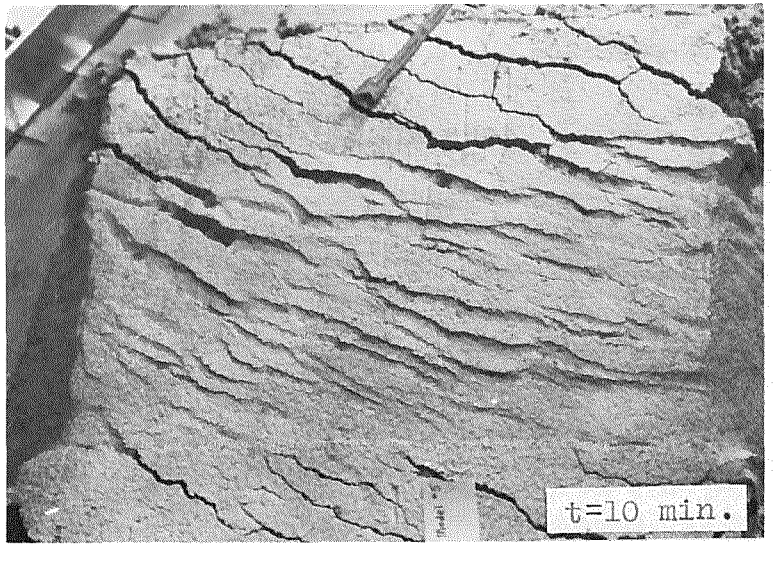

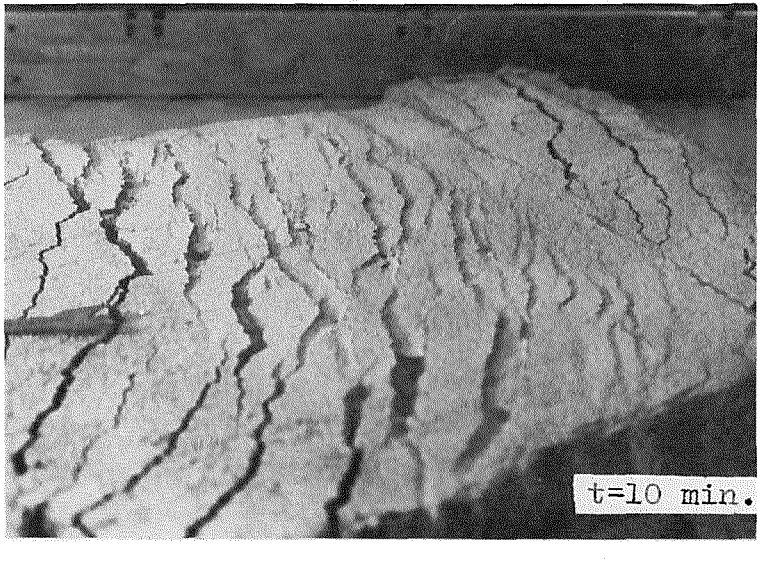

Model 9

The geometry of model 9 is essentially the same as model 8 with the addition of a "damp" sand (now 5cc water/500cc sand) transverse ridge trending N55W across the dry sand zone (Figure 16). The ridge is 3 cm wide with a dip of 60^{o} on its flanks. The purpose of this modification in geometry is to create a structural situation similar to that which may have existed between the Deerfield and Hartford basins prior to and/or during initial valley formation. Observation of fracture behavior here may offer some insight into the effects of such a structure on internal graben mechanics and deformation.

Results and conclusions. The sequence of photographs (Figures 16a, b) for time t = 0, 2, 4, 6, and 10 minutes (extension: 3, 6, 9, and 15%) shows three things:

1. The development in the ridge of grabens which propagate into the weaker dry sand and become less well defined.

2. The en echelon nature of faulting along the eastern 30^{o} dipping anisotropy.

3. Fault displacement along the N55W trending sides of the ridge.

This model reflects some of the deformative behavior previously discussed in the text and in the block diagrams to follow.

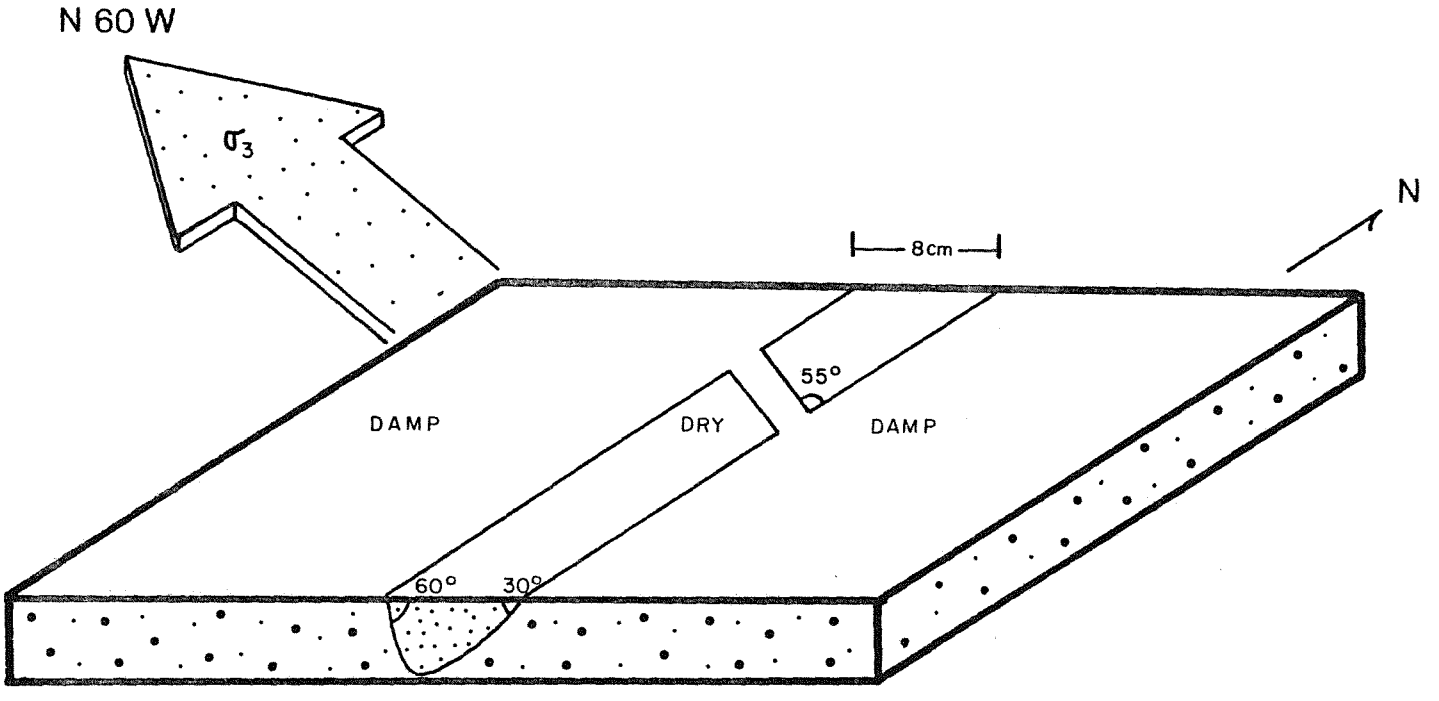

Figure 16. Schematic diagram showing starting geometry for model 9.

Figure 16a. Model 9

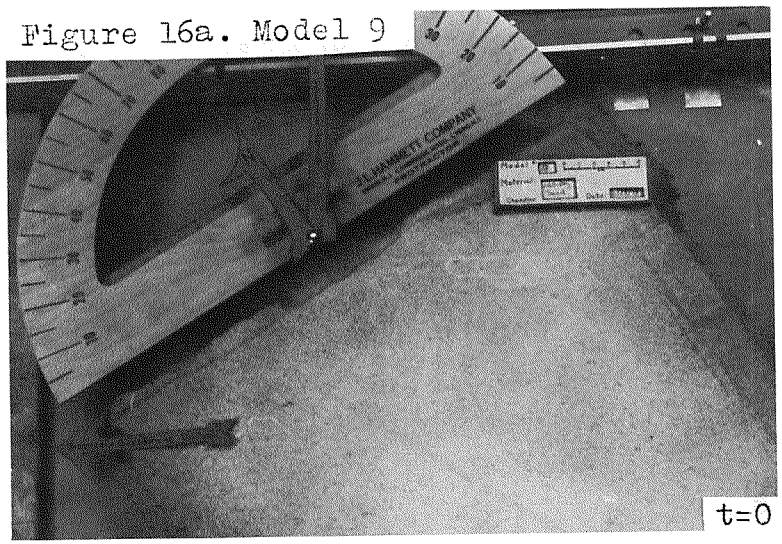

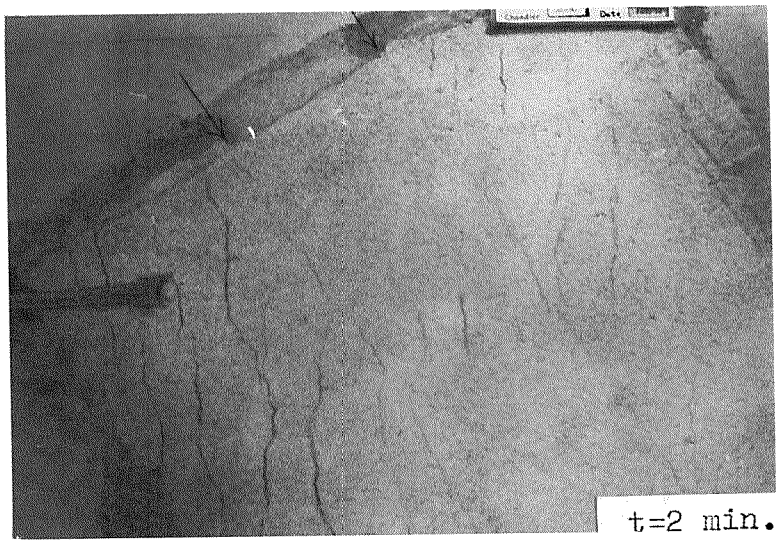

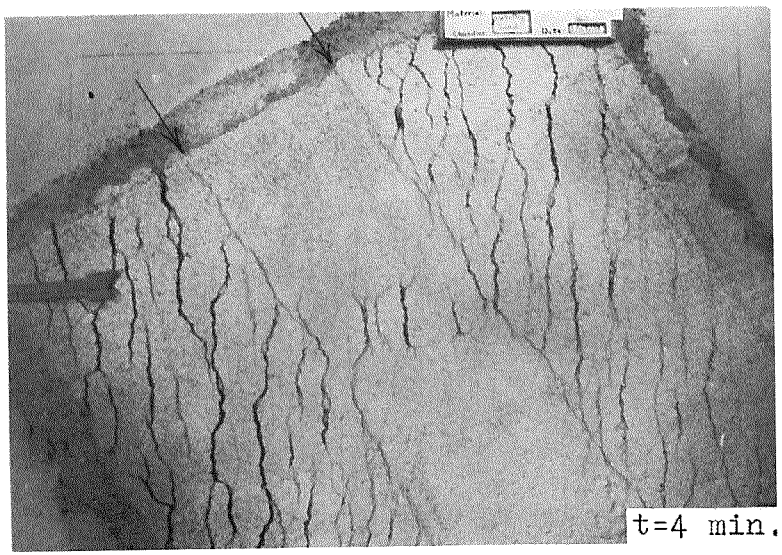

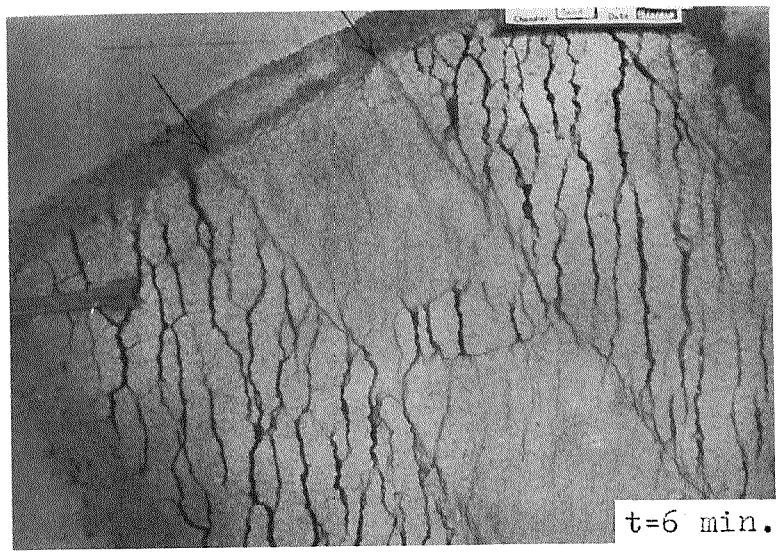

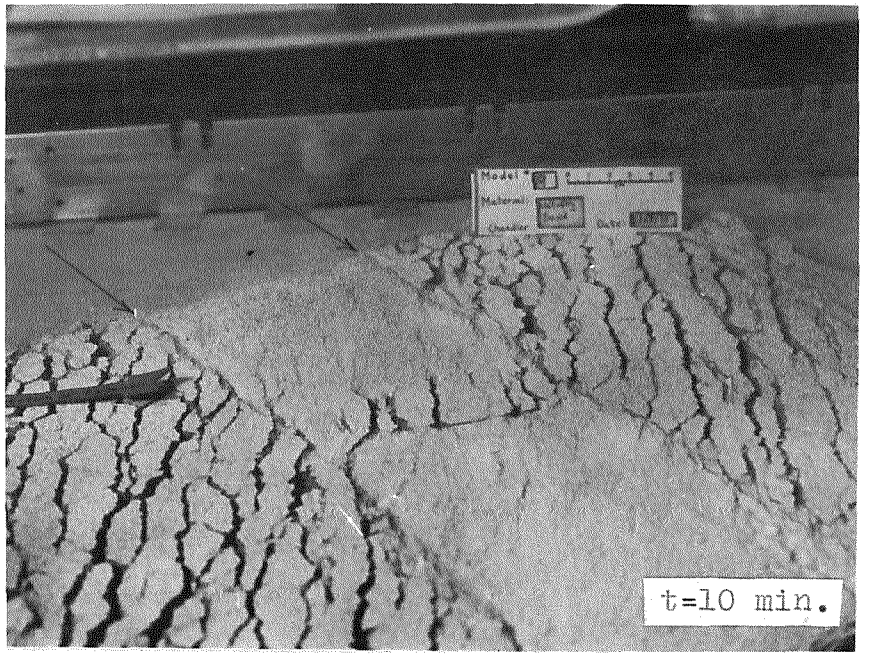

Figure 16b. Oblique view of model 9 showing displacement along flanks of transverse ridge.

Summary: A Possible Deformational Model

The data examined and the speculations made in this and previous sections are best summarized in a series of block diagrams depicting what the author feels may have been the sequence of development of the Connecticut Valley and related structures in the Amherst-Belchertown region. The sequence of diagrams shown in Figures 17a, b, c, d, and e, are captioned and described in the accompanying text. All diagrams are shown with basin fill removed and erosion of the eastern highlands continuous throughout. However, the pre-Triassic erosion surface that was present during the time shown in Figures 17a, b has been removed for reasons of clarity. Erosional unroofing of the Belchertown Intrusive Complex probably occurred somewhere during the time shown in Figures 17b and 17c.

BLOCK DIAGRAMS SHOWING

EVOLUTION OF THE CONNECTICUT VALLEY

STRUCTURES IN THE AMHERST-BELCHERTOWN

REGION

(Figures: 17a, b, c, d, and e)

Description: Figure 17a.

This schematic diagram shows the probable geologic setting of the study area during initial rifting. Note proposed continuation of the Belchertown Intrusive Complex across valley. Extension N60W (S60E) has begun with development of a N30E fracture set resulting in some minor displacement along the N55-70W "pre-Mesozoic" fracture set. Note the curvature of the originally N30E fractures to a more north-south trend as the elements forming the basement anisotropy (domes and complex) are encountered.

Description: Figure 17b.

Rifting is now well developed as the eastern border zone of the valley is initiated as a series of en echelon, splaying listric faults controlled by the anisotropies in the basement rocks. Displacement continues along the N55-70W "pre-Mesozoic" fracture set as the valley subsides.

Description: Figure 17c.

Probable first appearance of the Holyoke Basalt by extrusion occurred during this period. The valley continues to subside with further splaying and fault development. The telescope view accompanying the diagram shows the Holyoke Basalt and other valley fill superimposed on the crystalline rocks along the indicated line of sight.

Description: Figure 17d.

Differential subsidence of the valley initiates warping (flexuring) of the edge of the Holyoke Basalt. Major displacements along the "pre-Mesozoic" fracture set occur with probable initiation of a left-lateral shear couple at this time (Wise, personal communication, 1978). The transverse Amherst Block also manifests itself at this time, with Mt. Warner representing a surface expression of the block piercing the basin fill.

Description: Figure 17e.

The Connecticut Valley as it might appear today with the basin fill removed. The basement configuration that may have given rise to the apparent "bend" in the Holyoke Range is shown. Alternatives exist for the age and mode of formation of the N55-70W faults, shown here as resulting from tectonic heredity. It is conceivable that the N55-70W fractures are merely the orthogonal partners (Poisson effect) to the N30E fractures, both having been derived from the same Mesozoic age stress system. The anisotropy created by the Belchertown Intrusive Complex and its possible continuation across the valley may also have influenced the development of the N55-70W fractures.

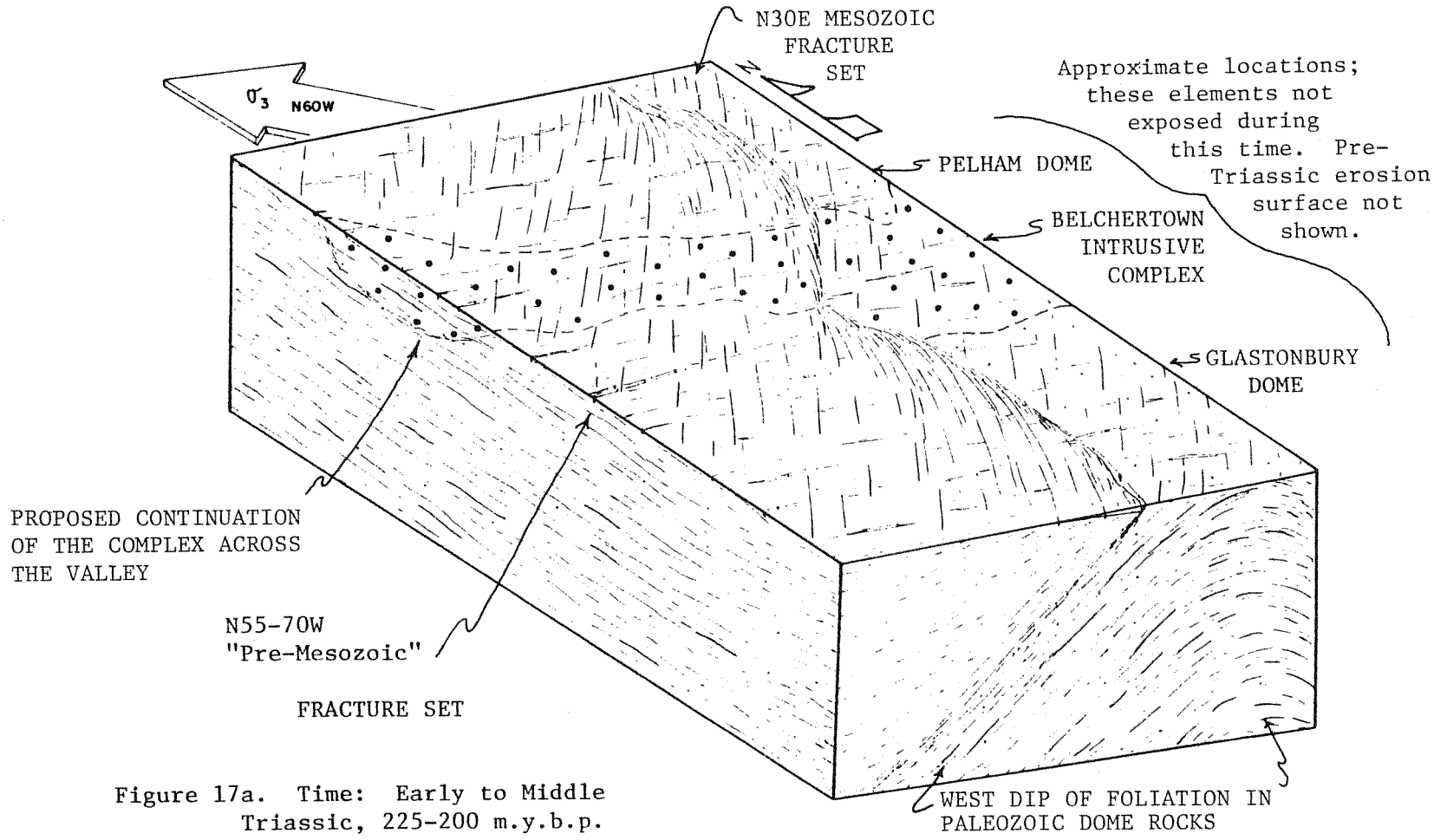

Figure 17a. Time: Early to Middle Triassic, 225-200 m.y.b.p.

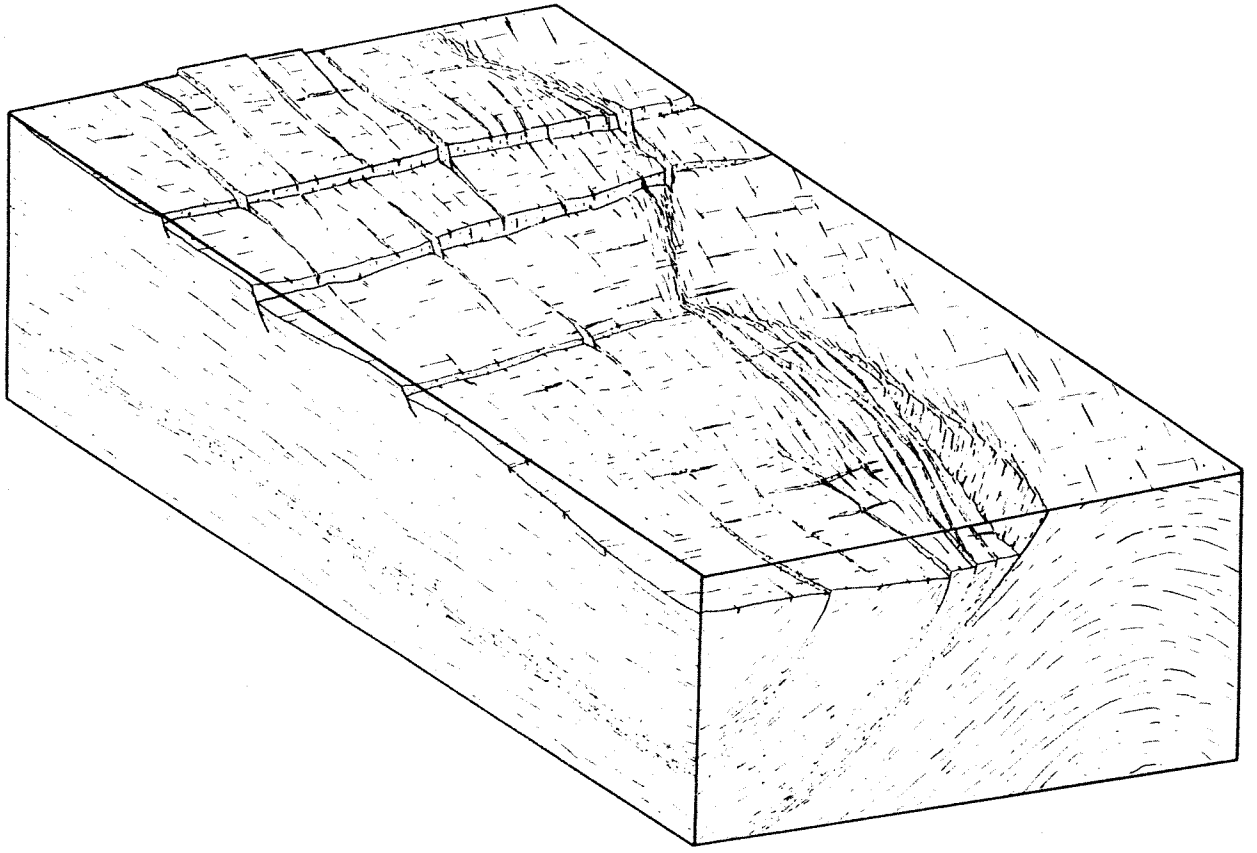

Figure 17b. Time: Late Triassic, 195-190 m.y.b.p.

Figure 17c. Time: Latest Triassic to Early Jurassic, 190-180 m.y.b.p.

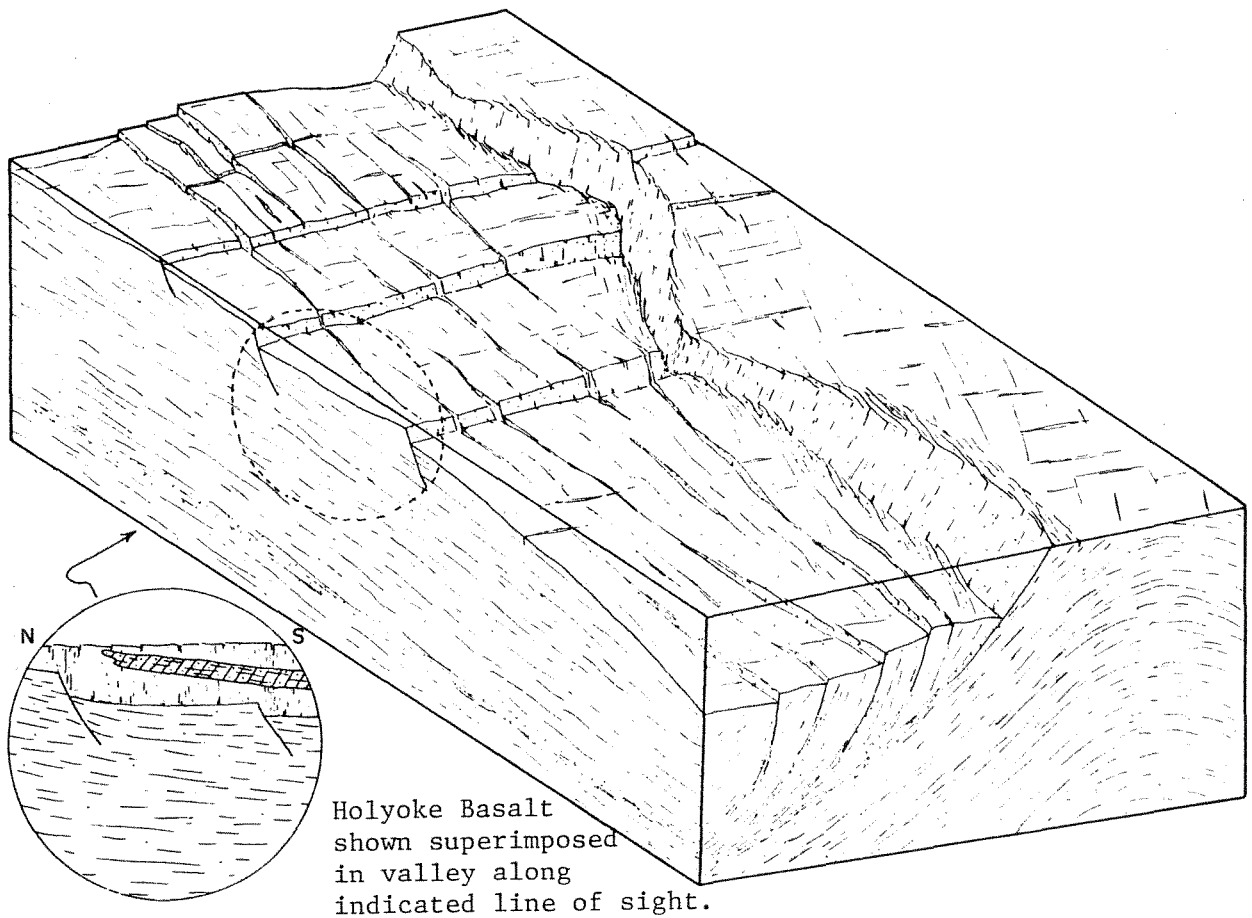

Figure 17d. Time: Early Jurassic, 180-175 m.y.b.p.

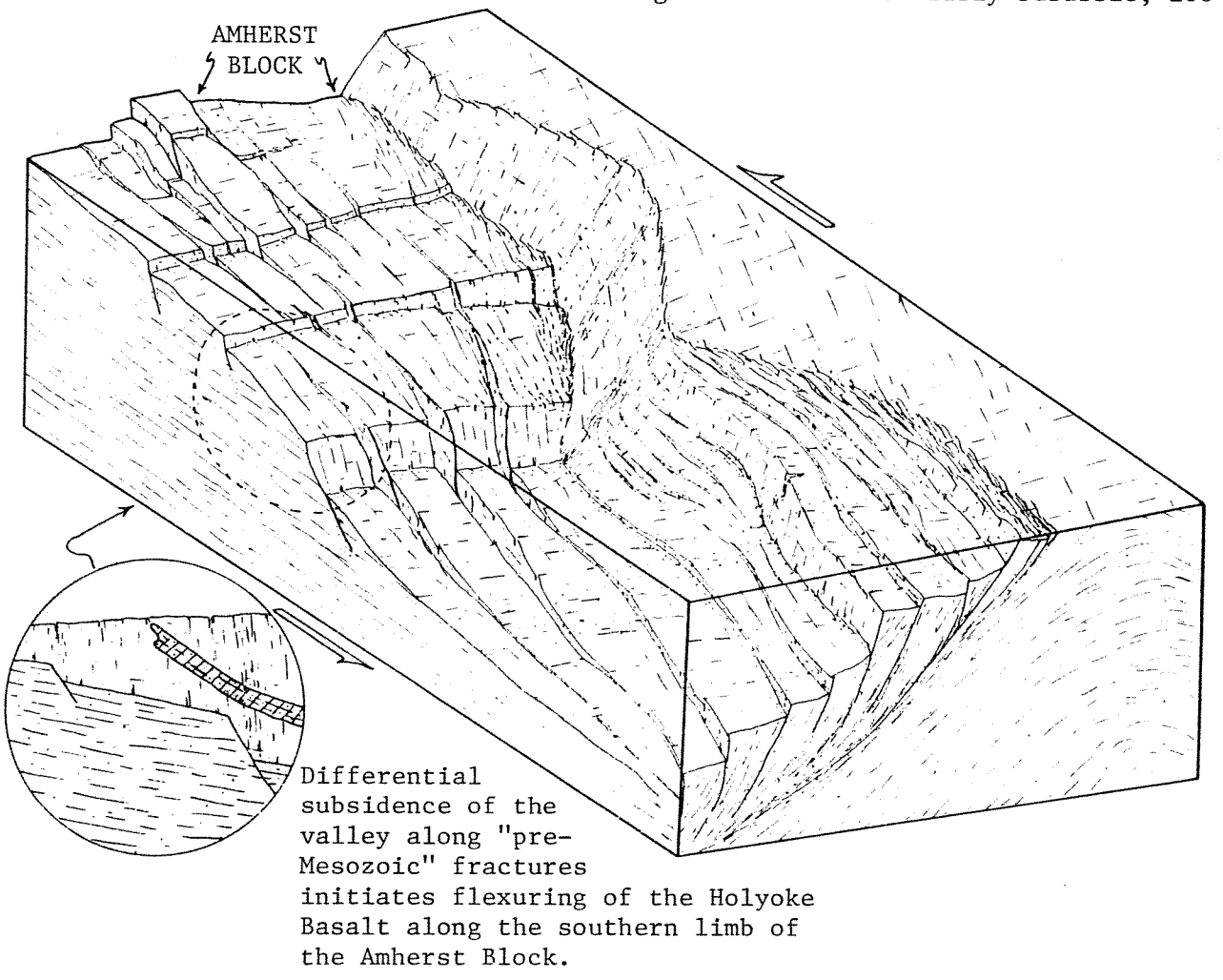

Differential subsidence of the valley along "pre-Mesozoic" fractures initiates flexuring of the Holyoke Basalt along the southern limb of the Amherst Block.

Figure 17e. Time: Latest Jurassic to present, 140 m.y.b.p.

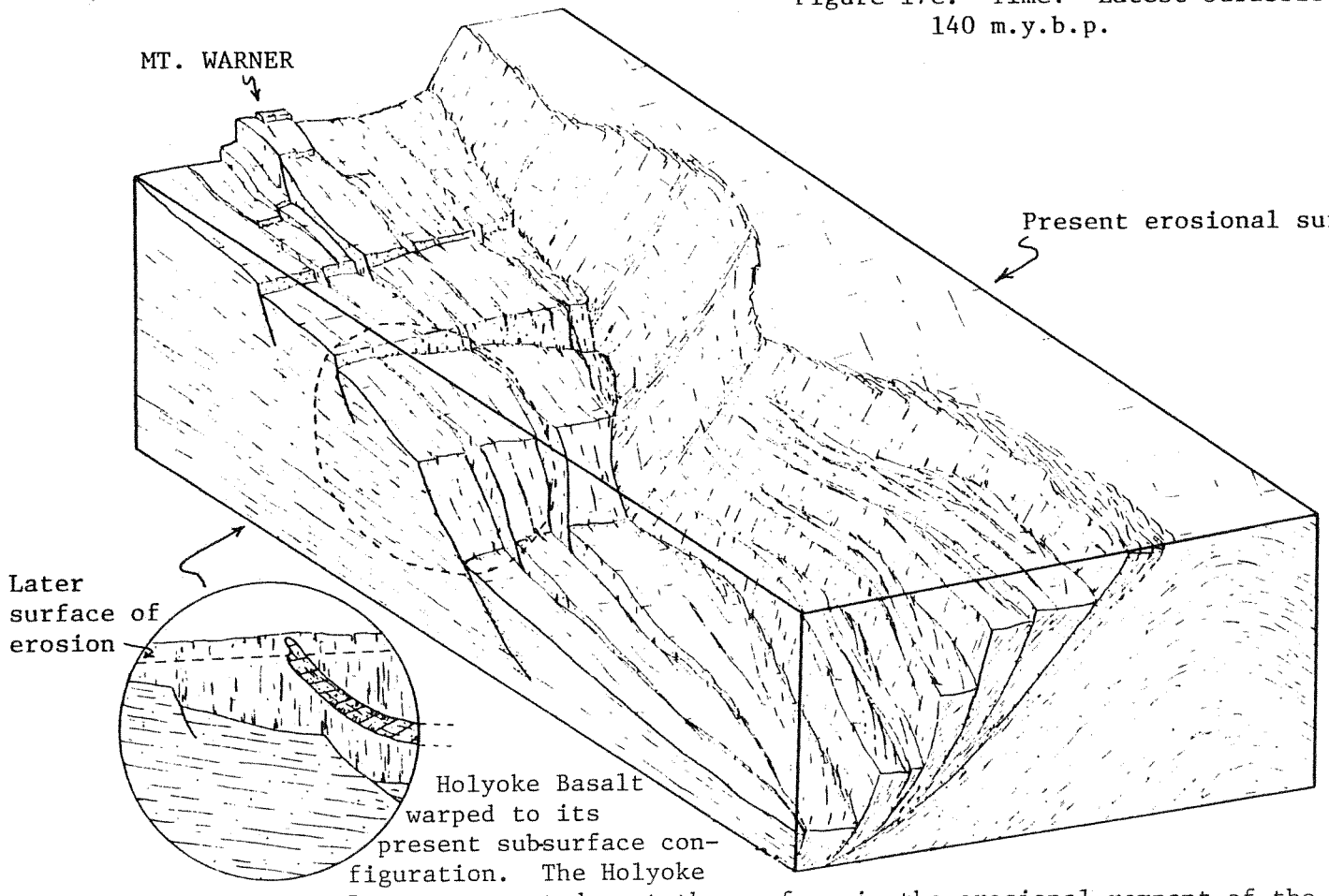

CONCLUSIONS

The complexities of the Amherst-Belchertown region examined in this study are unique in the context of the overall geology and structure of the Connecticut Valley. The border fault experiences some of its more pronounced changes in strike in this region as it bounds the Belchertown Intrusive Complex creating a salient and an abrupt re-entrant just to the north. The Holyoke Range, which appears to have been channeled into this re-entrant created by the northern portion of the complex and the Amherst Block, is not as complex a feature, genetically or structurally, as it might first appear.

Two major movement senses appear within the study area as is evident from two sets of predominant dip-sip normal faults. The strongest extensile motion is oriented around N80E-S80W as interpreted from slickensides on faults in both Mesozoic and Paleozoic rocks. A second extensile motion is oriented around N30E-S30W and restricted to faults in rocks of Paleozoic age. The first set of fault motions is associated with the regional Mesozoic stress system whereas the second set of motions appears related to the "pre-Mesozoic" system active over the study area. The following statements can be made about the area as a result of this study:

1. Extensile stresses at the time of valley formation were probably oriented around N60W-S60E giving rise to the

predominant N30E fracture pattern seen in the study area.

2. The N75W to N90W orientation of σ_3 suggested by dikes and veins and the more north-south sets of joint and fault orientations may be a manifestation of the curvature of the σ_3 stress trajectory as the fractures encountered anisotropies in the basement rocks.
3. Mt. Warner is simply part of the transverse Amherst Block which separated the Hartford and Deerfield basins at their time of origin, and continued to move differentially to upwarp the Holyoke Range along its southern flank. The block may well have been controlled by a relatively rigid westward continuation of the Belchertown Intrusive Complex beneath it (Figure 5).
4. A set of N55-70W fractures characterizes the Paleozoic rocks; especially at the Mt. Warner and Bagg Hill areas, and may well be defining the strike of the Amherst Block "horst" system.
5. There is no evidence that the study area has undergone appreciable strike-slip motion, in contrast to the Bain (1941) model which interprets the Holyoke Range as a massive drag fold due to right-lateral shearing motion on the basin.
6. The Holyoke Range represents the erosional outcrop of an east-west trending monoclinal flexure of the Holyoke Basalt

on the southern flank of the Amherst Block.

7. The gravity technique discussed has promise in future studies for defining simple contacts or faults in the valley and may be useful in providing initial starting points for 2-dimensional Talwani block models.
8. The catalogue of water well logs and locations provides additional constraints for locating contacts and/or faults and interpreting the topography of the basin fill.
9. Simple sand model results suggest that the eastern border fault may have initiated, not as one continuous fault, but as a series of en echelon, splaying listric faults whose orientations were controlled by basement anisotropy. With time, these coalesced to form the eastern boundary of the valley and the zone of later major displacements.

Suggestions for Future Study

Future work in geophysics probably will provide the answers to the many questions raised here about the deeper nature of the Connecticut Valley.

1. The use of Vibro-seismic techniques may help to define the geometry of the eastern border fault and the basement rocks underlying the basin fill.
2. A detailed gravity and ground magnetics study may serve to define further the geometry of the Amherst Block.
3. More detailed studies should be made of the older events associated with initiation of the border fault. Petrologic

and geochemical studies of the rocks in the vicinity of the border fault may provide some information as to the degree and nature of igneous activity during valley formation, and its effect on faulting.

REFERENCES CITED

Ahmad, Farrukh, 1975, Geological interpretation of gravity and aeromagnetic surveys in the Bronson Hill anticlinorium, Southwestern New Hampshire: Ph.D. Thesis, University of Massachusetts, 170 p.

Anderson, E. M., 1951, The dynamics of faulting: London, Oliver and Boyd, 206 p.

Ashenden, D. D., 1973, Stratigraphy and structure of the Pelham dome, north-central Massachusetts: University of Massachusetts, Dept. of Geology, Contribution No. 16, 132 p.

Ashwal, L. D., and Hargraves, R. B., 1977, Paleomagnetic evidence for tectonic rotation of the Belchertown Pluton, west-central Massachusetts: Journal of Geophysical Research, Vol. 82, No. 8, p. 1315-1324.

Ashwal, L. D., Leo, G. W., Robinson, Peter, Zartman, R. E., Hall, D. J., 1979, The Belchertown quartz monzodiorite pluton, west-central Massachusetts: a syntectonic Acadian intrusion: American Journal of Science (in press).

Badgley, P. C., 1965, Structural and tectonic principles: Harper and Row pub., 521 p.

Bain, G. W., 1932, The northern area of the Connecticut Valley Triassic: Am. Jour. Sci., V. 23, p. 57-77.

_____, 1941, The Holyoke Range and Connecticut Valley structure: Am. Journal Sci., V. 239, p. 261-275.

Bain, G. W., and Beebe, J. H., 1954, Scale model reproduction of tension faults: Am. Jour. of Science, V. 252 (12), p. 745-754.

_____, 1957, Triassic age rift structures in eastern North America: Trans. N.Y. Acad. Sci., V. 19, p. 489-502.

Balk, R., 1937, Structural behavior of igneous rocks: Geol. Soc. America Mem. 5, 177 p.

_____, 1957, Geology of the Mt. Holyoke Quadrangle, Massachusetts: Geol. Soc. Amer. Bull. 69, p. 481-504.

Barrell, J., 1915, Central Connecticut in the geologic past: Conn. Geol. and Nat. Hist. Surv., Bull. 23, 44 p.

Beloussou, V. V., 1961, Experimental Geology: Sci. American, V. 204, p. 97-106.

Billings, M. P., 1954, Structural Geology: Englewood Cliffs, N.J., Prentice-Hall, 514 p.

Boucot, A. J., 1961, Stratigraphy of the Moose River synclinorium, Maine: U.S. Geol. Survey Bull. 1111-E, 188 p.

Boucot, A. J., and Arndt, R. H., 1960, Fossils of the Littleton Formation (Lower Devonian) of New Hampshire: U.S. Geol. Survey Professional Paper 334-B, p. 41-53.

Bromery, R. W., 1967, Simple-Bouquer gravity map of Massachusetts: U.S. Geol. Survey Geophysical Investigation Map GP-612.

Cloos, E., 1955, Experimental analysis of fracture patterns: Geol. Soc. Am. Bull., V. 66, p. 241-256.

Coleman, K. G., 1974, Geologic background of the Red Sea: in The Geology of Continental Margins, Burke, C. A. and Drake, C. L., editors, Springer-Verlag, pub., p. 743-751.

Cornet, B., Traverse, A., McDonald, N. G., 1973, Fossil spores, pollen, and fishes from Connecticut indicate Early Jurassic age for part of the Newark Group: Sci., V. 182, p. 1243-1247.

Cornet, B., and Traverse, A., 1975, Palynological contributions to the chronology and stratigraphy of the Hartford Basin in Connecticut and Massachusetts: Geosci. and Man, V. 11, p. 1-33.

Currie, J. B., 1966, Experimental structural geology: Earth-Science Reviews, V. 1 (1): p. 51-67.

Deboer, J., 1968, Paleomagnetic differentiation and correlation of Late Triassic volcanic rocks in the central Appalachians (with special reference to the Connecticut Valley): Geol. Soc. Am., V. 79, p. 609-626.

DeSitter, L. U., 1956, Structural Geology: McGraw-Hill Series in the Geological Sciences, McGraw-Hill publ., 551 p.

Donath, F. A., 1961, Experimental study of shear failure in anisotropic rocks: Geol. Soc. Am. Bull. 72, p. 985.

Donath, F. A., 1962, Analysis of basin-range structure south-central Oregon: Geol. Soc. Am. Bull., V. 73, p. 1-16.

Ellen, S. D., 1964, A gravity survey of the northern Connecticut Valley Triassic basin: Senior thesis, Department of Geology, Amherst College, 68 p.

Emerson, B. K., 1898, Geology of Old Hampshire County, Massachusetts; comprising Franklin, Hampden, and Hampshire Counties: U.S. Geol. Survey Mon. 29, 790 p.

Faul, H., Stern, T. W., Thomas, H. H., Elmore, P. L. D., 1963, Ages of intrusion and metamorphism in the northern Appalachians: Amer. Jour. Sci., V. 261, p. 1-19.

Foose, R. M., and Cunningham, C. G., 1968, Pre-glacial Connecticut River course near Amherst, Massachusetts: Geol. Soc. Am., Vol. 79, p. 1415-1418.

Gilbert, F. P., Popenoe, Peter and Philbin, P. W., 1968, Aeromagnetic map of the Palmer Quadrangle, Hampden, Hampshire and Worcester Counties, Massachusetts: U.S. Survey Geophysical Investigations Map GP-617.

_____, 1968, Aeromagnetic map of the Ludlow Quadrangle, Hampden and Hampshire Counties, Massachusetts: U.S. Geol. Survey Geophysical Investigations Map GP-619.

_____, 1969, Aeromagnetic map of the Mt. Toby Quadrangle and part of the Greenfield Quadrangle, Franklin and Hampshire Counties, Massachusetts: U.S. Geological Survey Geophysical Investigations Map GP-660.

_____, 1969, Aeromagnetic map of the Mt. Holyoke Quadrangle, Hampshire and Hampden Counties, Massachusetts: U.S. Geol. Survey Geophysical Investigation Map GP-662.

Gilbert, F. P., Popenoe, Peter and Smith, E.P., 1969, Aeromagnetic map of the Belchertown Quadrangle, Hampshire County, Massachusetts: U.S. Geol. Survey Geophysical Investigations Map GP-663.

_____, 1969, Aeromagnetic map of the Winsor Dam Quadrangle, Hampshire, Worcester and Franklin Counties, Massachusetts: U.S. Geol. Survey Geophysical Investigations Map GP-664.

Goldstein, A. G., 1976, Brittle fracture history of the Montague Basin, north-central Massachusetts: Contrib. No. 25 (M.S. Thesis), Dept. of Geology, Univ. of Massachusetts, Amherst, Mass., 108 p.

Guthrie, J. O., 1972, Geology of the northern portion of the Belchertown Instusive Complex: Contrib. No. 8 (M.S. Thesis), Dept. of Geology, Univ. of Massachusetts, Amherst, Mass., 110 p.

Gzovsky, M.V., 1959, The use of scale models in tectonophysics: International Geol. Review, V. 1(4): p. 31-47.

Hafner, J., 1951, Stress distribution and faulting: Geol. Soc. Am. Bull., V. 62, p. 373-398.

Hall, D. J., 1973, Geology and geophysics of the Belchertown Batholith, west-central Massachusetts: Ph.D. thesis, Univ. of Massachusetts, 110 p.

Harris, N. B., 1974, Geology and magnetics at the eastern end of the Holyoke Range, Belchertown, Massachusetts: Senior thesis, Department of Geology, Amherst College, 92 p.

Hubbert, M. K., 1937, Theory of scale models as applied to geologic structures: Geol. Soc. Am. Bull., V. 48, p. 1459-1521.

Hubert, J. F., Reed, A. A., Dowdall, W. L., Gilchrist, J. M., 1978, Guide to the redbeds of central Connecticut, Contrib. No. 32, Department of Geology and Geography, Univ. of Massachusetts, 127 p.

Illies, J. H., and Fuchs, K., 1974, Approaches to taphrogenesis: Inter-Union Commission on Geodynamics, Scientific Report no. 8, 460 p.

Kick, J. F., 1975, A gravity study of the gneiss dome terrain of north-central Massachusetts: Ph.D. thesis, Univ. of Massachusetts, 179 p.

Klein, G. de V., 1969, Deposition of Triassic sedimentary rocks in separate basins, eastern North America: Geol. Soc. Am. Bull., V. 80, p. 1825-1832.

Koide, H., and Bhattacharji, S., 1975, Mechanistic interpretation of rift valley formation: Science, V. 189, p. 791-793.

Krynine, P. D., 1950, Petrology, stratigraphy, and origin of the Triassic sedimentary rocks of Connecticut: Conn. Geol. and Nat. Hist. Surv., Bull. 73, 239 p.

Laird, H. S., 1974, Geology of the Pelham Dome near Montague, west-central Massachusetts: Contrib. No. 14 (M.S. thesis), Dept. of Geology, Univ. of Massachusetts, Amherst, Mass. 84 p.

Laughton, A. S., 1966, The Gulf of Aden in relation to the Red Sea and Afar depression of Ethiopia: in The World Rift System, T. N. Irvine, editor, Geologic Survey of Canada, paper 66-14.

Lindholm, R. C., 1978, Triassic-Jurassic faulting in eastern North America - A model based on pre-Triassic structures: Geology, V. 6, p. 365-368.

Longwell, C. R., 1922, Notes on the structure of the Triassic rocks in southern Connecticut: Am. Jour. Sci., V. 4, p. 223-236.

Lyons, J. B., and Livingston, D. E., 1977, Rb-Sr age of the New Hampshire Plutonic Series: Geological Society of America Bull., V. 88, p. 1808-1812.

May, P. R., 1971, Pattern of Triassic-Jurassic diabase dikes around the North Atlantic in context of the pre-drift position of the continents: Geol. Soc. Am. Bull., V. 82, p. 1285-1292.

McConnell, R. B., 1972, Geologic development of the rift system of Eastern Africa: Geol. Soc. Am. Bull., V. 83, p. 2549-2572.

McGill, G. E., and Stromquist, A. W., 1974, A model for graben formation by subsurface flow: Canyonlands National Park, Utah: Contrib. No. 15, Dept. of Geology and Geography, University of Massachusetts, Amherst, Mass., 79 p.

McHone, J. G., 1978, Distribution orientation and ages of mafic dikes in central New England (in press).

McKenzie, D. P., Davies, D., and Molnar, P., 1970, Plate tectonics of the Red Sea and East Africa: Nature, V. 226, p. 243-248.

Means, W. D., 1976, Stress and strain: Springer-Verlag publ., New York, 339 p.

Moore, G. E., 1949, Structure and metamorphism of the Keene-Brattleboro area, New Hampshire-Vermont: Geol. Soc. of America Bulletin, V. 60, no. 10, p. 1613-1670.

Naylor, R. S., 1971, Acadian orogeny: an abrupt and brief event: Science, vol. 172, p. 558-560.

Naylor, R. S., Boone, G. M., Boudette, E. L., Ashenden, D. D., and Robinson, Peter, 1973, Pre-Ordovician rocks in the Bronson Hill and Boundary Mountain anticlinoria, New England, U.S.A.: Trans. Am. Geophys. Union, (Abstract), v. 54, p. 495.

Nettleton, L. L., and Elkins, T. A., 1947, Geologic models made from granular materials: Am. Geophys. Union Trans., v. 28(3), p. 451-466.

Northeast Utilities Service Co., 1974, Montague Nuclear Power Station, preliminary safety analysis report, Supplement 6, Docket No. 50-496 and 497.

Oertel, G., 1965, The mechanism of faulting in clay experiments: Tectonophysics, v. 2(5), p. 343-393.

Pferd, J., 1975, A computer based system for the collection of detailed structural data from metamorphic terrains (Abs.): abstracts with programs, northeast section, 10th Annual Meeting of Geol. Soc. Am., p. 106.

Piepul, R., 1975, An analysis of jointing and faulting at the southern end of the eastern border fault, Connecticut: M.Sc. thesis, Univ. of Massachusetts, 109 p., contri. no. 23.

Price, N. J., 1966, Fault and joint development in brittle and semi-brittle rock: Pergamon Press, Oxford, 175 p.

Profett, J. M., 1977, Cenozoic geology of the Yerington district, Nevada, and implications for the nature and origin of Basin and Range faulting: Geol. Soc. Am. Bull., V. 88, p. 247-266.

Ratcliff, N. M., 1977, Ramapo fracture zone through time: Inheritance of geological structures: Lamont-Doherty Geological Observatory, Sponsors; Symposium on the geological development of the New York Bight, p. 3-7.

Reeseman, R. H., 1973, K-Ar dating of Upper Triassic lavas of Connecticut Valley, New England: Geol. Soc. Am. abst., v. 5, p. 211.

Robinson, Peter, 1966, Alumino-silicate polymorphs and Paleozoic erosion rates in central Massachusetts (abstract): Transactions of the American Geophysical Union, v. 47, p. 424.

_____, 1967, Gneiss domes and recumbent folds of the Orange area, west-central Massachusetts: Guidebook for field trips in the Connecticut Valley, N.E.I.G.C. 59th Annual Meeting, p. 17-47.

Russell, I. C., 1878, On the physical history of the Triassic formation in New Jersey and the Connecticut Valley: Annals N.Y. Acad. Sci., v. 1, p. 220-254.

Russell, I. C., 1880, On the former extent of the Triassic formation of the Atlantic states: Am. Nat., v. 14, p. 703-712.

Sanders, J. E., 1960, Structural history of Triassic rocks of the Connecticut Valley belt and its regional implications: N.Y. Acad. Sci. Trans., v. 23, p. 119-132.

_____, 1963, Late Triassic tectonic history of northeastern United States: Am. Jour. Sci., v. 261, p. 501-524.

Sanford, A. R., 1959, Analytical and experimental study of simple geologic structures: Geol. Soc. of Amer. Bull. v. 70(1), p. 19-52.

Stanley, J. M., 1977, Simplified gravity interpretation by gradients-the geologic contact: Geophysics, v. 42, no. 6, p. 1230-1235.

Stevens, R. L., 1977, Sedimentology of the Sugarloaf Arkose, Deerfield Basin, Massachusetts: research report for M.S. degree, Univ. of Mass., Amherst, 84 p.

Stewart, J. H., 1971, Basin and Range structure: A system of horsts and grabens produced by deep-seated extension: Geol. Soc. Am. Bull., v. 82, p. 1019-1044.

Stoeck, P. L., 1971, Petrology and contact effects of the Hatfield Pluton of Belchertown tonalite in the Whately-Northampton area, western Massachusetts: M.Sc. thesis, Univ. of Massachusetts, 83 p., contrib. no. 7.

Stromquist, A. W., 1976, Geometry and growth of grabens, Lower Red Lake Canyon area, Canyonlands National Park, Utah: Contribution no. 28 (Master's thesis), Department of Geology and Geography, University of Massachusetts, Amherst, 118 p.

Talwani, M., Worzel, J. L., and Landsman, M., 1959, Rapid gravity computations for two-dimensional bodies with application to the Mendocino submarine fracture zone: Jour. Geophys. Research., v. 64, p. 49-59.

Wheeler, G., 1937, The west wall of the New England Triassic lowland: Connecticut State Geol. Nat. History Survey Bull. 58, p. 73.

_____, 1939, Triassic fault line deflections and associated warpings: Jour. Geol., v. 47, p. 337-370.

Willard, M. E., 1951, Bedrock geology of the Mt. Toby Quadrangle, Massachusetts: U.S. Geol. Survey Geol. Quad. Map GQ-8.

Willard, M.E., 1956, Bedrock geology of the Williamsburg quadrangle, Massachusetts: U.S. Geol. Survey Geol. Quad. Map GQ-85.

Williams, G., 1976, An analysis of brittle deformation in the area of the northern portion of the Pelham Dome, north-central Massachusetts: Senior thesis, Univ. of Massachusetts, 47 p.

Willis, B., 1936, East African plateaus and rift valleys: Carnegie Institute, Washington, publication no. 470, 358 p.

APPENDIX I

WELL LOGS AND LOCATIONS

General Statement

Driller's jargon is reasonably consistent among different well drillers. Based on known geology in the vicinity of the wells, a reasonably reliable interpretation can be given to the driller's jargon and lend some degree of meaning and credibility to the logs.

Common Jargon	Interpretation
"redrock"/"brownrock"(harder) -------	arkose (ss), shale, red till, etc.
"blackrock," "greyrock," or "granite" -------	Paleozoic schists, gneisses, tonolite, granodiorite, etc.
"traprock" ----------	basalt
"puddin rock" ----------	conglomerate or till
"ledge" ----------	bedrock
"bedrock" ----------	any of the above
"white quartz rock" ----------	pegmatite or silicified zone
"soft rock" ----------	till ?

INDEX MAP

Well location maps on the following pages are indexed here by letter.

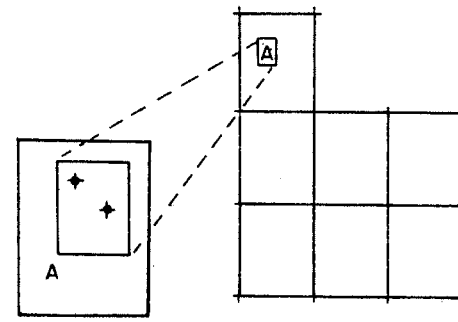

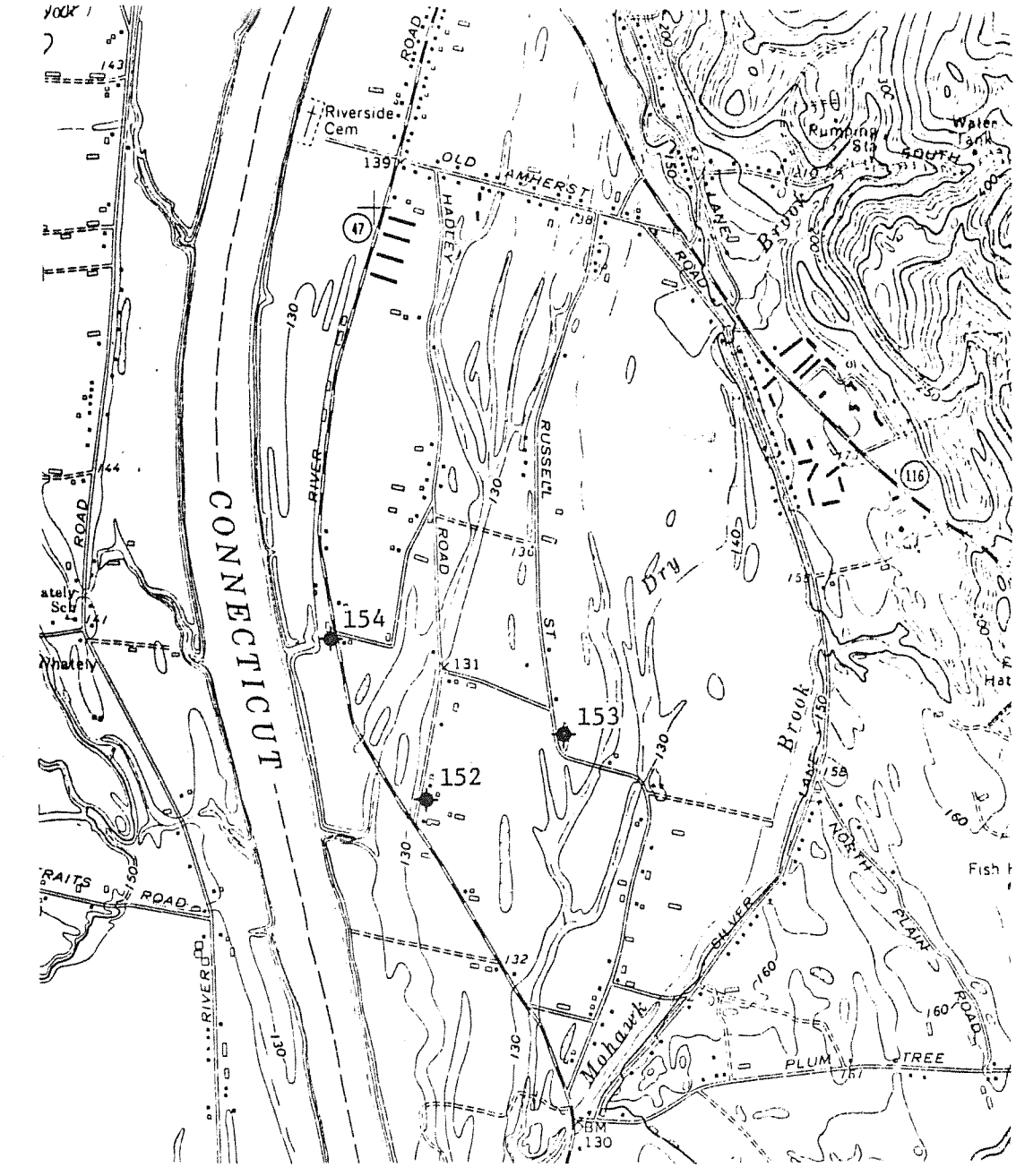

A

Well #	Log
152	Till from 197' to 341', bedrock at 344'
153	"Ledge" (arkose?) at 270'
154	Bedrock at 224'

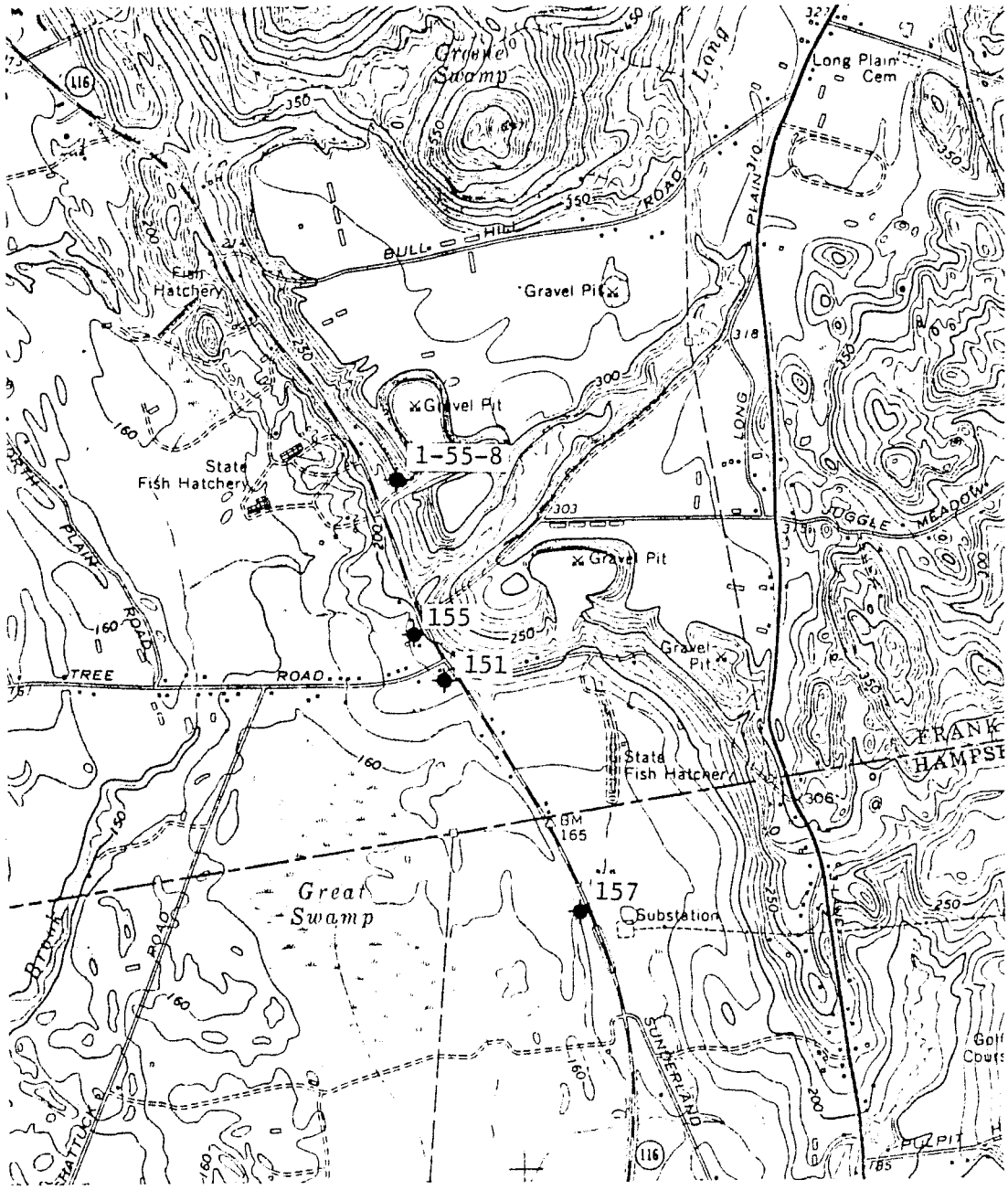

B

Well #	Log
1-55-8	"Redrock" at 376'
151	Bedrock at 274'
155	Sand and gravel to 376', Triassic bedrock at 376'
157	Bedrock at 233'

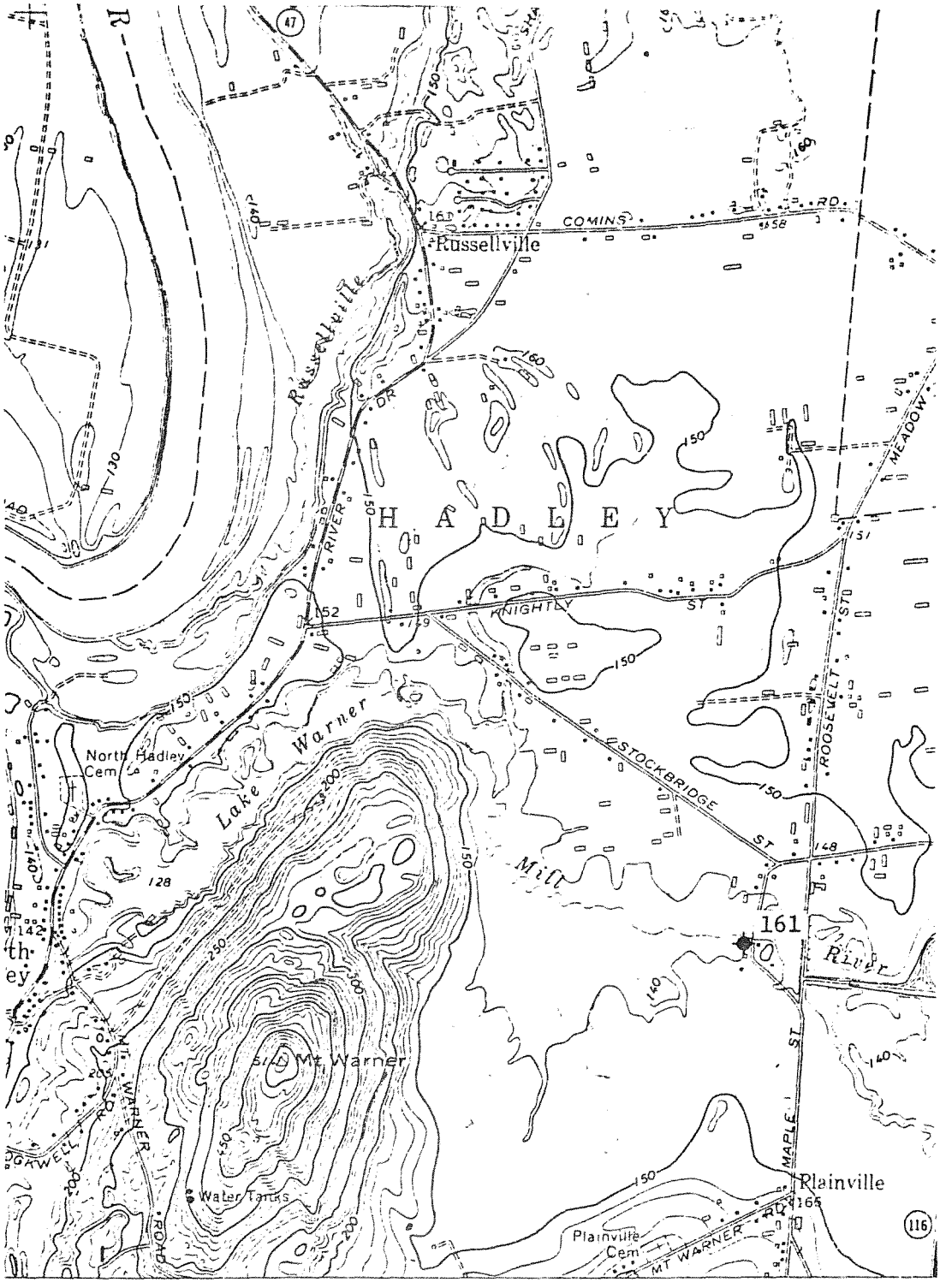

C

Well #	Log
161	Bedrock at 62'

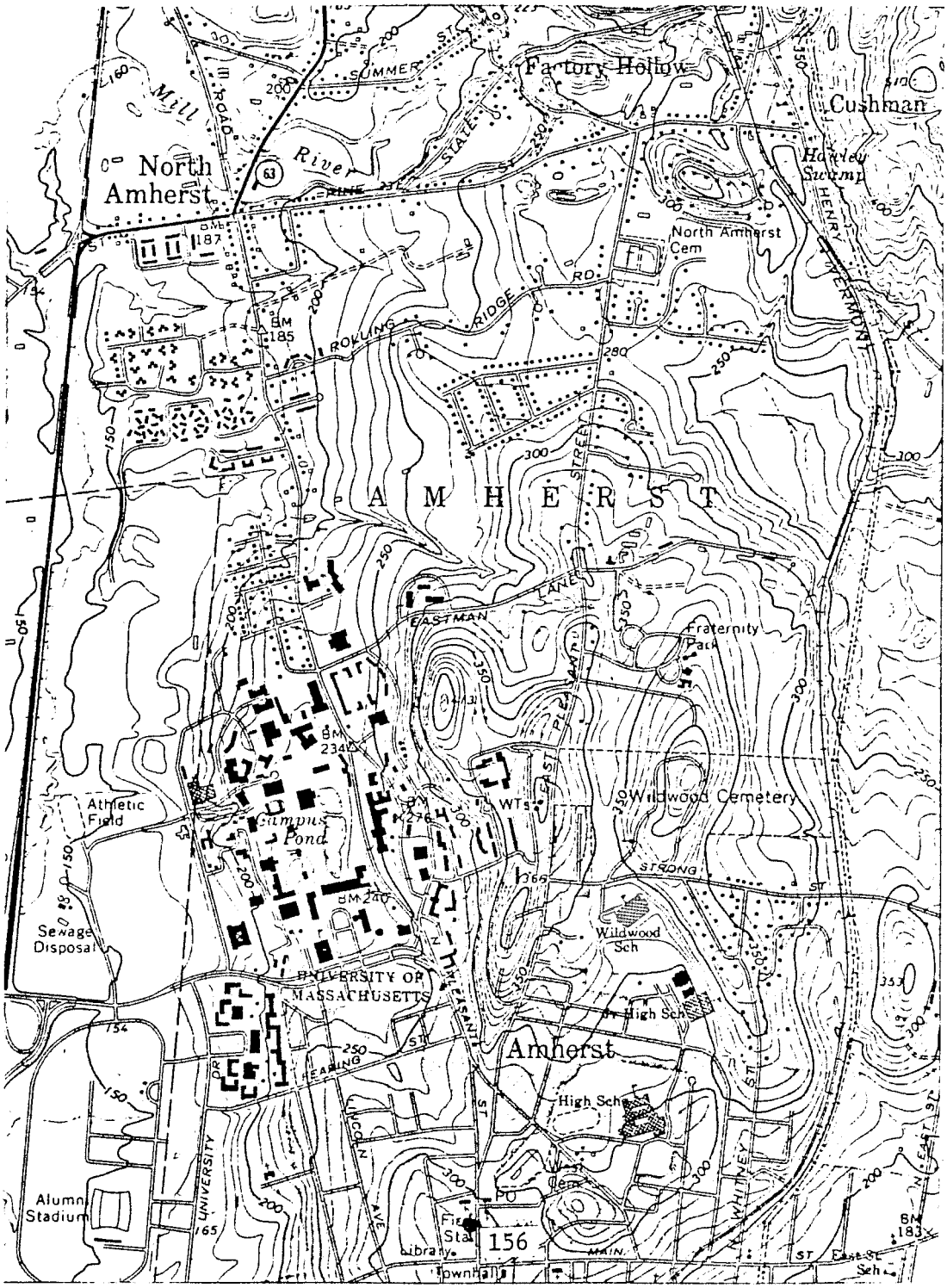

D

Well #	Log
156	Total depth, 470', "sedimentary breccia" to 50', Triassic bedrock from 50' to 330', "gneiss" from 330' to 470'.

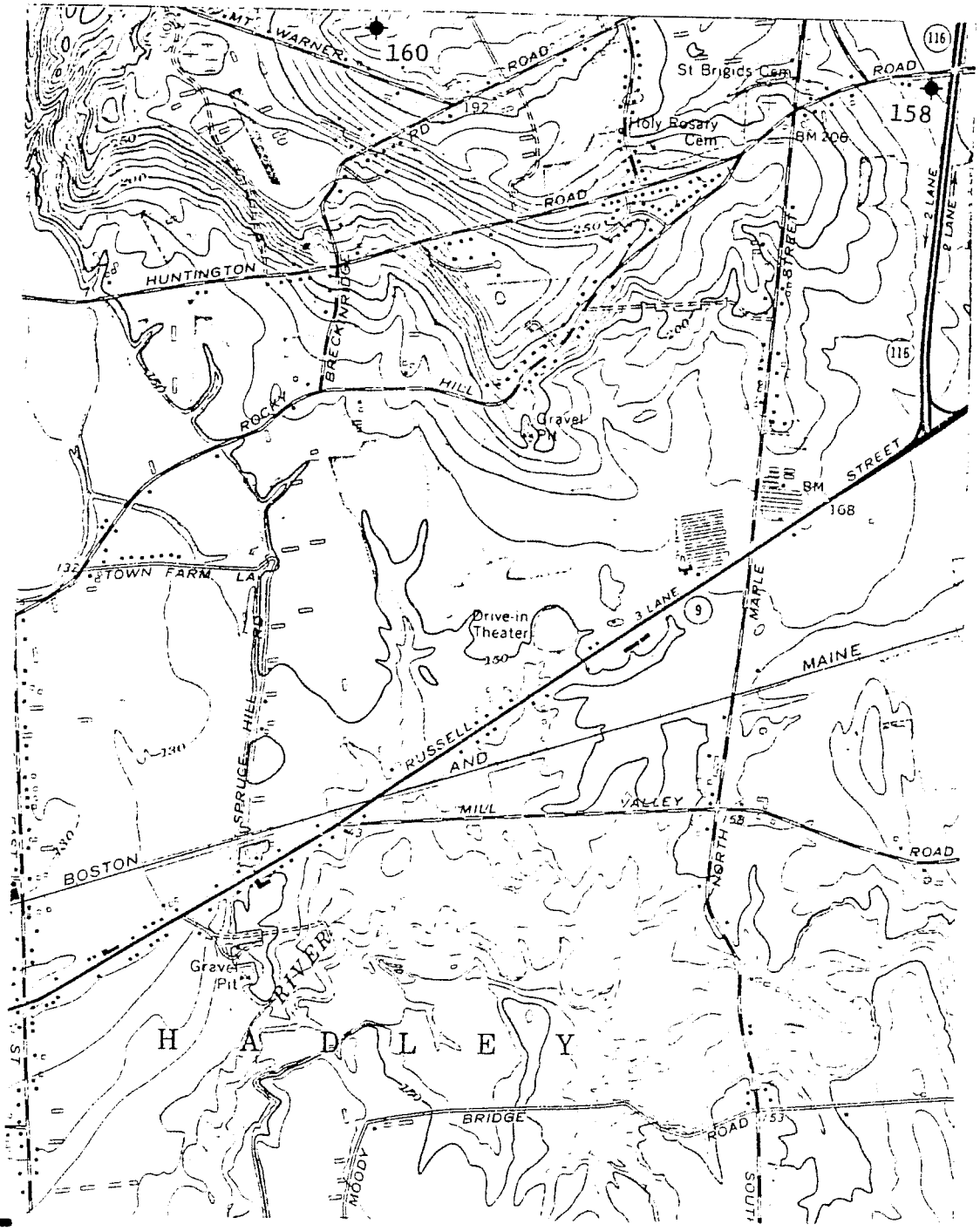

E

Well #	Log
158	"Triassic"at 30', bedrock at 100'
160	Sand and gravel to 223'

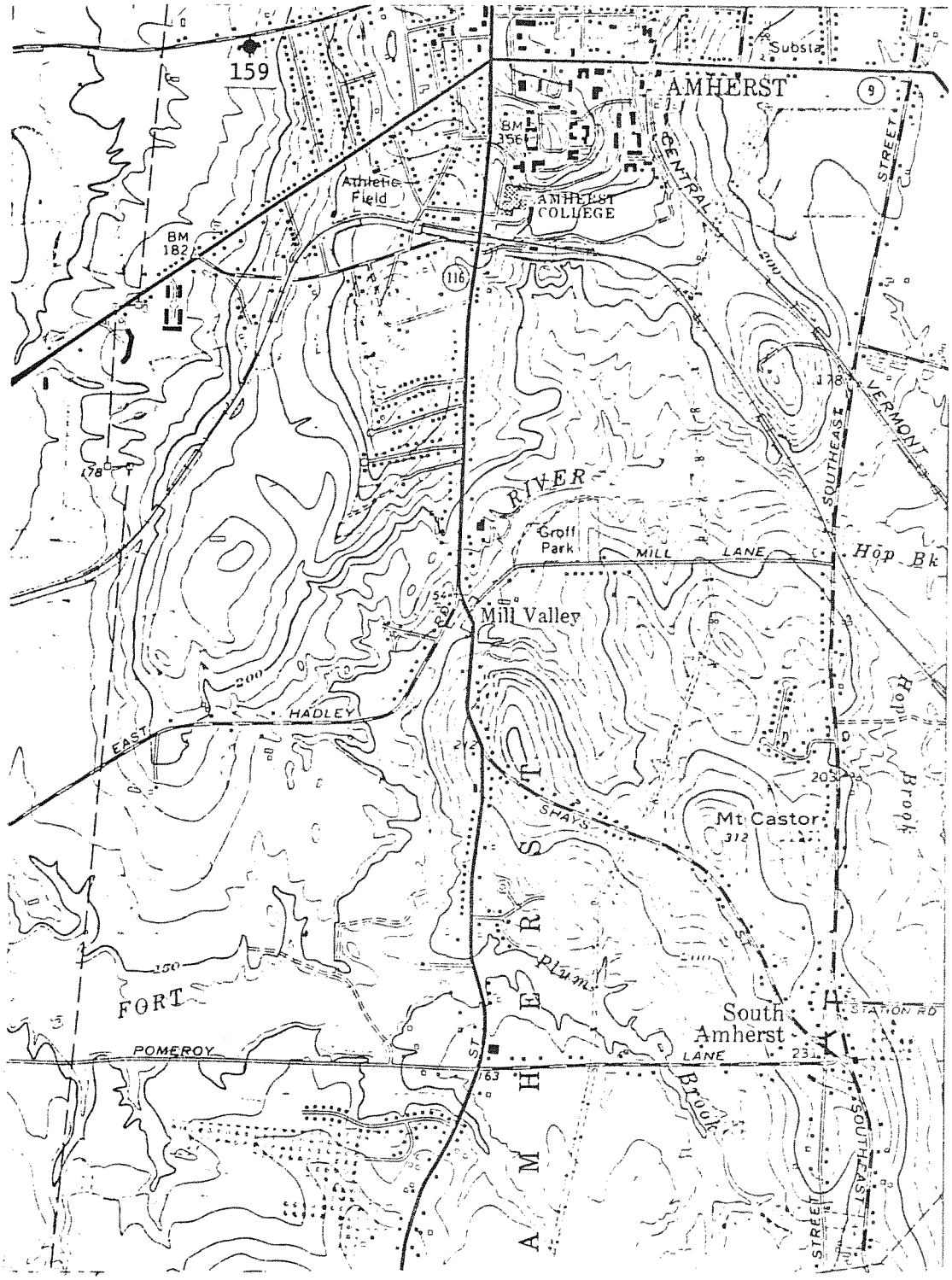

F

Well #	Log
159	"Triassic" at 50', "bedrock" at 159'

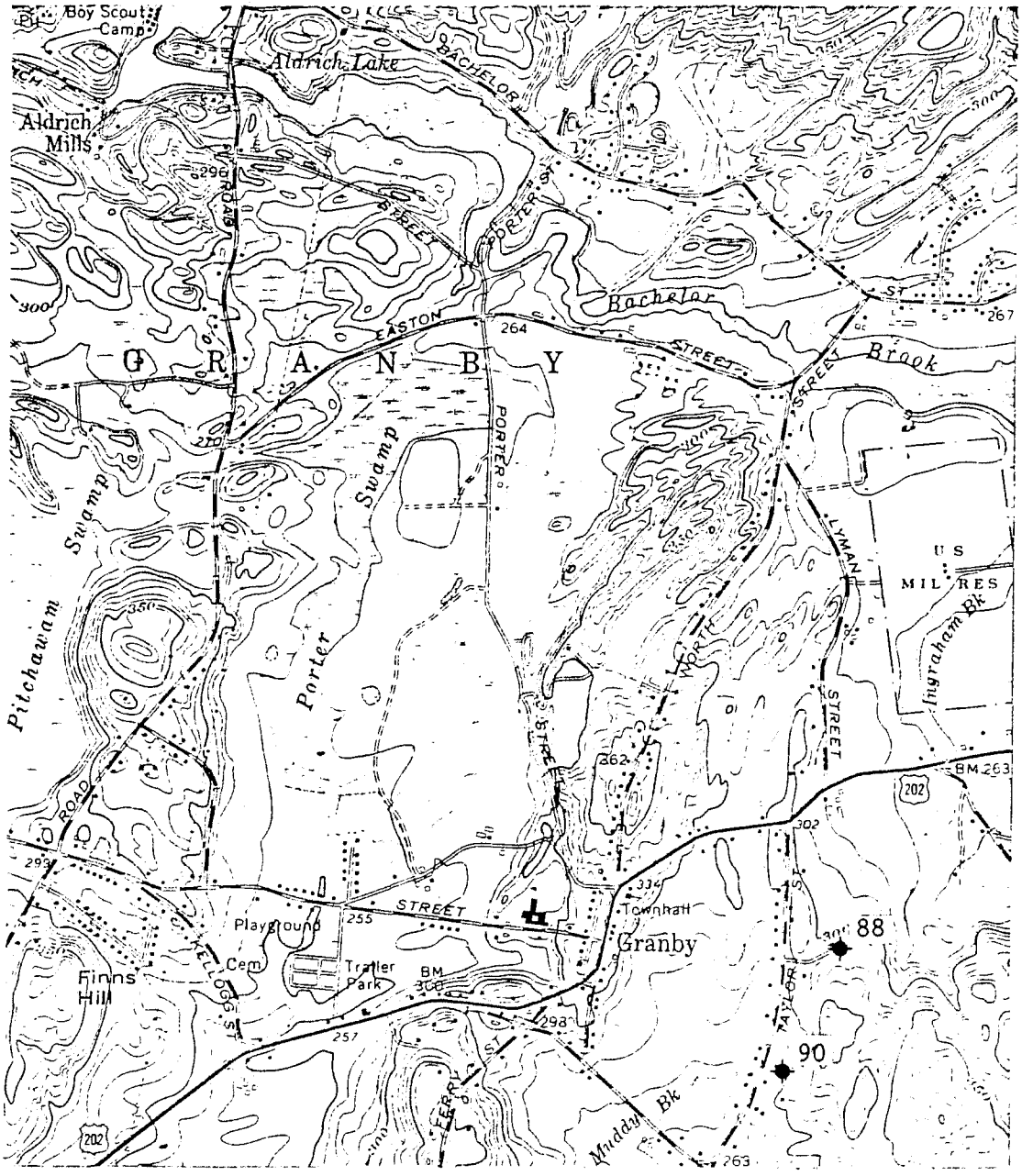

G

Well #	Log
88	Total depth 123', "greyrock" ledge at 12'
90	Total depth 173', ledge at 14'; puddin rock

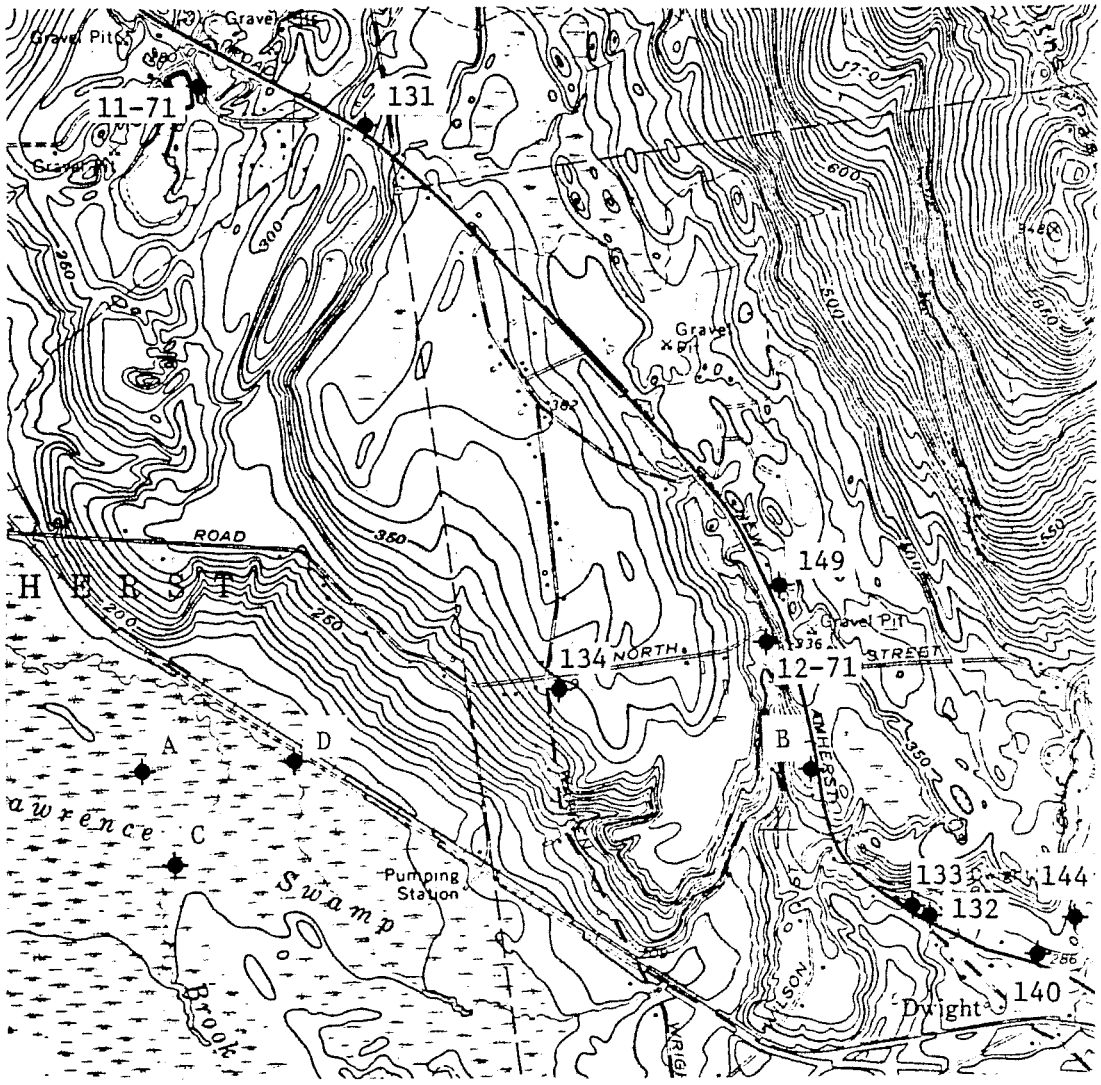

H

Well #	Log
11-71	"Redrock" at 75'
12-71	"Redrock at 99'
131	Total depth 280', "redrock" at 40'
132	Total depth 260', "redrock" at 78'
133	Total depth 400', "redrock 80' to 360', "white quartz rock" at 360'
134	Total depth 180', sandstone at 60', "redrock" at 140', "hard white rock" at 160'
140	Total depth 300', "granite" at 8'
144	Total depth 450', "greyrock" at 30'
149	Total depth 330', "softrock" from 56' to 212', "granite" at 212'

"H" continued:

Well #	Log
A	Total depth 100'+, 0 to 85' gravel and red till, 85-90' sand, "schist" at 91'
B	Sand and gravel 0-45', arkose 45-275', 275-706' "greyrock" (schist and dome gneisses)
C	Total depth 100'+, 0-85' gravel and red till, 85-90' sand, arkose at 90'
D	Arkose at 45'

I

Well #	Log
Zone 1	See additional logs.
9	Total depth 399', "brownrock" at 12'
16	Total depth 163', "greyrock" at 5'
138	Total depth 75', red sandstone at 63'
142	Total depth 150', sandstone at 9'
143	Total depth 75', "greyrock" at 42'
150	Total depth 80', "granite" at 30'

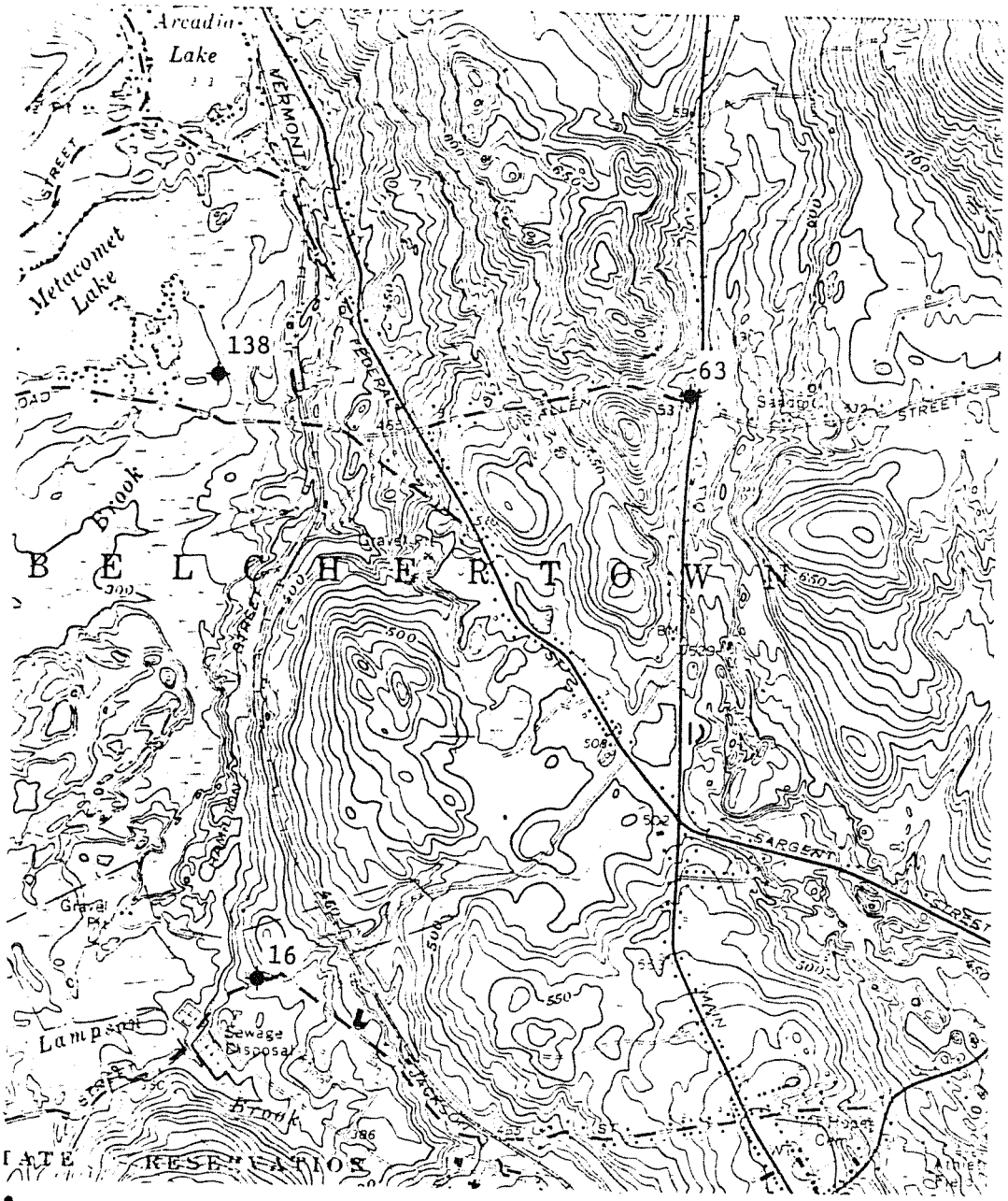

Well #	Log
16	Total depth 163', "greyrock" at 5'
63	Total depth 213', "greyrock" at 8'
138	Total depth 75', red sandstone at 63'

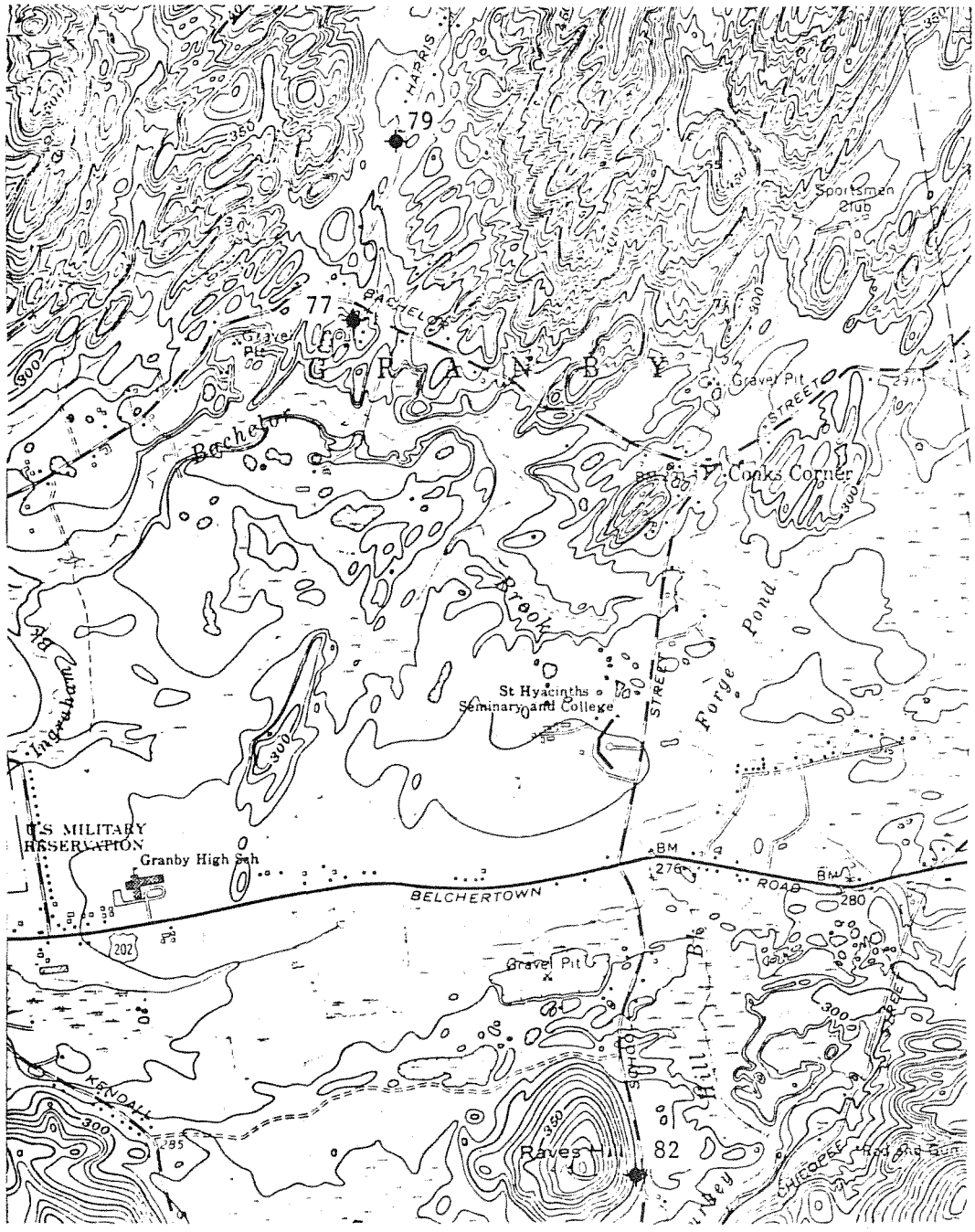

K

Well #	Log
77	Depth 133', "traprock" at 28'
79	Depth 174', "traprock" at 16'
82	Depth 249', "puddin stone" at 9'

Well #	Log
Zones 2 and 3	See additional logs
13	Depth 235', "redrock" at 135'?
45	Depth 69', "redrock" at 6'
69	Depth 224', "greyrock" at 40'
70	Sandstone at 9'
75	Depth 307', at 139', "redrock" then "grey-white rock"
147	Depth 125', red standstone at 15'

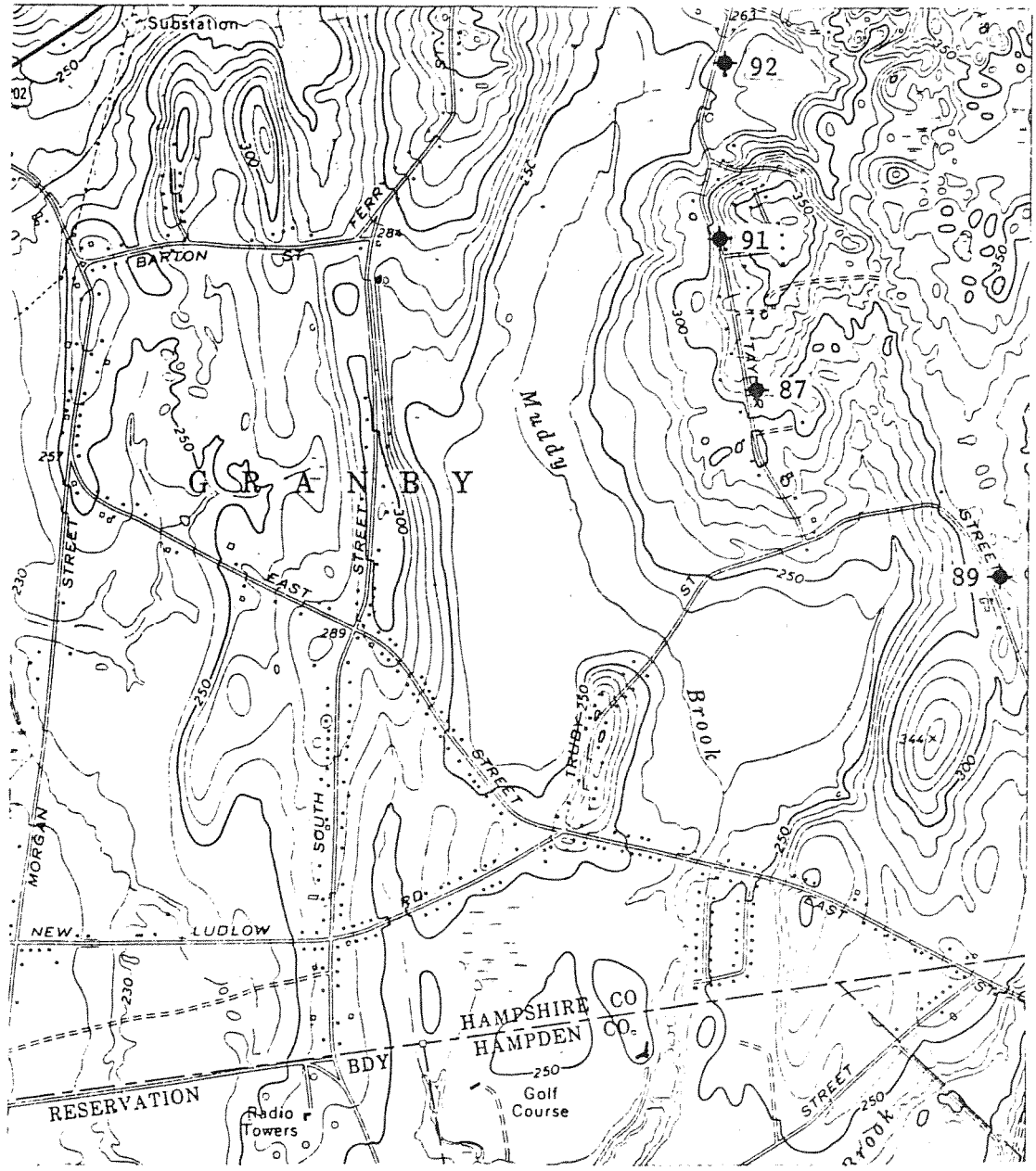

M

Well #	Log
87	Depth 322', "redrock" at 9'
89	Depth 296', "redrock" at 24'
91	Depth 448', "redrock" at 11'
92	Depth 97', "redrock" at 25', "traprock" at 60', "puddin rock" at 75'

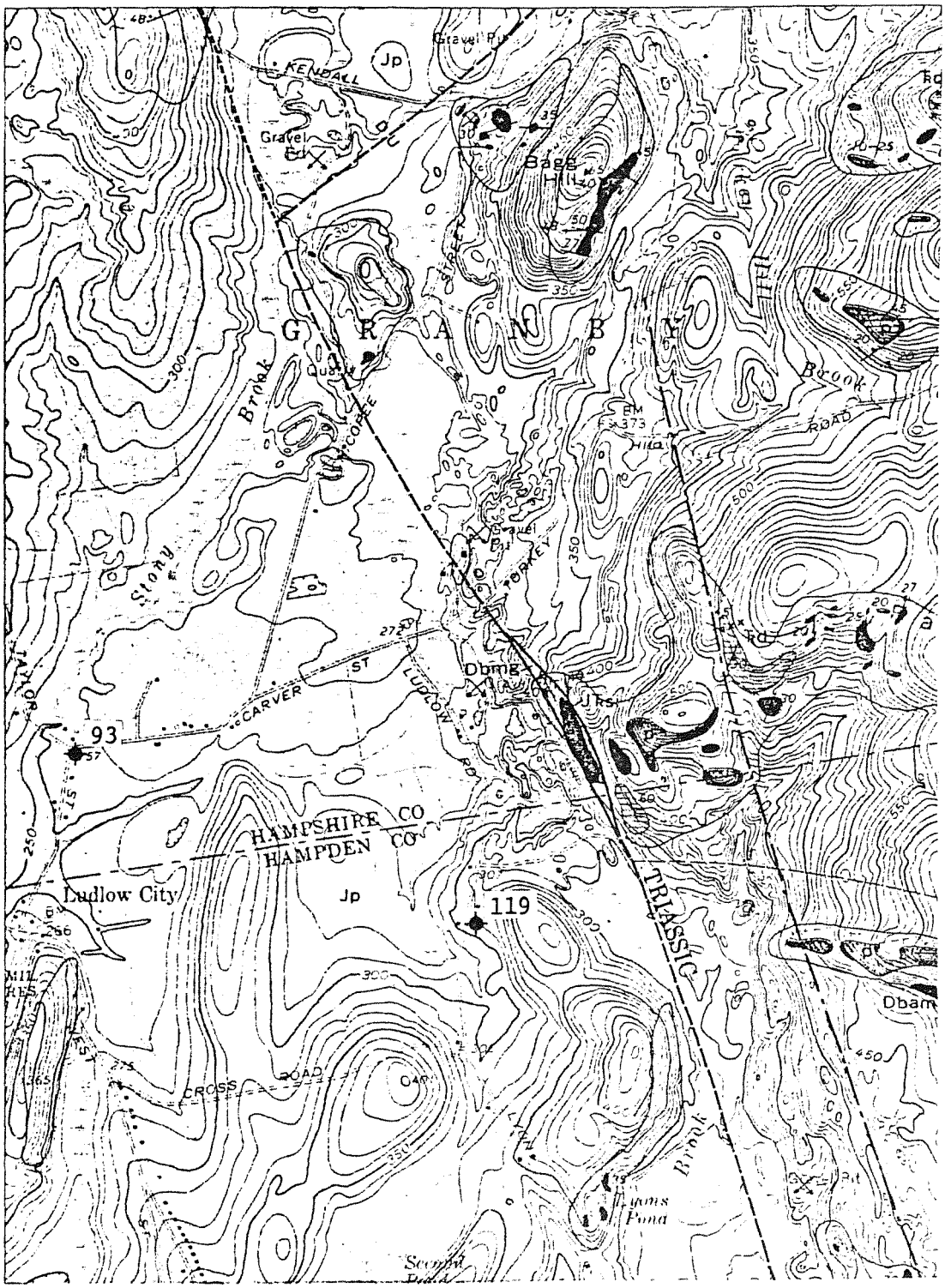

N

Well #	Log
93	Depth 128', red sandstone at 32'
119	Depth 412', sandstone at 18'

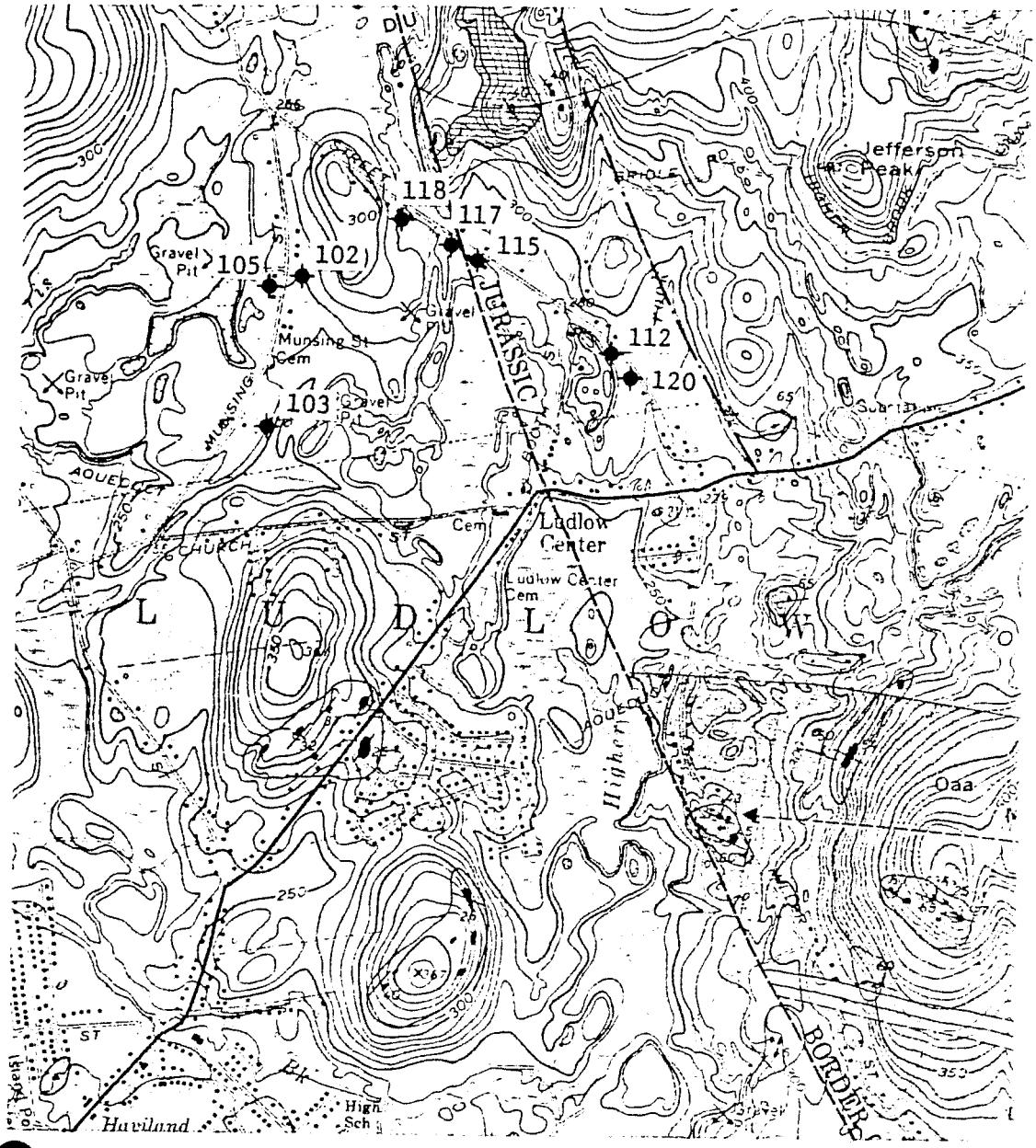

Well #	Log
102	Depth 233', "redrock" at 15'
103	Depth 100', "redrock" at 93'
105	Depth 223', "redrock" at 14'
112	Depth 272', "blackrock" at 22'
115	Depth 346', "greyrock" at 20'
117	Depth 72', "granite" at 25'
118	Depth 222', "greyrock"? at 10'
120	Depth 124', "greyrock" at 21'

Additional Logs: For wells too closely spaced to show on maps, but with considerable data useful in contouring of bedrock surface.

Zone 1. Stebbins Street (Lamascola, contractor)

Lot #	Depth	Lithology	
3	224'	sandstone at	8'
4	140'	"	9'
5	124'	"	14'
6	249'	"	18'
7	124'	"	16'
8	274'	"	10'
9	149'	"	2'

Zone 2. Pinebrook Drive, Rolling Acres

Lot #	Depth	Lithology	
1	124'	sandstone at	62'
3	98'	"	55'
4	174'	"	62'
5	73'	"	47'
6	323'	"	58'
7	99'	"	24'
8	99'	"	25'
9	124'	"	32'
10	224'	"	32'
12	199'	"	40'
14	174'	"	52'
16	109'	"	73'
18	123'	"	78'
19	122'	"	62'
23	74'	"	54'
24	149'	"	69'
25	399'	"	81'
34	224'	"	61'

Zone 3. Clearbook Drive, Rolling Acres

Lot #	Depth	Lithology	
11	--	sandstone at	28'
13	--	"	36'
15	--	"	58'
17	--	"	54'
20	--	"	53'
21	--	"	47'

APPENDIX II

BRITTLE PETROFABRIC DATA

SEPARATED BY DOMAIN AND STATION

All data are contoured on the lower hemisphere of an equal-area net.

Contours are as indicated.

APPENDIX IIA

BELCHERTOWN INTRUSIVE COMPLEX DOMAIN (BCD)

Annotation:

A. "Pre-Mesozoic" fracture system (Bagg Hill).
B. "Pre-Mesozoic" fracture system.
C. Mesozoic fracture system.

APPENDIX IIB

AMHERST BLOCK DOMAIN (ABD)
(includes Mt. Warner)

Annotation:

A. "Pre-Mesozoic" fracture system.
B. Mesozoic fracture system.

APPENDIX IIA

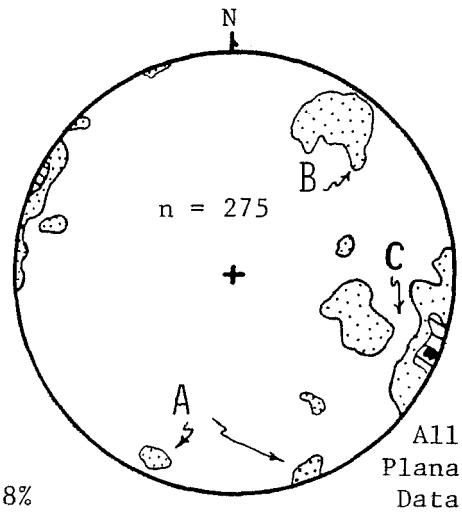

2,5,8%

All Planar Data

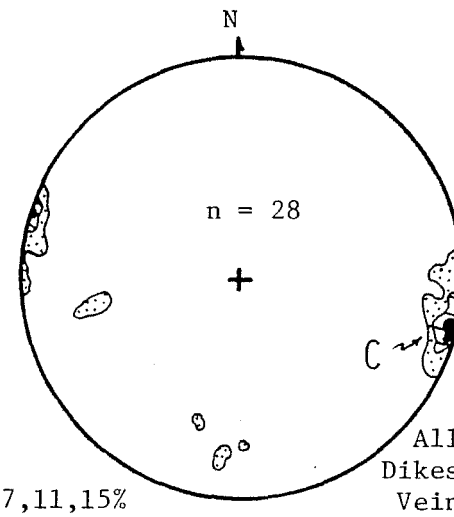

7,11,15%

All Dikes and Veins

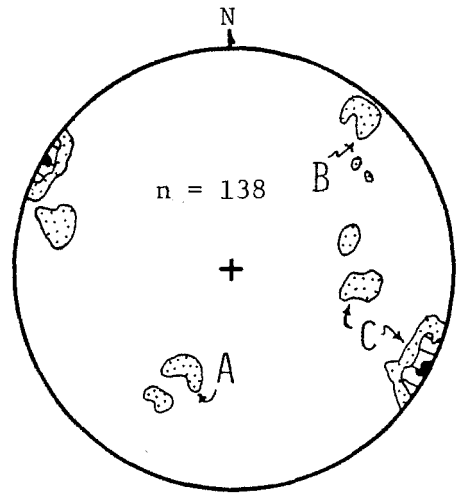

3,6,9%

All Joints

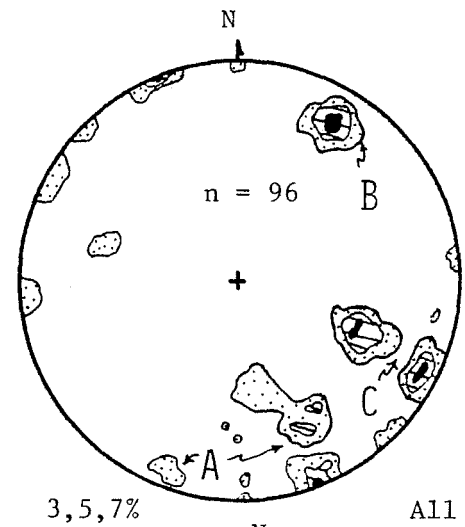

3,5,7%

All Faults

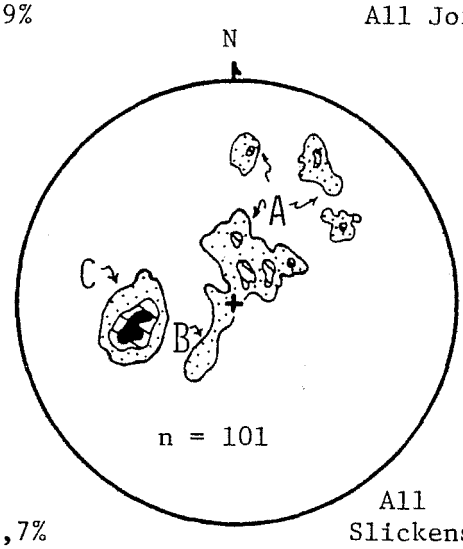

3,5,7%

All Slickensides

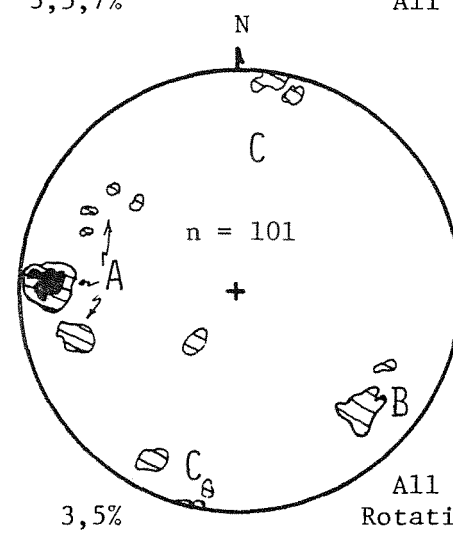

3,5%

All Rotation Axes

APPENDIX IIB

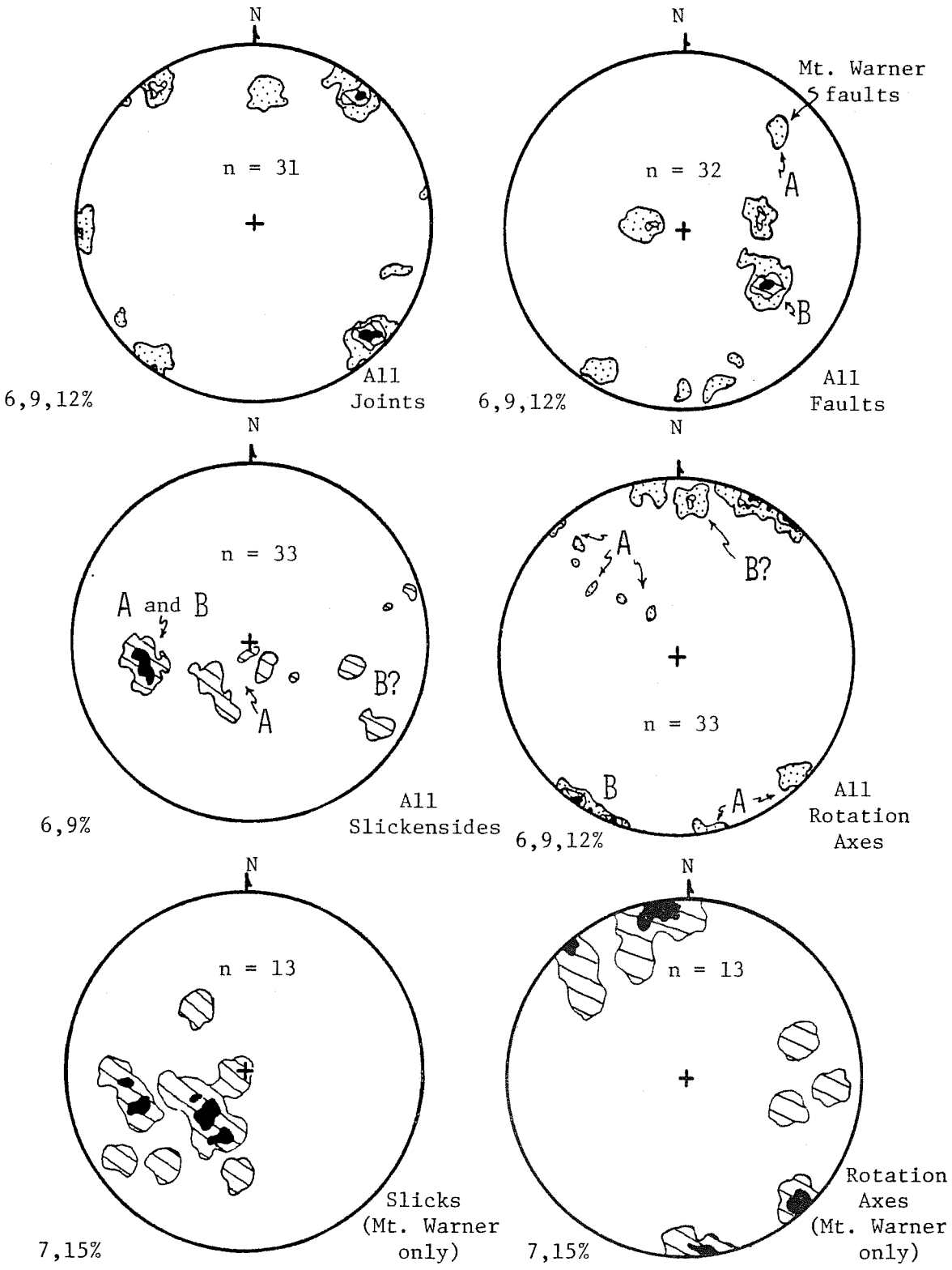

APPENDIX IIC

FRACTURE DATA FROM SIGNIFICANT STATIONS

Precise descriptions and locations for individual stations located in Figure 11 are given in Appendix IID. The purpose of examining fracture data by station is to define further and isolate the development of specific fracture patterns within and between domains.

Stations in the Belchertown Intrusive Complex Domain (BCD)

Stations 19 and 20 are located in the quarry at Bagg Hill in the northwest corner of the Ludlow quadrangle (Figure 11). The outcrop is in close proximity to the border fault and is highly fractured and faulted. These stations combined show two dominant fault orientations, one at N70W, 80NE and a second N72E, 70-80^{o}NW. A number of minor poorly defined sets are also present. Slickensides for these dominant faults plunge steeply to the north-northeast and their rotation axes (σ_2) trend between N60W and S73W, plunging 20^{o}W. A minor set of rotation axes trends generally north-south and plunges 15^{o}S. It is interesting to note the correspondence between the N70W orientation of faulting and the N55-70W trend in foliation measured by Hall (1973) at Bagg Hill. This suggests that the foliation may have been a controlling factor, along with stress orientation, during faulting.

Station 22 is located in the southeast portion of the complex. Jointing at this station is well developed with maxima oriented N63W, 25 SW and N75W, 50NNE. Faults, though rare, are oriented predominantly N23W, 80-90SW and at N71E, 60NW. Slickensides for these faults give somewhat uncertain motion senses. Rotation axes show maxima trending N86W, 10W; N58W, 45NW; and N25W, 40NW.

Station 24 is located near the Spillway at Quabbin Reservoir within the Spillway Stock of the Belchertown Intrusive Complex. Joints show a dominant N28E orientation and are nearly vertical. A second minor set is found at N8E, 50W. Faults cluster nicely and are oriented N27E, 55-85NW. Slickensides for these faults plunge predominantly to the west-southwest and rotation axes (σ_2)trend N14E, 10°N.

Station 39 shows well developed joint maxima at N32E, 80NW; N12E, 75E; and a minor set at N56W dipping both 80SW and 50NE. Faults show maxima oriented N56W, 75-80SW and a second set nearly vertical at N36E. Slickensides for the NW set show fault motion to the northeast with a west-southwest motion sense indicated by the slickensides for the NE set. Rotation axes for these faults show dominant trends at S42W, 60SW and S48E, 25SE.

Joints at station 40 are generally randomly oriented, but maxima do appear oriented N10W, 45-75W; and N27E, 80NW.

Stations Located Within the Mesozoic Basin

Station 33 is located near the Notch in the Holyoke Range. Dominant joint sets appear oriented N10E, 70NW; N64E, 45SE and minor sets at N75W, vertical; and N75E, 65NNE.

Station 45 near the Holyoke Dam shows two joint sets oriented N10W, 75W; and N38E, 70NW.

Faults measured in the vicinity of the east end of the Holyoke Range by Danesh (1977) show maxima oriented N8E, 80W and 60E, and N33E, 65NW. Slickensides for these faults plunge to the west-northwest and to the northeast. Rotation axes (σ_2) trend dominantly N6E, 10°S.

Poles to bedding within Mesozoic rocks of the study area show a well defined maximum oriented N44E, 65SE. It should be noted that the majority of the bedding readings were taken at outcrops in close proximity to the border fault and the eastern end of the Holyoke Range.

Stations 19 and 20 (Bagg Hill, BCD)

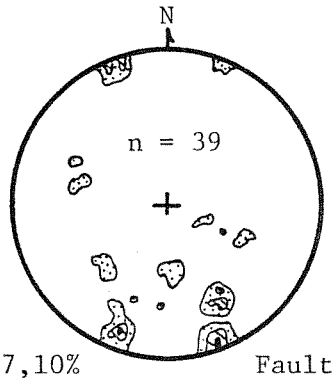

5,7,10% Faults

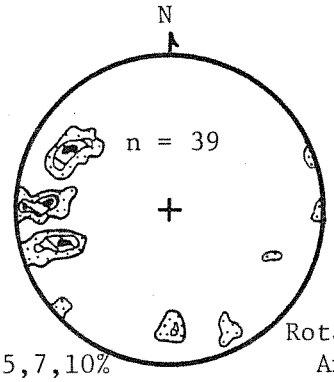

5,7,10% Rotation Axes

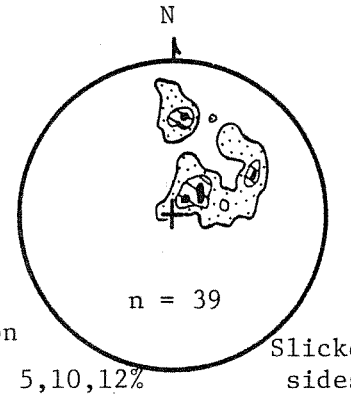

5,10,12% Slicken-sides

Station 22 (BCD)

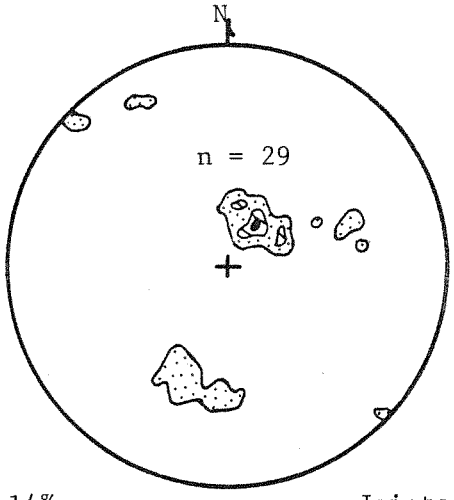

6,10,14% Joints

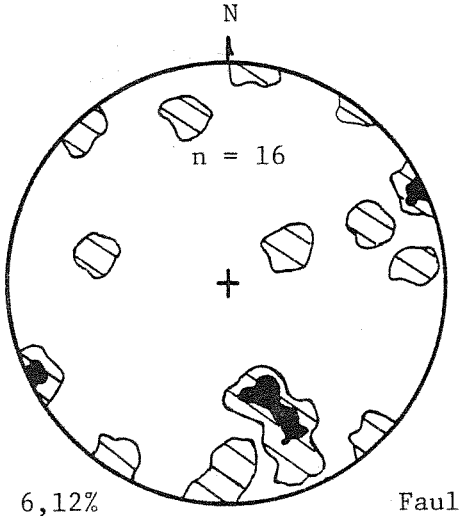

6,12% Faults

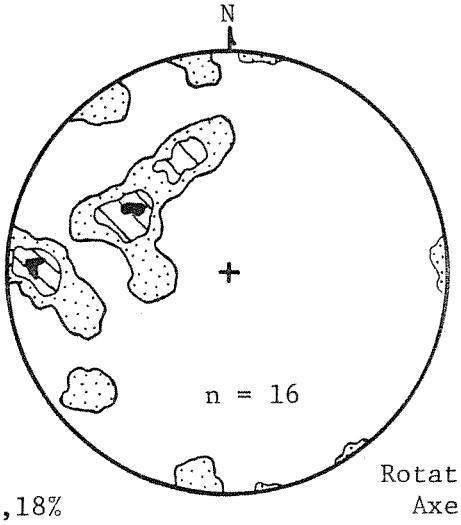

6,12,18% Rotation Axes

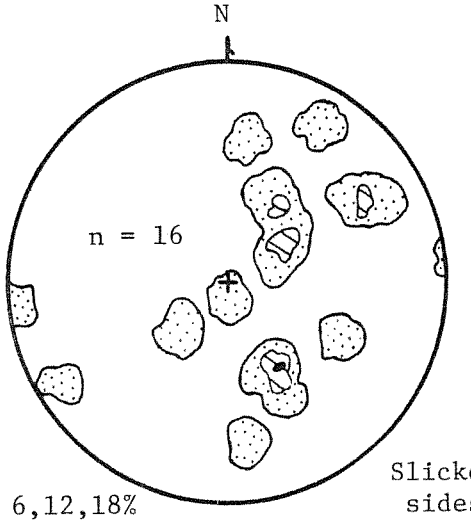

6,12,18% Slicken-sides

Station 24
(BCD)

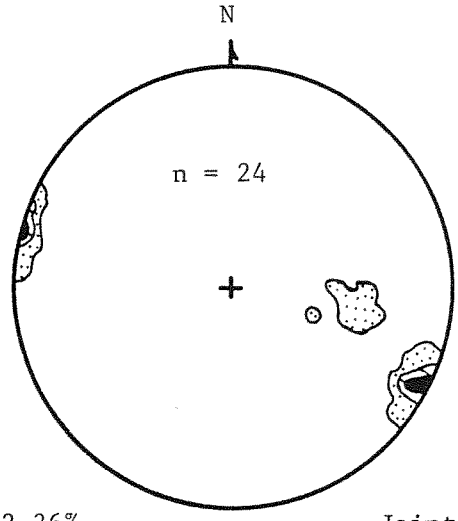

8,22,36% Joints

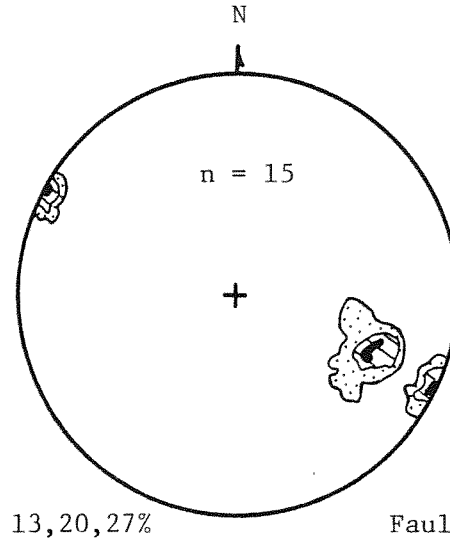

13,20,27% Faults

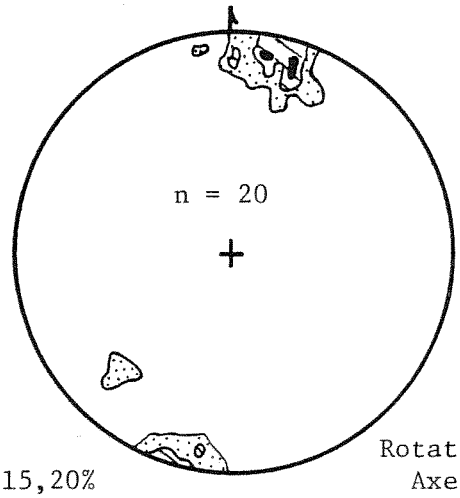

10,15,20% Rotation Axes

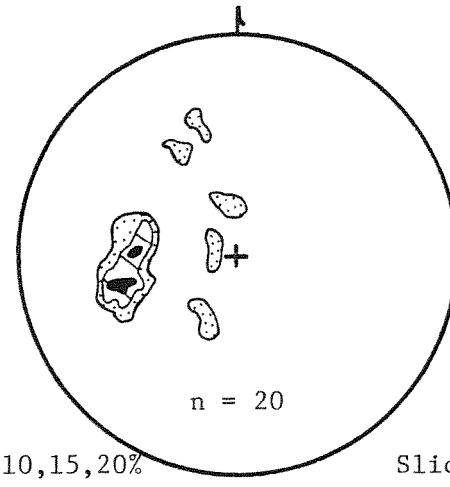

10,15,20% Slicken-sides

Station 39
(BCD)

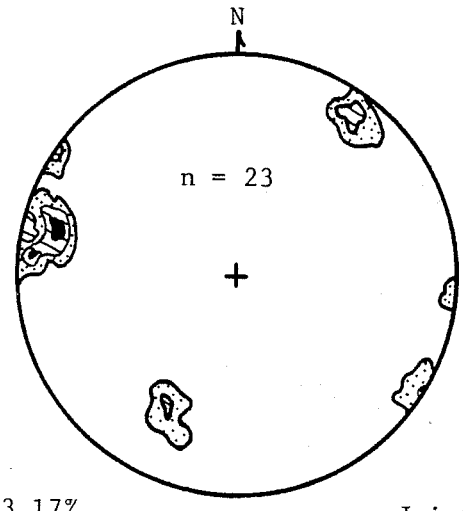

8,13,17%

Joints

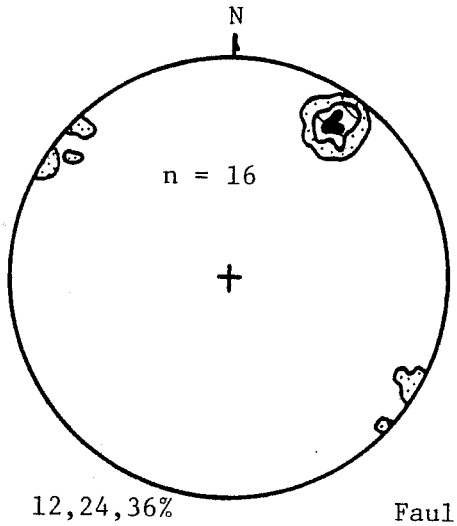

12,24,36%

Faults

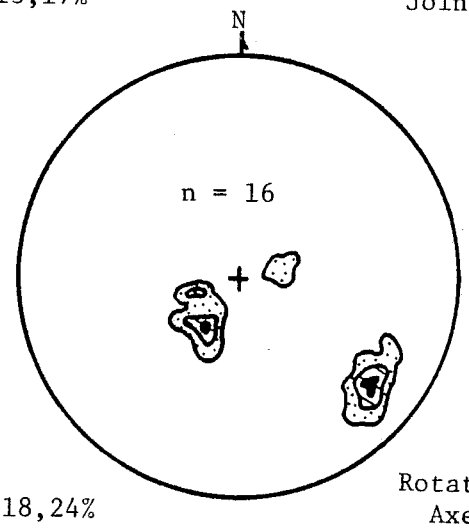

12,18,24%

Rotation
Axes

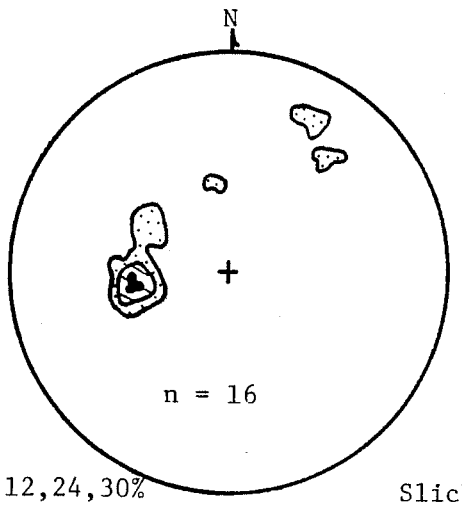

12,24,30%

Slicken-
sides

Station 40 (BCD)

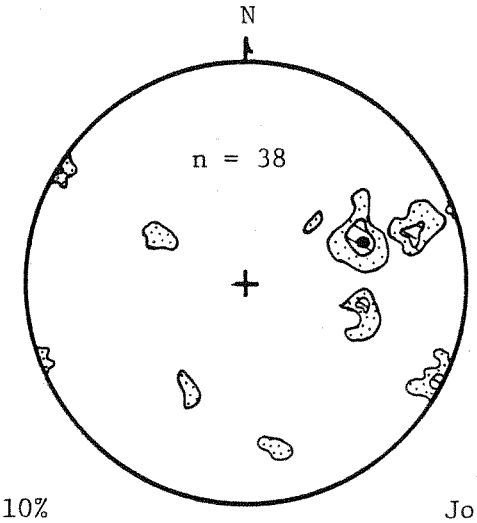

5,7,10% Joints

Stations within the basin

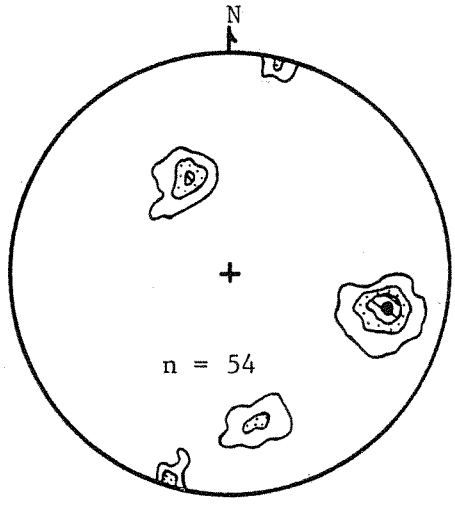

5,7,11,15% Joints

Station 33

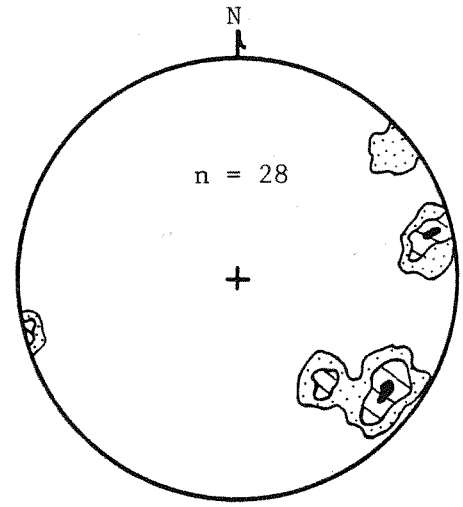

7,10,17% Joints

Station 45

Data from east end of Holyoke Range (Danesh, 1977).

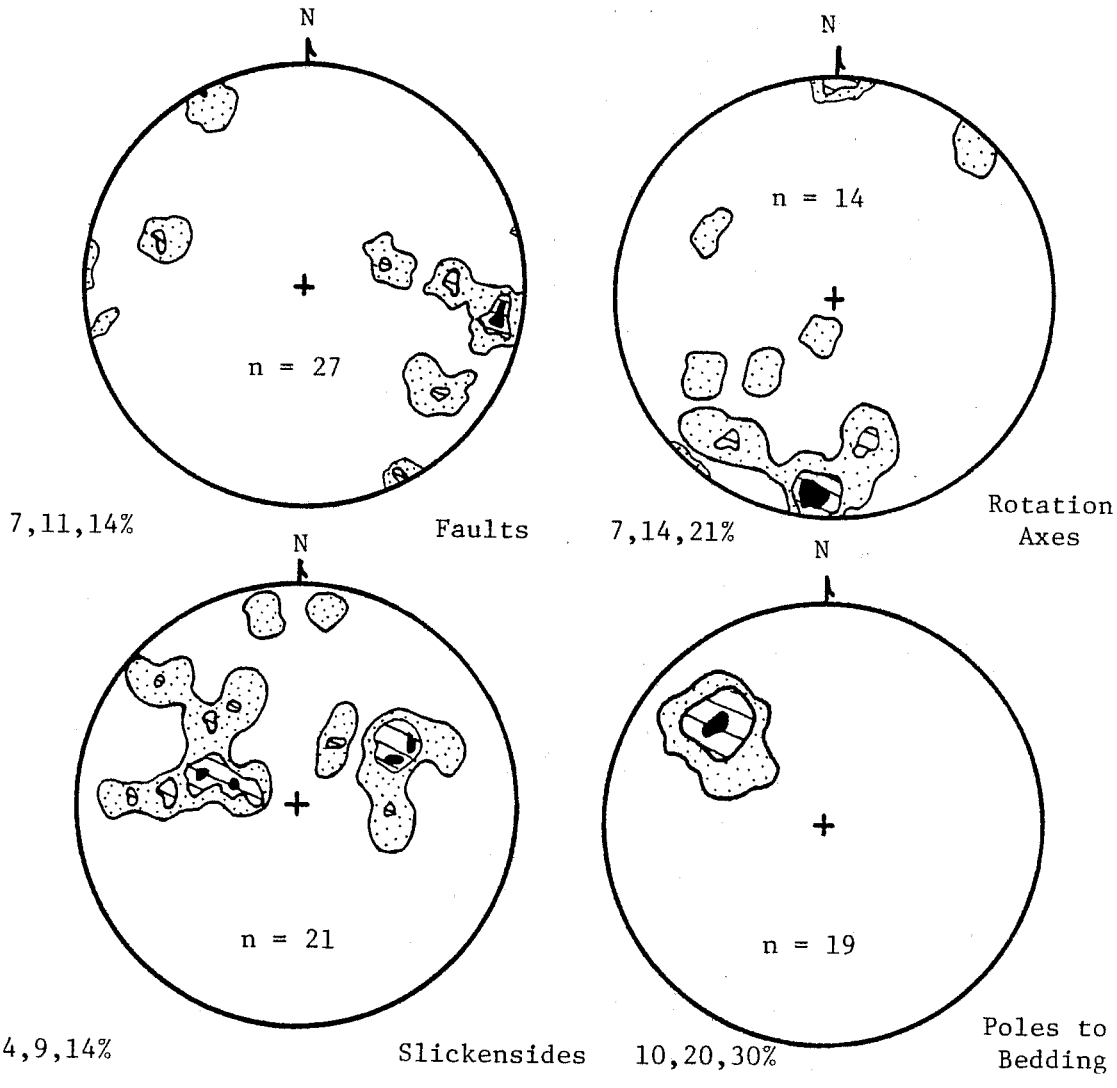

APPENDIX IID

MAJOR FRACTURE STATION DESCRIPTIONS

Universal Transverse Mercator (UTM) coordinates for stations given in E-W, N-S order.

Stations in the Belchertown Intrusive Complex:

Stations 19 and 20 (combined); UTM: 708100, 4680000

Quarry at Bagg Hill with large (2000') exposure of the Belchertown Intrusive Complex. Highly faulted, cut by many massive pegmatite dikes (sericitized). Rocks vary in texture from a massive granodiorite to a well foliated, gneissic texture. Faulting is prominent in the more foliated rocks. Fault to joint ratio is extremely high.

Station 22; UTM: 716300, 4673700

Extensive railroad cut (1000'-1500') along powerlines, inaccessible in places. Massive granodiorite, well faulted and jointed.

Station 24; UTM: 719550, 4685000

Road cut 200 ft. east of Spillway at Quabbin Reservoir. Exposure in the Spillway Stock of the Belchertown Intrusive Complex; well jointed, cut by dikes and quartz veins.

Station 39; UTM: 720000, 4675500

Railroad cut in the granodiorite, foliated in places. Some fault planes covered by quartz containing pink spary-tooth calcite. Micro-fractures in quartz do not cut calcite.

Station 40; UTM: 715300, 4673550

Granodiorite forming natural cliff, near Chicopee River, well jointed.

Stations in the Mesozoic basin:

Station 26; UTM: 699650, 4694100

Exposure of Partridge Fm. along Mt. Warner Road (several exposures) near Mt. Warner in rust-weathering schist and massive pegmatite.

APPENDIX IID (Continued)

Station 33; UTM: 705800, 4686050

Road cut in the Holyoke Basalt across from Notch quarry.

Station 45; UTM: 698000, 4675900

Spillway at the Holyoke Dam. Faulting and jointing in ss. and shales occurs along bedding in most cases.

APPENDIX III

SUMMARY/RESULTS OF GRAVITY TRAVERSE ALONG COMINS ROAD FROM NORTH AMHERST TO ROUTE 47

APPENDIX IIIA

Index map showing location of traverse in the Mt. Toby quadrangle from B-B'. Previous contact between Amherst Block (p"Ṛ") and basin sediments ("Ṛ") as mapped by Willard (1951) is shown along with the revised contact location. Gravity stations 0 (B') to 14 are spaced every 200', stations 14 to 69 every 100', and 69 to 74 (B) every 200'. Even stations between 14 and 69 are not shown.

APPENDIX IIIA

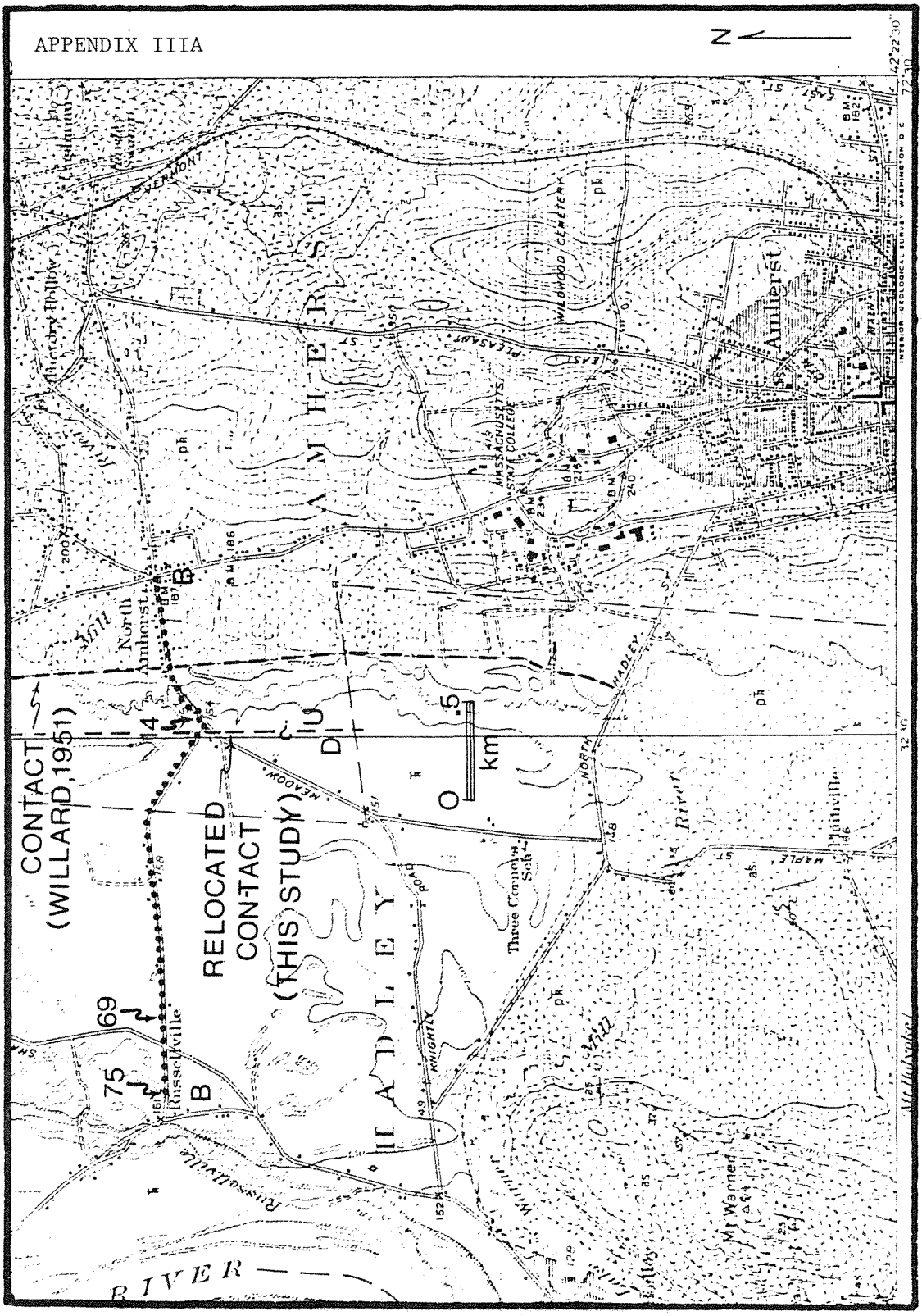

APPENDIX IIIB: Gravity data from Comins Road gravity traverse.

0TOTAL NUMBER STATIONS= 75
0- - - - - - - - - - - - - - - - - - - -COMPUTATION PRINT OUT- - - - - - - - - - - - - - - - - -
0
0---BOUGUER DENSITY USED=2.67

0 STATION	LATITUDE	LONGITUDE	ELEVATION	THEORETICAL GRAVITY	OBSERVED GRAVITY	BOUGUER ANOMOLY
0	42.4095	72.5833	186.9	980395.90	980378.78	-5.91
1	42.4094	72.5833	182.2	980395.89	980379.02	-5.95
2	42.4093	72.5833	177.1	980395.88	980379.29	-5.98
3	42.4092	72.5833	172.5	980395.87	980379.59	-5.95
4	42.4091	72.5833	169.8	980395.86	980379.67	-6.02
5	42.4090	72.5833	166.8	980395.85	980379.86	-6.00
6	42.4089	72.5833	163.7	980395.84	980380.12	-5.91
7	42.4088	72.5833	160.9	980395.83	980380.43	-5.76
8	42.4087	72.5833	158.1	980395.83	980380.76	-5.59
9	42.4083	72.5833	159.6	980395.79	980380.82	-5.41
10	42.4079	72.5833	158.6	980395.75	980380.82	-5.43
11	42.4075	72.5833	156.1	980395.72	980381.11	-5.25
12	42.4071	72.5833	156.1	980395.68	980380.72	-5.60
13	42.4067	72.5833	154.7	980395.65	980380.69	-5.68
14	42.4067	72.5833	153.8	980395.65	980380.62	-5.81
15	42.4069	72.5833	154.4	980395.66	980380.44	-5.97
16	42.4071	72.5833	154.4	980395.68	980380.32	-6.09
17	42.4073	72.5833	154.7	980395.70	980380.32	-6.21
18	42.4075	72.5833	154.6	980395.72	980380.14	-6.30
19	42.4077	72.5833	155.0	980395.74	980380.03	-6.42

APPENDIX IIIB: cont'd.

20	42.4079	72.5833	154.9	980395.75	980379.97	-6.51
21	42.4081	72.5833	154.7	980395.77	980379.91	-6.59
22	42.4083	72.5833	155.1	980395.79	980379.75	-6.74
23	42.4085	72.5833	155.2	980395.81	980379.79	-6.72
24	42.4087	72.5833	155.0	980395.83	980379.72	-6.76
25	42.4089	72.5833	156.4	980395.84	980379.64	-6.83
26	42.4091	72.5833	156.7	980395.86	980379.63	-6.84
27	42.4093	72.5833	156.9	980395.88	980379.51	-6.96
28	42.4095	72.5833	157.0	980395.90	980379.60	-6.89
29	42.4097	72.5833	156.9	980395.92	980379.56	-6.95
30	42.4099	72.5833	157.2	980395.93	980379.55	-6.96
31	42.4101	72.5833	157.2	980395.95	980379.51	-7.02
32	42.4103	72.5833	156.5	980395.97	980379.58	-7.01
33	42.4105	72.5833	155.8	980395.99	980379.64	-7.01
34	42.4104	72.5833	155.5	980395.98	980379.56	-7.10
35	42.4104	72.5833	155.8	980395.98	980379.55	-7.09
36	42.4104	72.5833	156.6	980395.98	980379.48	-7.11
37	42.4104	72.5833	156.7	980395.98	980379.45	-7.14
38	42.4104	72.5833	156.8	980395.98	980379.43	-7.15
39	42.4103	72.5833	157.2	980395.97	980379.41	-7.14
40	42.4103	72.5833	157.6	980395.97	980379.38	-7.15
41	42.4103	72.5833	157.9	980395.97	980379.28	-7.23
42	42.4103	72.5833	158.4	980395.97	980379.25	-7.23
43	42.4103	72.5833	157.4	980395.97	980379.26	-7.28
44	42.4102	72.5833	156.7	980395.96	980379.30	-7.27
45	42.4102	72.5833	156.6	980395.96	980379.25	-7.32
46	42.4102	72.5833	157.0	980395.96	980379.14	-7.41
47	42.4102	72.5833	157.3	980395.96	980379.12	-7.41

APPENDIX IIIB: cont'd.

48	42.4102	72.5833	157.5	980395.96	980379.06	-7.47
49	42.4101	72.5833	157.0	980395.95	980378.99	-7.56
50	42.4101	72.5833	156.2	980395.95	980379.07	-7.52
51	42.4101	72.5833	155.1	980395.95	980379.06	-7.60
52	42.4101	72.5833	154.0	980395.95	980379.06	-7.67
53	42.4101	72.5833	153.5	980395.95	980379.05	-7.70
54	42.4101	72.5833	153.8	980395.95	980379.00	-7.74
55	42.4100	72.5833	154.3	980395.94	980378.96	-7.73
56	42.4100	72.5833	154.8	980395.94	980378.91	-7.76
57	42.4100	72.5833	155.4	980395.94	980378.85	-7.78
58	42.4100	72.5833	155.2	980395.94	980378.89	-7.75
59	42.4100	72.5833	155.2	980395.94	980378.85	-7.79
60	42.4099	72.5833	155.0	980395.93	980378.89	-7.75
61	42.4099	72.5833	154.0	980395.93	980378.88	-7.82
62	42.4099	72.5833	155.2	980395.93	980378.88	-7.76
63	42.4099	72.5833	155.4	980395.93	980378.93	-7.69
64	42.4099	72.5833	155.4	980395.93	980378.95	-7.67
65	42.4098	72.5833	155.6	980395.92	980379.01	-7.59
66	42.4098	72.5833	155.2	980395.92	980379.06	-7.56
67	42.4098	72.5833	155.4	980395.92	980379.05	-7.57
68	42.4098	72.5833	155.4	980395.92	980379.09	-7.52
69	42.4098	72.5833	155.7	980395.92	980379.10	-7.49
70	42.4097	72.5833	154.6	980395.92	980379.06	-7.47
71	42.4097	72.5833	155.8	980395.92	980379.19	-7.39
72	42.4097	72.5833	155.5	980395.92	980379.29	-7.31
73	42.4096	72.5833	156.6	980395.91	980379.43	-7.15
74	42.4096	72.5833	158.6	980395.91	980379.35	-7.05

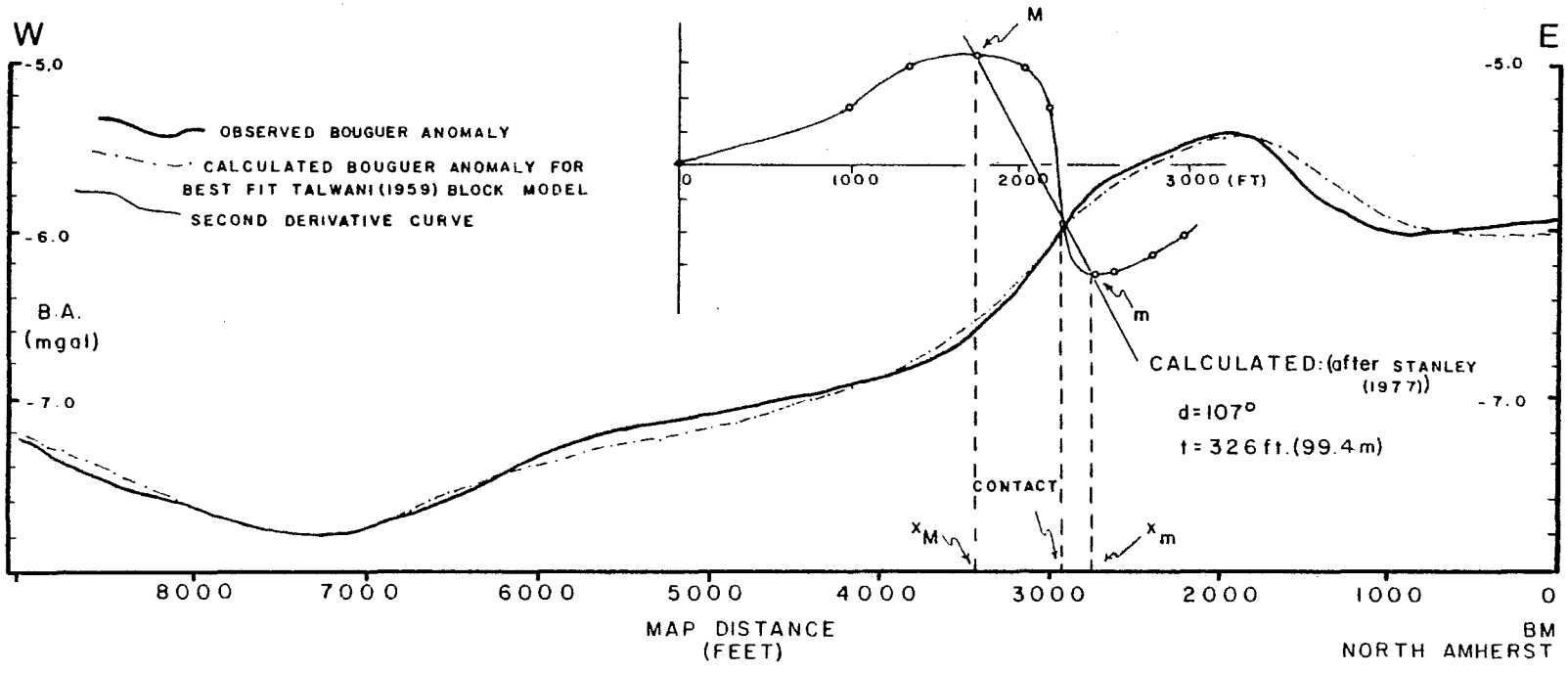

APPENDIX IIIC: Observed Bouguer gravity profile along Comins Road with calculated Bouguer gravity profile for Talwani block model and second derivative curve superimposed.

CRITICAL POINTS:

$x_M = -495$

$x_m = 185$

$M = 1.25 \times 10^{-6}$

$m = -2.25 \times 10^{-6}$

CONTACT: Point where line through M and m intersects the second derivative curve.

APPENDIX IIID

DESCRIPTION OF THE METHOD FOR DEFINING A GEOLOGIC CONTACT

Stanley (1977) describes the theory and application of a simple method for on-site interpretation of gravity anomalies arising from a geological contact. The method employs the second horizontal derivative of the gravity anomaly and has a high immunity to regional and topographic interference and is independent of latitude.

All that is required is a relatively short length of traverse across the area believed to contain a contact, as in the model shown in Figure 1 of Appendix IIIE. The observed anomaly is then plotted along the line of traverse and from this, the first and second derivative curves can be calculated (Figures 3a, b, c, of Appendix IIIE). From the second derivative curve, four critical points are of interest, e.g., M, m, x_M, and x_m. These points represent the maximum and minimum points on the second derivative curve and their respective x coordinates. They can be used in the equations in Table 1 of Appendix IIIE to calculate values for t, the depth to the shoulder of the contact, and d, the supplement to the angle of dip of the contact, as shown in Figure 1 of Appendix IIIE. The map location of the contact is defined by the point where the straight line drawn through M and m intersects the second derivative curve.

This method was applied to the anomaly profile shown in Appendix IIIC. The section of the curve showing the maximum gradient was chosen. The behavior of the west end of the profile has already been interpreted as being due to a buried stream channel (Foose and Cunningham, 1968). To determine the second derivative curves for observed anomalies, a computer program was developed and adapted to the Wang computer system for easy usage (Appendix IIIF). An example of the data input and the corresponding printout is shown in Appendix IIIG.

$$(M + m)/(M - m) = \cos d. \qquad \text{(determine } d\text{)}$$
$$x_M - x_m = -2t/\sin d \qquad \text{(determine } t\text{)}$$
$$M - m = (2G\rho \sin d)/t \qquad \text{(determine } \rho\text{)}$$

$$x_0 = t/\tan d. = (x_M + x_m)/2$$
$$-x_M \cdot x_m = t^2$$
$$g_{xx}(0) = (2G\rho \sin d.\cos d)/t = M + m$$

TABLE 1

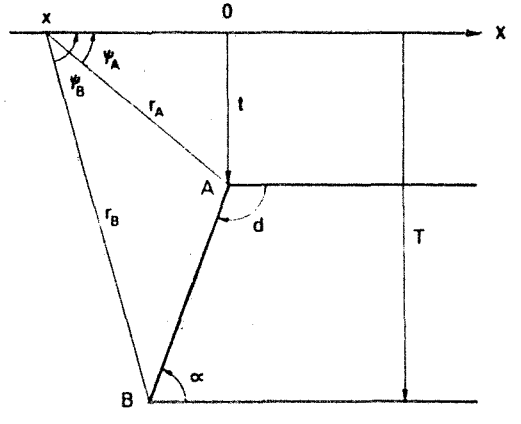

FIG. 1. Geometry of the geological contact model.

FIGURE 3

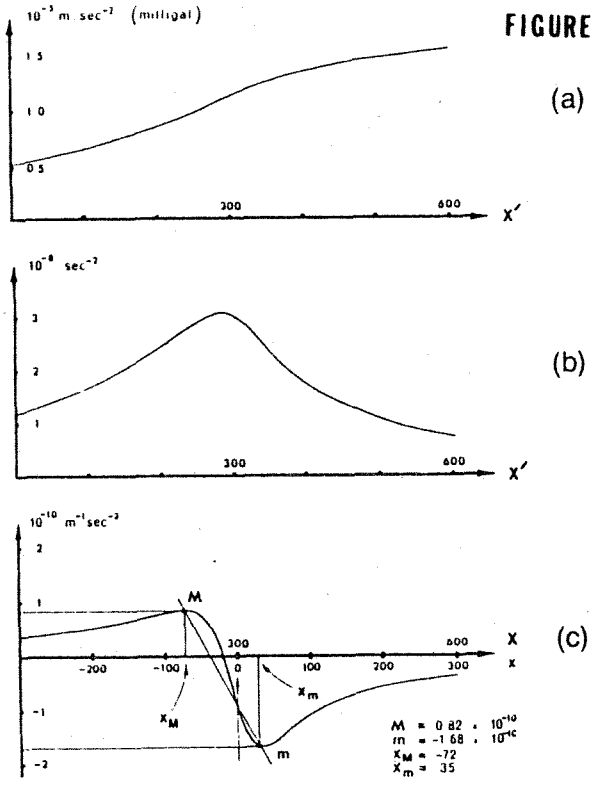

Table 1. Equations which link the coordinates of the four characteristic points with the unknown parameters of the contact. The choice between these relationships will depend upon which of the four characteristic points are best defined on the second derivative gravity profile. The usual choice is the first three equations.

FIG. 3(a) Bouguer profile across a contact model. (b) The horizontal gradient anomaly across the same contact model. (c) The second derivative of the above Bouguer profile. Identified on this profile are the characteristic points from which the parameters of the contact may be calculated.

FROM STANLEY (1977)

APPENDIX IIIF: Wang computer program for calculating coordinates for second derivative curves.

```
10 REM ************************************
20 REM              DERIV
30 REM ------------------------------------------
40 REM DESIGNED FOR USE WITH THE TECHNIQUE DEVELOPED
50 REM BY STANLEY IN "GEOPHYSICS",VOL.42,NO.6,P.1230-
60 REM 1235,October 1977: "SIMPLIFIED GRAVITY
70 REM INTERPRETATION BY GRADIENTS--THE GEOLOGICAL
80 REM CONTACT"
90 REM ------------------------------------------
100 REM TAKES SERIES OF VALUES AT SUCCESSIVE STATIONS
110 REM AND CALCULATES SLOPES AND THEN 2ND DERIVATIVE
120 REM FROM THESE SLOPES
130 REM ------------------------------------------
140 REM            CHANDLER 1/23/78
150 REM ------------------------------------------
160 REM X(I)=MAP DIST. TO POINT
170 REM Y(I)=ANOMALY AT THAT POINT
180 REM ------------------------------------------
190 DIM X(100),Y(100),D1(100),D2(100),X1(100),X2(100)
200 DIM X7(100)
210 INPUT "N=",N
220 FOR I=1 TO N
230 INPUT "X AND Y", X(I),Y(I)
240 PRINT "X=";X(I),"Y=";Y(I)
250 NEXT I
260 FOR I=1 TO N
270 J=I+1
280 X1(I)=X(I)+((X(J)-X(I))/2)
290 D1(I)=(Y(J)-Y(I))/(X(J)-X(I))
300 NEXT I
310 FOR I=2 TO N
320 J=I-1
330 X2(J)=X1(J)+((X1(I)-X1(J))/2)
340 D2(I)=(D1(I)-D1(J))/(X1(I)-X1(J))
350 NEXT I
360 SELECT PRINT 211
370 FOR I=1 TO N
380 PRINT "X=";X(I),"Y=";Y(I)
390 NEXT I
400 PRINT
410 PRINT
420 FOR I=1 TO N
430 PRINT "X1=";X1(I),"D1=";D1(I)
440 NEXT I
450 PRINT
460 PRINT
470 FOR I=1 TO N
480 IF I=1 THEN 510
490 X7(I)=X2(I-1)
500 GO TO 520
510 X7(I)=0
520 PRINT "X2=";X7(I),"D2=";D2(I)
530 NEXT I
540 PRINT
550 PRINT
560 END
```

APPENDIX IIIG

Data input: X and Y coordinates of observed anomaly.

X (map distance)	Y (Bouguer anomaly)
600	-7.02
800	-6.97
1000	-6.92
1200	-6.87
1400	-6.81
1600	-6.72
1800	-6.57
2000	-6.37
2200	-6.13
2400	-5.86
2600	-5.68
2800	-5.58
3000	-5.51
3200	-5.43
3400	-5.36

Second derivative program printout: coordinates of points defining second derivative curve shown in Appendix IIIC.

X (map distance)	Y (second derivative)
0	0
1000	6.25xE -08
1400	8.13xE -07
1800	1.25xE -06
2000	1.0xE -06
2200	6.25xE -08
2400	-2.25xE -06
2600	-1.75xE -06
2800	-7.5xE -07
3000	-1.25xE -07

APPENDIX IIIH

CALCULATION OF d AND t FOR COMINS ROAD GRAVITY PROFILE

From Table 1., Appendix IIIE;

1) $(M+m)/(M-m) = \cos d$

From second derivative curve; $M = 1.25 \times 10^{-6}$, $m = 2.25 \times 10^{-6}$ so:

$$\cos d = \frac{-1.0 \times 10^{-6}}{3.5 \times 10^{-6}} = -.286$$

$$d = 106.5^{o}$$

2) $x_M - x_m = -2t/\sin d$

From second derivative curve; $x_M = -495$, $x_m = 185$ so:

$$t = \frac{-680}{-2} \sin d = 340(.9588)$$

$$t = 326\text{ft. } (99.4\text{m})$$

Note: This calculated value for t is in excellent agreement with well data for the area around the Amherst Block (see Appendix I, maps A and B).

APPENDIX III I: Coordinates for corners of best fit Talwani block model.

```
LIST
DATA1          5000.0   .1   30   5
2.4  11  BLOCK1

      0.0        0.0
  10000.0        0.0
  10000.0        .17
  5002.31        .17
  5002.30       .070
  5001.80       .075
  5001.79        .12
  5000.70        .12
   5000.6        .20
  5000.00       .080
      0.0        .07
  2.74   6    BLOCK2
   5001.8       .075
   5002.3        .07
  5002.31        .17
  10000.0        .17
  10000.0        1.0
   5001.6        1.0
  2.67   8    BLOCK3
      0.0        1.0
   5000.0       .080
   5000.6        .20
  5000.70        .12
  5001.79        .12
  5001.65       .752
   5000.0       .655
      0.0       .655
  2.74   6    BLOCK4
      0.0       .655
   5000.0       .655
  5001.65       .752
 5001.451      1.625
   5000.0       1.55
      0.0       1.55
  2.82   7    BLOCK5
      0.0       1.55
   5000.0       1.55
5001.4510      1.625
   5001.6        1.0
  10000.0        1.0
  10000.0        5.0
      0.0        5.0
      0.0        0.0 10000.0    0.0 10000.0  5.0   0.0   5.0
```

APPENDIX III J: Calculated bouguer anomaly for best fit Talwani block model.

```
DATA1          16.04.33        78/03/05.
BLOCK1           2.40
BLOCK2           2.74
BLOCK3           2.67
BLOCK4           2.74
BLOCK5           2.82
5000.0          583.2          0.0000
5000.1          583.1          -.0012
5000.2          582.9          -.0027
5000.3          582.8          -.0045
5000.4          582.7          -.0065
5000.5          582.7          -.0088
5000.6          582.7          -.0115
5000.7          582.9          -.0144
5000.8          583.0          -.0178
5000.9          583.1          -.0216
5001.0          583.2          -.0257
5001.1          583.2          -.0304
5001.2          583.3          -.0354
5001.3          583.4          -.0407
5001.4          583.5          -.0462
5001.5          583.6          -.0517
5001.6          583.8          -.0567
5001.7          584.0          -.0602
5001.8          584.4          -.0594
5001.9          584.7          -.0523
5002.0          584.9          -.0441
5002.1          585.0          -.0368
5002.2          585.0          -.0304
5002.3          584.8          -.0249
5002.4          584.6          -.0202
5002.5          584.5          -.0161
5002.6          584.5          -.0125
5002.7          584.5          -.0095
5002.8          584.6          -.0068
5002.9          584.6          -.0045

OMODEL CHECK
STATION 1 =      -.001411
STATION 2 =      -.004875
STATION 3 =      -.001750
      .264 CP SECONDS EXECUTION TIME
```

APPENDIX IIIK

Best fit Talwani block model and calculated anomaly for density stratigraphy shown.